



TÉCNICO
LISBOA



EXPERIMENTAL CHARACTERIZATION OF ELECTRIC MOTORS AND JET ENGINES FOR BLENDED WING BODY FLIGHT TEST MODELS

Yahiya Ajraoui

Thesis to obtain the Master of Science Degree in

Aerospace Engineering

Supervisor(s): Prof. Afzal Suleman
Prof. Dario Giuseppe Pastrone

Examination Committee

Chairperson: Prof. Fernando José Parracho Lau
Supervisor: Prof. Afzal Suleman
Member of the Committee: Dr. Jayachandran Peethambaran Kuzhichalil

November 2019

PRIVATE AND CONFIDENTIAL
©Bombardier Inc. or its subsidiaries. All right reserved.

Dedicated to my family, my friends
and whoever believed in me along this journey

Acknowledgments

Having reached the end of this course of study, it is my duty to thank all those who contributed to the achievement of this goal. First of all, I thank Allah for having given me the luck to achieve my studies in a peaceful and pleasant way, helping me with difficulties, and I thank him even more for having given me two incredibly attentive and very patient parents who have had to endure me, as well as support, for all this time. Having the fortune of being the first graduate in aerospace in my family, and of my village of origin, I see it not only as a success of mine, but as a triumph of my father El Hassan, I feel embarrassed by not having done even better. Due to my thanks, my mother Nadia is sure to be there too. She introduced me to love the mathematical and physical sciences from an early age, motivating me to always aim for the maximum.

Warm thanks certainly go to my little sisters who have always supported me, but not endured, for the whole course of studies and therefore I wish them to do even better in the future. To thank the friends who followed me on this long journey is the minimum! I could not even imagine how it would have gone without them all, their contribution is indescribable. I do not mention anyone simply because they are many, and to forget someone by distraction would make me more sick than the person in question. However, they are worthy of note the CfAR team who followed me in this mission, making this thesis research be as professional as entertaining.

Last but not least, I express my gratitude to all the professors I have had on this along this path, and I find no better way to do it than how our prophet Muhammad taught us by saying in every prayer "Allah have mercy on all those who have taught". Among the many who have had as teachers, I consider to be a debtor and therefore noteworthy the following: the teacher Maddalena D'agostino, prof. Antonella Denora, prof. Vicino, professor Giuseppe Lofrese, professor Giuseppe Addam and professor Casalino. Special gifts certainly go to my supervisors professor Suleman who have given me the possibility to try the "Canadian experience", a dream came true, and for having followed me during this journey, making the job much easier and interesting!

THANKS YOU ALL!

Resumo

Recentemente, os veículos aéreos não tripulados (UAVs) têm demonstrado um potencial significativo como meio de validação de um conceito no domínio aeroespacial, uma etapa essencial antes de se prosseguir com os testes em escala real.

O Center for Aerospace Research (CfAR), especializado na produção de Demonstradores de Testes de Vôo, tem concentrado recentemente a maioria dos seus esforços nos modelos em escala do Blended Wing Body (BWB) da Bombardier. Esta nova configuração de aviões consiste em uma forma híbrida com características únicas, capazes de aproveitar as vantagens das asas e das aeronaves tradicionais, tornando-a um objeto de estudo interessante nos últimos anos.

Um primeiro protótipo feito pelo CfAR é o modelo à escala de 7% (FTV7%), que já está em testes de voo, enquanto que o outro, o modelo de 16,5% (FTV16,5%), ainda não está pronto para voar. Cada um destes modelos é uma combinação de inúmeros sistemas e subsistemas que precisam de ser testados e validados para obter os resultados previstos.

O objetivo da presente dissertação é realizar um projeto paralelo e o desenvolvimento da caracterização do sistema de propulsão para ambos os modelos FTV7% e FTV16,5%. O primeiro monta um par de Ventilador Elétrico (EDF), enquanto o outro um par de motores de turbina a jato. Testando o motor EDF, obtendo-se mapas de desempenho e detectando-se vibrações inesperadas. No modelo de 16,5%, os esforços foram colocados mais no projeto e desenvolvimento de uma bancada de teste instrumentada, incluindo uma interface gráfica Labview (GUI). Um projeto preliminar dos próximos testes foi também realizado.

Palavras-chave: UAV, Sistema Propulsivo, EDF, Motores a Jato, Banco de Ensaios, Ensaios.

Abstract

In recent times, Unmanned aerial vehicles (UAVs) have demonstrated a significant potential as mean of concept validation in aerospace domain, an essential step before proceed with real scale testing.

The Center for Aerospace Research (CfAR), specialized in production of Flight Test Demonstrators, recently has focused most of its efforts on the Blended Wing Body (BWB) scaled models on behalf of Bombardier. This new planes configuration consists of an hybrid shape with unique features able to match benefits from both flying wing and traditional aircrafts, making it a worthwhile object of study in the last few years.

A first prototype made by CfAR is the 7% scale model (FTV7%) which is already under flight testing, while the other, the 16.5% model (FTV16.5%), is not ready to fly yet. Each of this models is a combination of numerous systems and subsystems that need to be tested and validated in order to get the predicted results.

The objective of the present dissertation is to carry out a parallel design and development of propulsion system characterization for both FTV7% and FTV16.5% models. The first one mounts a pair of Electric Ducted Fan (EDF), while the other a couple of Jet turbine engines.

The EDF motor have been ground tested obtaining useful performance maps and detecting unexpected vibrations.

Concerning the 16.5% model, the efforts were addressed more on the design and development of an instrumented test bench, including a Labview Graphic User Interface (GUI). A preliminary design of the upcoming tests has been done too.

Keywords: UAV, Propulsion System, EDF, Jet turbine, Testing, Test Rig.

Contents

- Acknowledgments v
- Resumo vii
- Abstract ix
- List of Tables xiii
- List of Figures xv
- Nomenclature xix
- Glossary xxi

- 1 Introduction 1**
- 1.1 Background and Motivation 1
- 1.2 State of the Art 4
 - 1.2.1 Unmanned Air Systems 4
 - 1.2.2 Propulsion in Scaled Flight Test Models 4
 - 1.2.3 Testing of Propulsion Systems 5
- 1.3 Thesis Objectives 7
- 1.4 Thesis Roadmap 7

- 2 Engine Characterization 9**
- 2.1 Electric Ducted Fan (EDF) 10
 - 2.1.1 Theoretical Overview 10
 - 2.1.2 Characterization of an EDF 14
- 2.2 Gas Turbine Engine 15
 - 2.2.1 Theoretical Overview 15
 - 2.2.2 Gas Turbine Engines for UAVs Propulsion 19
 - 2.2.3 Characterization of a Micro Turbine Engine 21

- 3 EDF Testing 23**
- 3.1 Schubeler DS-51-AXI 24
- 3.2 Objectives and Functional Requirements 25
- 3.3 Previous Work 25
- 3.4 Test Rig Design 27
 - 3.4.1 Software Design 28

3.4.2	Test Planning	29
3.5	Experimental Set Up	30
3.6	Testing and Results	34
3.6.1	ESC Testing	35
3.6.2	Thrust Test Results	36
3.6.3	Vibration Analysis	40
3.7	Concluding Remarks	42
4	Turbine Jet Testing	43
4.1	JetCat Engine	44
4.2	Objectives and Functional Requirements	45
4.3	Previous Work	46
4.4	Test Bench Design and Equipment Selection	47
4.4.1	Testing Location	47
4.4.2	Test Rig Design	48
4.4.3	Sensors and Equipment Selection	51
4.5	Software Development	58
4.5.1	LabView GUI Design	58
4.6	Experimental Set Up	60
4.7	Concluding Remarks	61
5	Future Work and Reccomandations	63
5.1	EDF motor	63
5.1.1	Software Updates	63
5.1.2	Testing	64
5.2	Turbine Jet Engine	65
5.2.1	Software Updates	65
5.2.2	Testing	65
5.3	Recommendations	67
6	Conclusions	69
	Bibliography	71
A	EDF Documentation & Software	75
A.1	Coupled Electric Motor and EDF Aerodynamics Model	75
A.2	Matlab script	77
B	Jet Turbine Documentation & Software	83
B.1	JetCat Instruction Manual & Test Checklist	83
B.2	Compressor and Turbine maps	88

List of Tables

3.1	EDF parameters.	24
3.2	Block Inputs.	26
3.3	Block Outputs.	26
3.4	ESC parameters.	31
3.5	battery parameters.	33
3.6	Thrust vs throttle relevant values.	40
3.7	Throttle vs thrust relevant values.	40
3.8	Throttle, RPM and frequency detected values.	42
4.1	JetCat P500 PRO parameters.	44
4.2	PCB 356A43 specifications.	54
4.3	PCB 352C04 specifications.	54

List of Figures

1.1	New aircraft configurations.	1
1.2	X-48B Blande Wing Body aircraft scale model.	2
1.3	Center for Aerospace Research, University of Victoria.	2
1.4	Blended Wing Body aircraft.	3
1.5	UAVs application.	4
1.6	Propulsion systems for UAVs application.	5
1.7	Test rig for Electric Ducted Fan.	6
1.8	Test rig for Jet turbine engines.	6
2.1	Propulsion systems for UAVs application.	10
2.2	Electric Ducted Fan components.	10
2.3	Electric Ducted Fan work principle.	11
2.4	EDF characterization outputs.	14
2.5	Schematic diagram of a Gas Turbine.	15
2.6	Typical compressors configurations in Gas Turbines.	16
2.7	Typical compressor map.	17
2.8	Typical turbine map.	18
2.9	Old and modern micro turbine engines.	19
2.10	Some arrangements of MTEs.	20
2.11	Gas turbine characterization outputs.	21
2.12	Gas turbine Thermal characterization.	22
3.1	BWB EDF motors.	23
3.2	Schubeler DS-51-AXI.	24
3.3	Example Implementation of Block Flying at 80% throttle, SL, 25m/s.	25
3.4	"THRUST-TORQUE TESTER.vi" interface.	27
3.5	EDF test rig.	28
3.6	LabVIEW GUI knob.	28
3.7	EDF mount.	30
3.8	Castle Phoenix Edge 120 HV.	31
3.9	CfAR customized power box.	31

3.10 NI data acquisition devices.	32
3.11 LiPo batteries.	33
3.12 Safety protection and Stop button.	33
3.13 EDF test rig assembled.	34
3.14 Scheme of the performed tests and analysis	34
3.15 Iteration process to find ESC lower limit	35
3.16 Experimental average values of thrust tests.	36
3.17 Throttle, Thrust (negative) and battery voltage for the four tests.	37
3.18 Average curve obtained from experimental thrust tests	38
3.19 Fitting curve and related equation for N.thrust to throttle curve.	38
3.20 Fitting curve and related equation for throttle to N. thrust curve.	39
3.21 experimental thrust curves fitted by 4th degree equation.	39
3.22 Torque load cell reading for test 1 and test 2 overlapped.	40
3.23 Time and frequency domain signal for test 1 and test 2	41
3.24 FFT results for each throttle command.	41
4.1 JetCat turbine jets.	43
4.2 JetCat P500 PRO.	44
4.3 Propulsion system already chosen components.	46
4.4 JetCat preliminary design.	47
4.5 Test rig chosen location.	48
4.6 JetCat mounting.	49
4.7 Test rig final design.	50
4.8 Sensors preliminary disposition.	51
4.9 Load cell position.	52
4.10 JetCat sensors.	53
4.11 3-axis PCB accelerometer	54
4.12 1-Axis PCB accelerometer.	54
4.13 National Instruments cDAQ board.	54
4.14 National Instruments modules.	55
4.15 Test rig Fuel tank.	55
4.16 Fuel line air trap.	56
4.17 Alternatives to flow-meter sensor.	56
4.18 Stop button location.	57
4.19 Multidisciplinary proces for JetCat tests.	58
4.20 LabVIEW GUI for JetCat testing.	59
4.21 Test bench set up.	60
4.22 Test rig realization.	61
5.1 cRIO data acquisition system.	63

5.2	New LabVIEW GUI for EDF testing.	64
5.3	Nacelle tests.	66
5.4	Dual Engine Control.	67
A.1	Block's mask parameters [21].	75
A.2	Simulink diagram [21].	76
B.1	compressor and turbine maps.	88

Nomenclature

α	Mass flow rate ratio
Ω	Angular velocity
η	Efficiency
γ	Heat capacity ratio
ρ	Mass density
c	Velocity of the air flux through a rotary machine
C_p	Heat capacity
e	Internal energy of the flux
f	Frequency
F	Thrust
h	Static enthalpy
h_0	Stagnation enthalpy
I_a	Specific thrust
M	Mach number
\dot{m}	Mass flow rate
p	Pressure
P	Power
\dot{Q}	Heat flow rate
T	Temperature
$TSFC$	Thrust Specific Fuel Consumption
u	Axial velocity
U	Tangential velocity

Glossary

BA	Bombardier
BWB	Blended Wing Body
cDAQ	compact Data Acquisition
cRIO	compact Real time Input Output
CAD	Computer-Aided Design
CFD	Computational Fluid Dynamics
CfAR	Centre for Aerospace Research
ECU	Engine Control Unit
EDF	Electric Ducted Fan
EGT	Exhaust Gas Temperature
ESC	Engine Speed Controller
FFT	Fast Fourier Transform
FTV	Flight Test Vehicle
GSU	Ground Station Unit
GUI	Graphic User Interface
MTE	Micro Turbine Engine
RC	Radio Controlled
RPM	Revolution Per Minute
TSFC	Thrust Specific Fuel Consumption
UAS	Unmanned Aircraft System
UAV	Unmanned Aerial Vehicle
UVic	University of Victoria

Chapter 1

Introduction

1.1 Background and Motivation

Throughout the ages, the attitude of humankind has been always that of seeking improvements and solutions for all the problems they face in every day life. The engineering field is the best example of the "problem-solving" attitude, and the objective of every engineer is always that of finding the best solution, either improving the existing one, or creating a new one.

Aerospace engineering sector at its side, has always demonstrated to be at the forefront in development of new concepts, showing consistent flexibility towards new technologies and new aircraft configurations, respecting though safety standards. "For years, the airline industry has been seeking game-changing aircraft", says John Grant, London-based senior analyst at OAG, the airline research and publishing firm. "Now they're finally arriving and are genuinely changing the way that carriers are able and willing to launch new services and frequencies". Specifically, Grant says the latest machines can take us farther, faster, and move us in greater comfort than ever before. And in the process, they'll burn less fuel—meaning that even if airfares don't drop as a result, they probably won't go up as fast as they would otherwise [1]. The giants of aerospace field are in continuous competition among each other in development of new concepts, and lots of efforts are made by big companies like Nasa and Boeing towards new aircraft configurations (Figure 1.1).



(a) NASA X-57 Maxwell.



(b) Boeing Truss-Braced Wing.

Figure 1.1: New aircraft configurations.

Bombardier could not remain idle to this trend, and started pushing researchers and developers towards the investigation of new aircraft configurations, that might improve BA planes performance. In recent years, one configuration in particular that BA is focusing on most, seems to be the Blended Wing Body (BWB) shape. This hybrid architecture with unique features able to match benefits from both flying wing and traditional aircrafts, has been a desirable case study for several companies in the last decade. No passenger planes have been made yet with this kind of configuration, but the American coalition Nasa-Boeing have already flown successfully a scale model of 20.4 feet wingspan, the X-48B (Figure 1.2) [2].



Figure 1.2: X-48B Blende Wing Body aircraft scale model.

BA in turn, is working on developing new BWB business jets, with an estimated entry into commercial service in 2035 [3]. The charge of building up Flight Test Vehicles (FTV) has been shared recently with the Center for Aerospace Research (CfAR) of University of Victoria (UVic), delegating most of design and manufacture tasks. The center of research, in collaboration with Quaternion Aerospace company, has shown high professionalism in UAV design, production and testing. For many years, they have been fabricating and testing both conventional and unconventional aircraft models, leading to a significant experience in the sector.



Figure 1.3: Center for Aerospace Research, University of Victoria.

The first scaled model of the new generation aircraft so far described has materialized in the 7% scale (Figure 1.4) of the large-scale aircraft, designed and developed paying attention to all the limits and difficulties occurring during the scaling down process[4].

The main task of this first prototype was mainly that of collecting aerodynamic data from flight tests, in order to validate and improve the control models used by the autopilot to maneuver the aircraft. Other aspects like engine performance, take off and landing on runway, and flight efficiency were quite neglected in this phase. Moving forward the project, a second generation of the same scale came to light, and this time was required to lower the risk of aircraft vital components damage (in terms of airframe and integrated systems), but also the exigency to check the behaviour of the aircraft in take off and landing stage. Another important demand was that of test the propulsive system to obtain reliable engine maps and data to be given to the autopilot. Until now, the flight team have been working with a valid, but not fully accurate model made following a theoretical approach integrated with statistical data from literature. The latter has been working pretty good, but there were some discrepancies that needed to be defeated. The best approach is an engine characterization, and that means to test the engines on test rig, and extract the desired data and integrate it with the already done model.



Figure 1.4: Blended Wing Body aircraft.

Along with the FTV7% testing, the Center for Aerospace research has started working on the design and development of a larger scale flight test demonstrator to get closer to what are the real physics and issues of the full scale aircraft. Actually the dimensions of the model are 16.5% of the full scale plane, with a wingspan that goes over 5 meters (detailed parameter specifications are confidential material). It is well known that every system and subsystem of the aircraft must be designed, tested and validated before start working on the plane. This procedures are even more complicated and time taking for unconventional plane configurations, and since the dimension now are getting bigger, there is no alternative of testing. Scaling up is good solution for preliminary design, but testing is mandatory for validation. This time the propulsive system will not be powered counting on theoretical models, but they will be fired and mounted on the plane only after a careful mapping of the system. The latter has been already chosen in the design phase, and it will consist of a pair of Jet turbines that will supply the required thrust in all

the flight stages.

1.2 State of the Art

1.2.1 Unmanned Air Systems

An unmanned aerial vehicle (UAV), also referred to as drone consists of an aircraft that flies without a human pilot on board, and may operate either under remote control by a human operator or autonomously by on board computer [1].

UAV technology is improving impressively in the last few years, and although it came to light in the military sector (Figure 1.5 a), it spread over various non-military fields. Nowadays, there exist so many kinds of UAVs with a lot of utilities in different areas such as disaster relief, border surveillance, wildfire fighting, inspection of pipelines as well as to spray pesticides on farms (Figure 1.5 b). That occurs because of the large advantage that they can access to points which are difficult or dangerous to the human being to go to. Furthermore, this typology of aircrafts is finding a wide use in aerospace companies themselves as flight test demonstrators for concept validation.



(a) MQ-4C Triton used for surveillance purposes.



(b) Pesticide drone.

Figure 1.5: UAVs application.

1.2.2 Propulsion in Scaled Flight Test Models

The propulsion system in UAV planes, as in traditional ones, has the role of supplying the required power to propel the aircraft for every flight phase. It has two major components: the propeller (or fan) that could be either ducted or not, and the motor/engine. The latter supplies power to the propeller that converts it into propulsive force, which is necessary for the aircraft to overcome inertial and drag forces to fly. Nevertheless, scaled aircrafts don't use always the same technologies of the traditional planes, for example, electric motors are used much more than turbines, and also the neglected piston engines are widely used in these models.

The process of selecting, characterising and running propulsion systems is a fundamental step for any UAV design, as well as the choice of correct combination of engine and propeller [5].

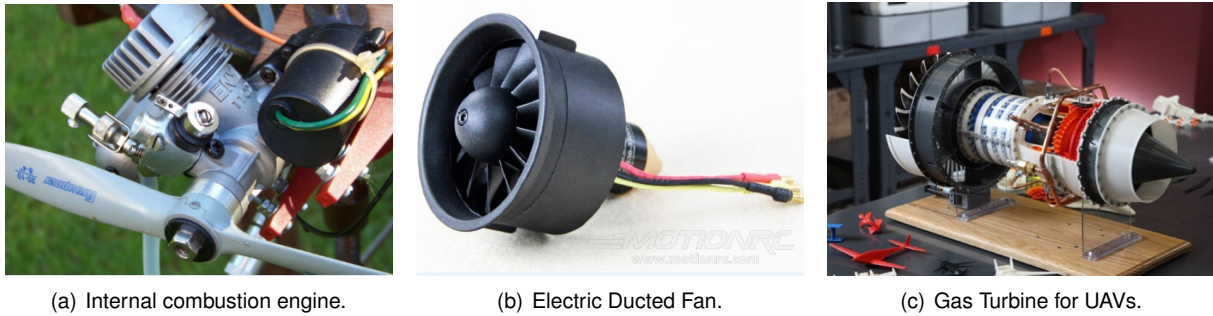


Figure 1.6: Propulsion systems for UAVs application.

Although lots of propellers and engines in the market are certified (sometimes even with complete data sheet characterisation), it happens quite often that either they have an excessive cost, or simply the chosen propulsive system doesn't have the required characterization. A relevant problem of the scaled models also, is that non-certified propeller systems are often manufactured for hobbyists and so, do not contain exhaustive data sheets. However, even if the engine is provided with all the required data sheets, it would be good practice to test the system before run it on the plane, since usually the aircraft is carrying expensive components, and losing control of the propulsive system may compromise the integrity of the whole craft. In this circumstances, results essential for any center of research, that works on flight test demonstrators, to design and develop a suitable propulsion system test rig, with the proper equipment, and execute ground tests before flight ones.

1.2.3 Testing of Propulsion Systems

A test bench is a virtual environment used to verify the fidelity of a design or model, which verifies the correct interfacing and responses. Developing a test rig environment is often time-consuming task for an advanced verification team, but pays back saving time, effort and money through the ability to verify ideas and their implementation. The required features from a test bench might be the following : Re-usability, Efficiency, Flexibility and the capability of reproduce as close as possible the real environment simulated [6].

Test benches may differ a lot among each other because of the countless variables that occurs during design and development. The noteworthy factors could be the following:

- the size of the system tested;
- the nature of the power supply;
- the environment that operators try to simulate;
- the entity of data investigated;
- Safety issues.

It is quite common to see small benches for electric ducted fan tests rather than for jet engines'. This is due mostly because the electric motors are commonly used only for hobbyists RC planes, or professionally by researchers aboard flight demonstrators. The set up of these kind of test rigs is generally quick, but requires carefulness in particular towards electric power sources and devices. An example of a simple test bench for an EDF motor is shown in Figure 1.7.

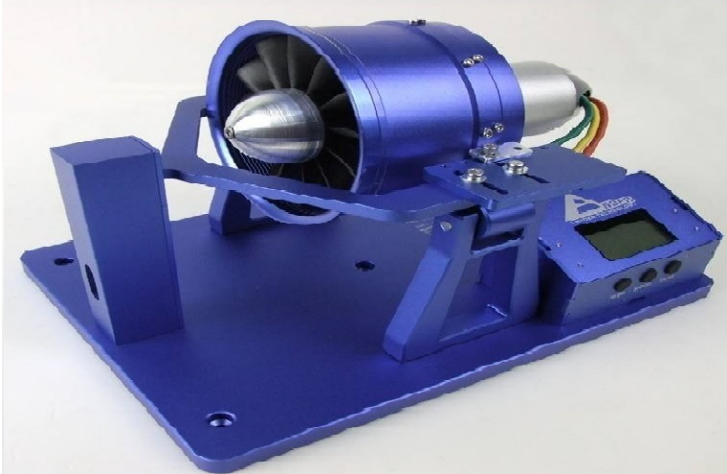


Figure 1.7: Test rig for Electric Ducted Fan.

From the other hand, Jet engine test benches can have any dimension, and this is due to the wide range of scale available for this reliable devices. Nowadays, is possible to find jet engines from the dimensions of few centimeters up to a pair of meters long. This variety of dimensions reflects of course not only on the dimension of the test rig, but also on safety procedures, and sometimes causes limitations to the tests wanted. Examples of Turbojets test rigs are given in Figure 1.8.



(a) Big scale Turbojet.



(b) Small scale turbojet.

Figure 1.8: Test rig for Jet turbine engines.

1.3 Thesis Objectives

The principle scope of this dissertation is that of set up suitable test benches for the propulsive systems of the two Blended Wing Body scale models. Moreover, it is intended also to accomplish ground tests for both systems, and analyze the collected data.

The essential targets of the thesis are itemized as follows:

- **FTV7%** propulsive system
 - design tests procedures;
 - modify and set up the existing test rig;
 - test the motors;
 - analyze the obtained data for engine characterization;

- **FTV16.5%** propulsive system
 - design both test rig and tests procedures;
 - select and order test bench equipment;
 - design a Graphic User Interface for the tests;
 - set up the test rig;
 - accomplish part of the tests;

1.4 Thesis Roadmap

The dissertation work has been organized in such a way that the two propulsive systems analysis are reported using a parallel approach, although some discrepancies often occur.

The framework of the current thesis is given itemized below.

Chapter 1: Introduction

This first chapter exposes the main features of Unmanned aerial vehicles (UAVs), explaining their usage and benefits in aerospace research along with a brief introduction to propulsive systems testing. Following, the main objectives of the thesis are presented in addition to a layout of the current dissertation.

Chapter 2: Engine Characterization

In the following chapter, the general guidelines for engine characterization are illustrated in parallel for both types of propulsive systems investigated. A first part is dedicated to the Electric Ducted Fan (EDF) discussing the characteristics of this type of motors, their performance and what is expected from a characterization of the latter. In the second half instead, the attentions are focused on gas turbine engines, recalling their main features and performances, but concentrating on the principal aspects relative to the

characterization.

Chapter 3: EDF Testing

In the following chapter, the work performed on the propulsive system of the FTV7% is analyzed in all its details. A single Electric Ducted Fan (EDF) has been tested to obtain the engine maps and to investigate some vibrations that occurred during the tests. The chapter presents all the phases of the tests, starting from the requirements, passing through the test rig design and set up, and concluding with results analysis and verification.

Chapter 4: Turbine Jet Testing

In the following chapter, the attention is moved towards the jet engine turbines, main characters of the propulsive system aboard the FTV16.5%. The chapter presents both the requirements and the theoretical model adopted in the design phase, before moving towards the test bench design and set up. The latter includes also software design for testing purposes. Unluckily the tests have not been performed, except for the equipment and in part for the software.

Chapter 5: Future Work

In the following chapter, it is possible to identify an exhaustive definition of the future work for both the typologies of propulsive systems. In relation to the EDF motors, the limits of the performed tests are discussed and specific tests are suggested to overcome the latter. With regard to the Jet engines instead, an adequate roadmap has been done for the upcoming tests .

Chapter 6: Conclusion

In this last chapter, the main achievements are brought into view and discussed in order to give the reader a final overview of the work done. Furthermore, lessons learned and recommendations are exposed with the objective of helping in future or similar application.

Appendix

Here is possible to find support documentation concerning both analysis. In detail, it contains Labview Graphic User Interface (GUI) of both the tests, as well as Matlab and Simulink scripts.

Chapter 2

Engine Characterization

One of the most important tasks in the phase of making a design of an UAV is to properly select its propulsion system. The primary initial data should include application and requirements for a UAV. The type of a propulsion system is directly linked with tasks and aims which the designed unit will execute. Moreover, it is necessary to take into account the required payload, essential for carrying equipment [7]. After being selected, the system needs to be tested before being integrated on the aircraft. There are many objectives behind testing the propulsive system of an aircraft. The preeminent are listed below:

- Check the integrity and readiness of the system;
- Check the authenticity of the received data sheet;
- Check that there is no interference between the propulsive system and other on board systems;
- Make a Characterization of the engine if not provided by the supplier, or recheck the given one.

In general the first three points are mandatory steps before the first flight, and this because there is the risk of damaging the aircraft if there is any leak in the system. For example, an uncounted interference in terms of vibration might damage the structure of the plane if not detected before the flight. The same importance has the verification of the authenticity of the provided data sheet, mistakes may occur either from the supplier or from the customer interpretation.

Last but not least, there is the engine characterization. The latter consists of obtaining the characteristic maps and tables that best describe the "engineering" behaviour of the propulsive system. These characteristics might be for example, thrust to throttle map, the efficiency trend, or the presence of certain vibrations. The level of detail of the engine characterization may vary a lot, depending on how important and precise is the analysis. Furthermore, the type of required characteristic maps and output data differ from one type of engine to another.

This very important step is often bypassed using theoretical models obtained in different ways, such as statistical data, scaling from other characterized engines, or simply using provided maps from the furnisher. That happens typically because the engine characterization is time consuming, and requires effort and expenses that usually companies cannot guarantee. Nevertheless, it must be said that the

trendy approach is mostly that of combining both, the analytical model, and few performed tests, in order to get as close as possible to the desired results. This last approach is the one adopted by the Center for Aerospace Research, and will be addressed in the current dissertation.

2.1 Electric Ducted Fan (EDF)

2.1.1 Theoretical Overview



Figure 2.1: Propulsion systems for UAVs application.

Electric Ducted Fans (EDF) are widely used as propulsion systems in vertical and/or short takeoff and landing (V/STOL) uninhabited aerial vehicles (UAVs), and that because they offer a higher static thrust/power ratio for a given diameter than open propellers. Furthermore, due to operational requirements (LiPo batteries, constructive simplicity, high reliability) and the cost price, this type of motors are being increasingly used to power various types of unmanned aircrafts respect to small engine jet.

A peculiar feature respect to the open fans motors is also that of providing impact protection for the rotating blades and improve personnel safety due to the enclosed fan structure as well as the lower noise level in the plane of the rotating fan blade [8]. The scheme of a common EDF motor is given below in Figure 2.2.

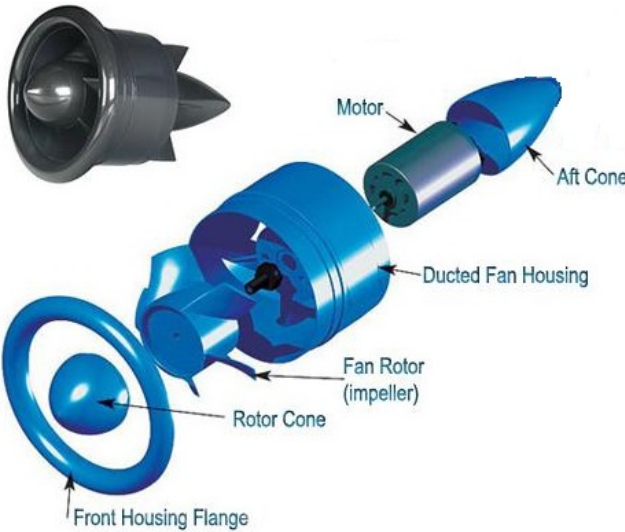


Figure 2.2: Electric Ducted Fan components.

The EDF propulsion concept is quite simple, and consists of an electric motor that drives an intubated (ducted) propeller. The intake air is compressed by the fan rotor, thus exhaust air has sufficient speed to power the UAV (Figure 2.3).

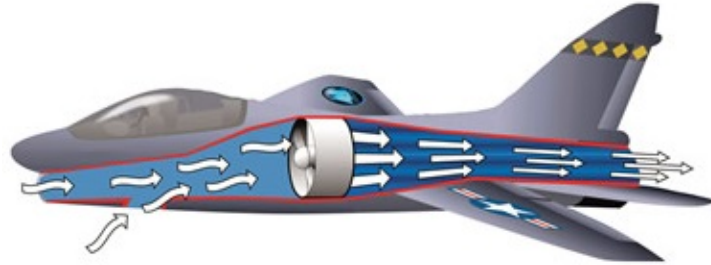


Figure 2.3: Electric Ducted Fan work principle.

The analytical approach of a 3-D rotor flowfield is pretty complex, and is quite often replaced by a simplified, inviscid actuator disk model. The latter is originated from the combination of the radial equilibrium equation, energy equation, and the conservation of angular momentum principle across the fan rotor. The first equation consists of the force balance in the radial direction at a given axial position, balancing the pressure forces in the radial direction with the centrifugal force. The following assumptions are made:

- The airflow is incompressible;
- The effective size of the EDF unit is determined by the Fan Swept Area;
- The ducts are frictionless (neglected boundary layer effect);
- Ducts can be assumed to be circular in cross section;
- Vorticity due to rotating parts is ignored;
- The bifurcation and joining of ducts can be ignored.

In this approach, a pressure change term is computed from the first principles at each radial position of the rotor from hub to tip. The magnitude of the static pressure jump term across the rotor is closely related to the amount of stagnation enthalpy change from the rotor inlet to exit. The stagnation enthalpy increase from the rotor inlet to exit is the same as the rate of energy provided to the fluid by the rotor per unit mass flow rate of the duct flow. The conservation of the angular momentum principle and energy equation suggests that the magnitude of this jump is mainly controlled by the tangential (swirl) component c_2 of the flow velocity in the absolute frame of reference at the exit of the rotor and rotor angular velocity (variables 1 and 2 are the blade inlet and exit angles measured from the axial direction). Since the tip Mach number of the rotor is designed not to be in the compressible flow range, it is reasonable to assume that the internal energy at the rotor inlet e_1 and exit e_2 is approximately the same, we can assume then

$$e_1 = e_2 \tag{2.1}$$

In a ducted fan rotor, it is reasonable to assume that the axial component of the absolute velocity vector is also conserved from inlet to exit ($c_{x2} = c_{x1}$), due to mass conservation considerations law. The flow is assumed to be swirl-free and axial at the rotor inlet where:

$$c_1 = c_{x1} \text{ and } c_{\theta1} = 0 \quad (2.2)$$

under design conditions. The relative velocity vector at the exit of the rotor w_2 is smaller than the relative velocity w_1 at the rotor inlet in a typical axial flow fan. While the relative flow w_2 is diffusing in the relative frame of reference, the absolute flow velocity vector c_2 is accelerated at the rotor exit because of added energy to the flow by the rotor.

Equation (2.3) represents the change of stagnation enthalpy (h_o)¹ in the ducted-fan rotor system. The right-hand side of this equation is the rate of work per unit mass flow rate of air passing from the rotor.

The right-hand side is also the same as the product of the rotor torque and angular speed of the fan rotor:

$$h_{o2} - h_{o1} = U (c_{\theta2} - c_{\theta1}) \quad (2.3)$$

where

$$U = \Omega r \text{ and } c_{\theta1} = 0 \quad (2.4)$$

which can also be written as:

$$\left(h_2 + \frac{c_2^2}{2} \right) - \left(h_1 + \frac{c_1^2}{2} \right) = U c_{\theta2} \quad (2.5)$$

$$\left(e_2 + \frac{p_2}{\rho_2} + \frac{c_2^2}{2} \right) - \left(e_1 + \frac{p_1}{\rho_1} + \frac{c_1^2}{2} \right) = U c_{\theta2} \quad (2.6)$$

Equation (2.3) is a simplified form of the energy equation and angular momentum conservation (combined) expressed from rotor inlet to exit of a ducted-fan unit. When $e_1 = e_2$ is substituted into Eq. (2.6) because of the assumed incompressibility condition, the Euler equation results in Eq. (2.7):

$$\frac{1}{\rho} (P_{o2} - P_{o1}) = U c_{\theta2} \quad (2.7)$$

Equation (2.7) could be rearranged as follows:

$$\left(p_2 + \rho \frac{c_2^2}{2} \right) - \left(p_1 + \rho \frac{c_1^2}{2} \right) = \rho U c_{\theta2} \quad (2.8)$$

Using Eqs. (2.7) and (2.8), an equation for the calculation of the static pressure jump between the rotor inlet and exit can be obtained:

¹ Stagnation enthalpy is the enthalpy of a flow at a stagnation point. It is the enthalpy at a stagnation point if the flow is brought to a stop from velocity v_1 . Total enthalpy h_t instead, is defined at every point in a flow field but stagnation enthalpy is only defined at a stagnation point. Total enthalpy is the same at every point in a flow field so the enthalpy at a stagnation point is numerically equal to the total enthalpy everywhere in the flow field.

$$\Delta p = p_2 - p_1 = \rho \left[U c_{\theta 2} - \frac{1}{2} (c_2^2 - c_1^2) \right] \quad (2.9)$$

Equation (2.9) allows the enforcing of a prescribed pressure jump p in the function of density, radial position, rotor angular speed, rotor exit swirl velocity $c_{\theta 2}$, c_1 , and c_2 . The rate of energy per unit mass flow rate added to the flow by the rotor is specified by the product $U c_{\theta 2}$, as shown in Eqs. (2.7) and (2.8). Equation (2.9) could be evaluated at each radial position between the rotor hub and tip, resulting in the radial distribution of the static pressure jump required by the general purpose viscous flow solver for a so-called fan-type boundary condition.

The "efficiency" of the fan is the nearness to which the energy required is matched by the energy provided, or $Efficiency = P_{flight}/P_{fan}$. As a percentage this is usually around 80%. The Power required from the motor, P_{motor} , also depends on the losses in the system due to friction in the duct, restrictions in the geometry of the duct and so on. Klaus Scharnhorst assumes (from an analysis of pipe flow theory, etc..) that $P_{motor} = P_{fan}/0.85$ is a reasonable approximation [9]. The efficiency of the motor is therefore:

$$Efficiency(motor) = \frac{P_{fan}}{P_{motor}} = 0.85 \text{ approx.} \quad (2.10)$$

After giving a theoretical model, it is time to take a look to the advantages and limitations of this type of technology. A list of prevalent lineaments is given.

Advantages :

- EDF unit does not need electricity fuel tanks and ignition systems (pipes, spark plugs, throttle servo), so easier to build;
- Since an electric motor does not get nearly as hot as a jet engine, the materials used do not have to tolerate high temperatures. This enables the use of more composites that may have more favorable mechanical properties than metal alloys;
- Ducted fans are quieter than propellers: they shield the blade noise, and reduce the tip speed;
- Power to weight ratio is generally higher than gas turbine engines;
- Thrust to weight ratio is generally higher than gas turbine engines;
- Dimensions are smaller wrt to open propellers;
- Ducted fans offer enhanced safety on the ground with respect to open propellers.

Drawbacks:

- Power source (LiPo batteries) specific energy very low respect to fuel based engines. This means that as the required power increases, the weight of batteries to carry on board increases drastically;
- Less efficient than a propeller at cruise (at lower thrust levels in particular);
- Requires high RPM and minimal vibration;

- Complex duct design (risk of stagnation) [10][11] [12].

2.1.2 Characterization of an EDF

The type of required characteristic maps and output data differ from one type of engine to another. The main researched curves during the characterization of an EDF motor are:

- Thrust curve known also as "performance curve", that shows the variation of the thrust through time;
- Thrust to throttle curve that shows the variation of the Thrust as a function of the commanded throttle;
- Thrust to RPM curve, that is quite similar to the previous one, having as x-axes the revolutions per minute instead of the command;
- Torque to RPM or to throttle curves;
- Consumed power with respect to time or to RPM;
- Efficiency curves.

The analysis might go deeper researching more detailed features such us: the aerodynamic behaviour of the fan and the casing of the ducted fan, as well as checking if there is any suspected vibration due to rotor imbalance. Some examples of EDF characterization outputs are given in Figure 2.4.

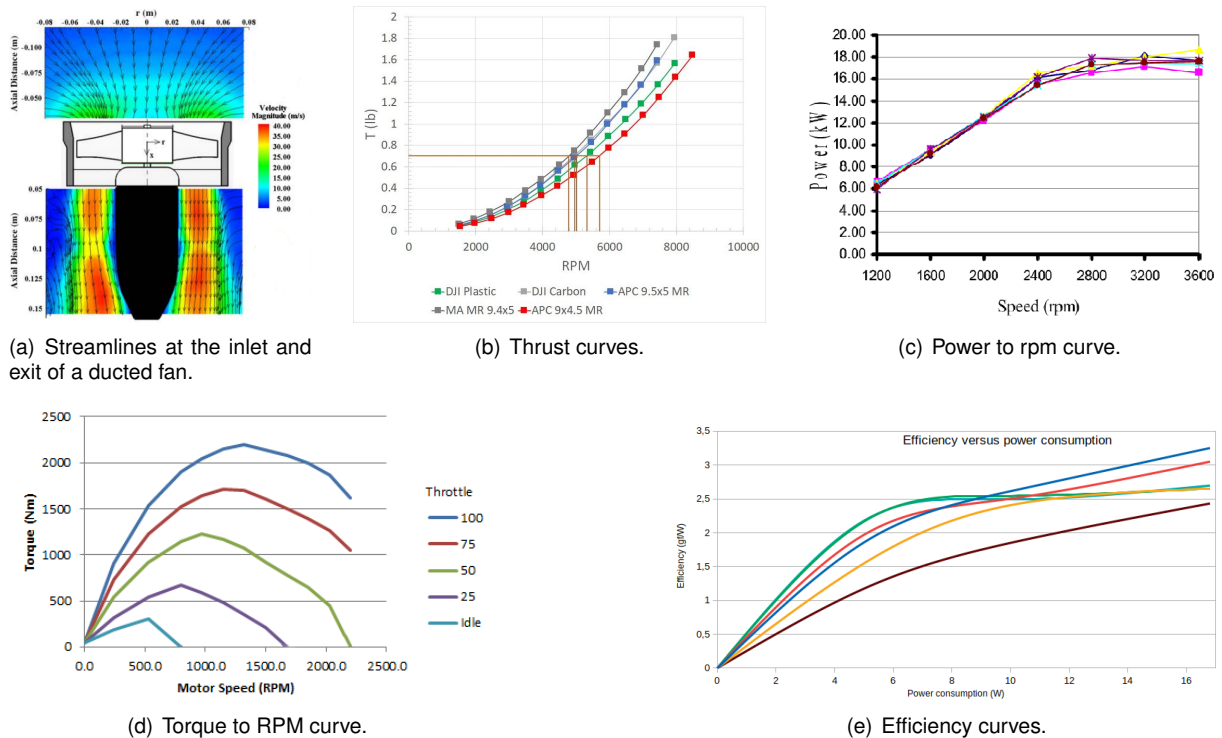


Figure 2.4: EDF characterization outputs.

All these tests and analysis are performed in base on the level of detail of the approach adopted. Anyhow, regardless the grade of detail, the analysis must be performed very carefully since the resulting model will be then implemented on the UAV's autopilot, therefore will be the reference for the autopilot maneuvers.

2.2 Gas Turbine Engine

2.2.1 Theoretical Overview

The gas turbine engine is compact, has a light weight and can operate using multiple fuels. This makes gas turbine engines suitable for many aerospace and industrial applications. The economics of power generation using gas turbine engines depends on the fuel cost, running efficiency, maintenance cost, and first cost, in that order [13].

The simple cycle of a gas turbine engine, known also as a Bryton cycle, consists of a compressor, combustor and turbine (Figure 2.5). The compressor is used to increase the pressure of air before combustion, thus allowing burning more fuel and getting more power from a plant of the same size. The combustor is used to add energy to the flow, while the turbine is used to drive the compressor as well as external load. The performance of this cycle can be improved further by different techniques such as intercooling the air during the compression process or reheat the fluid during the expansion in the turbine. There are also other means to improve the cycle performance, but all of these techniques have lateral drawbacks (extra weight, expensive, high-tec required etc.) which make them suitable only for certain kind of circumstances [14]. As well as in the case of EDF motors, an analytical approach of the

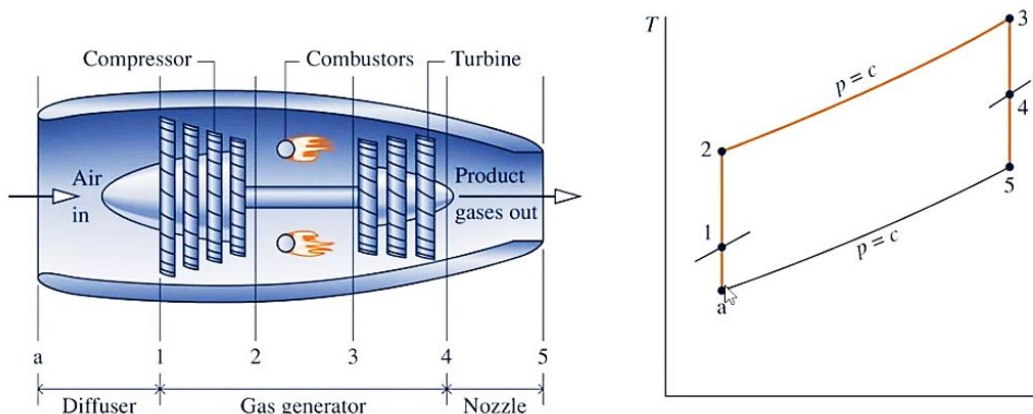


Figure 2.5: Schematic diagram of a Gas Turbine.

dynamics of a gas turbine engine is quite complex, therefore a simpler model will be adopted following the work performed by Rahman and Whidborne from Cranfield University [15].

In order to simulate a dynamic system, it is important to specify a set of minimum number of variables or states (X) that completely define the system dynamics. This was defined as $X(P_3, P_5, N)$ with an initial condition of $X_0(P_{3,0}, P_{5,0}, N_0)$, while the respective variation in time is expressed as $\dot{X}(\dot{P}_3, \dot{P}_5, \dot{N})$. Starting from ambient conditions (P_0, T_0, M_0) and considering that the engine is static (like in ground

testing condition, i.e. M_0), and assuming the flow process to be adiabatic, the equations are:

$$\frac{T_1}{T_0} = 1 + \frac{\gamma - 1}{2} M^2 \quad (2.11)$$

$$\frac{p_1}{p_0} = \left(\frac{T_1}{T_0} \right)^{\frac{\gamma}{\gamma-1}} = \left(1 + \frac{\gamma - 1}{2} M^2 \right)^{\frac{\gamma}{\gamma-1}} \quad (2.12)$$

The total temperature (T_1) represents the rise in temperature by bringing air molecules travelling at Mach number (M) to rest at the intake face. The total pressure at the intake face is a function of temperature ratio and is given by equation (2.12). Since no energy is added in the intake, the total temperature remains constant [16]. However, there is a loss in total pressure as the flow passes through the intake and this pressure loss is a measure of intake efficiency (η_I). Therefore, the intake exit conditions are:

$$T_2 = T_1 \quad (2.13)$$

$$p_2 = \eta_I p_1 \quad (2.14)$$

Moving into the compressor, it was assumed that the flow was adiabatic and non-reversible. The two typologies of compressors commonly used in turbojet engines are axial and centrifugal (Figure 2.6). The axial compressor directs the air flow parallel to the rotational axis whereas the centrifugal design directs the flow radially outward, perpendicular to the rotational axis. Small gas turbines, that produce less than 5 MW, are often designed around centrifugal compressors. Although these are less efficient than multi-stage axial compressors, centrifugal compressors are reliable and able to produce higher pressure ratios with a single stage than axial ones. Regardless of the exact geometry in the centrifugal



Figure 2.6: Typical compressors configurations in Gas Turbines.

compressor, the purpose is to redirect the air radially along the axis of rotation. Air flows along the blades of the compressor and is sent out in the radial direction by centrifugal force. The high-speed air accelerated by the compressor then enters the diffuser stage of the engine. The increase in pressure across the compressor is accompanied by increases in temperature and enthalpy. Change in enthalpy across an adiabatic compressor can be defined by:

$$\Delta h = TC_p \left(\left(\frac{p_3}{p_0} \right)^{\frac{\gamma}{\gamma-1}} - 1 \right) \quad (2.15)$$

This increase in enthalpy is proportional to the input power received from the turbine to the compressor, which can be seen in the following expression:

$$P = \frac{\dot{m}\Delta h}{\eta} \quad (2.16)$$

From empirical data and computer simulation, performance of a compressor can be represented by compressor maps. These charts plot performance characteristics of a compressor in order to understand the compressors' capabilities. Typically, mass flow rate and pressure ratio are plotted, although sometimes rotations per minute (RPM) or efficiency are seen. An example is presented below.

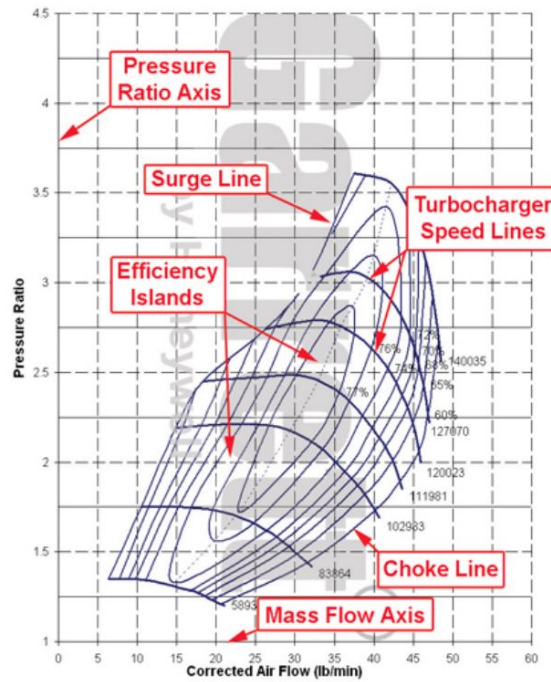


Figure 2.7: Typical compressor map.

The purpose of the next stage, the combustor, is to increase the flow temperature. This occurs through the release of energy from the combustion reaction which takes place thanks to the introduction of fuel. The difference downstream and upstream of the combustor can be evaluated starting from the energy conservation equation, which states that the total enthalpy variation is equal to the heat supplied to the flow, since the work carried out from outside is null. The enthalpy balance referred to the unit of time is written:

$$\dot{m}_a h_3 + \dot{m}_f h_f + \dot{Q} = (\dot{m}_a + \dot{m}_f) h_4 \quad (2.17)$$

The manipulation of the equation becomes particularly simple if is adopted the approximation that combustion flow rate is negligible compared to that of air . This hypothesis is in general reasonably verified in the turbojets, where to keep the temperature T4 within values acceptable to the structure of the turbine, an amount of air higher than the minimum quantity required for combustion is processed. The equation becomes:

$$\dot{m}_a h_3 + \dot{Q} = \dot{m}_a h_4 \rightarrow \Delta h_{34} = \frac{\dot{Q}}{\dot{m}_a} \quad (2.18)$$

that could be written also as:

$$\dot{m}_a c_p (T_4 - T_3) = \dot{Q} \quad (2.19)$$

having considered the c_p of air constant through the combustor.

The next stage is represented by the turbine. The role of this unit is that of providing the required power to run the compressor. The dynamic equilibrium between the two components requests that the power generated by the turbine is equal to that absorbed by the compressor. Skipping all the algebra in this phase, the result expressed as:

$$\Delta h_{45} = (h_4 - h_5) = \frac{\alpha (h_3 - h_2)}{\alpha + 1} \quad (2.20)$$

where $\alpha = \dot{m}_a / \dot{m}_f$.

From empirical data and computer simulation, likewise the compressor, performance of a turbine can be represented by turbine maps. These charts plot performance characteristics of a turbine in order to understand the component's capabilities. Typically, mass flow rate and pressure ratio are plotted, although sometimes rotations per minute (RPM) or efficiency are seen. An example is presented below:

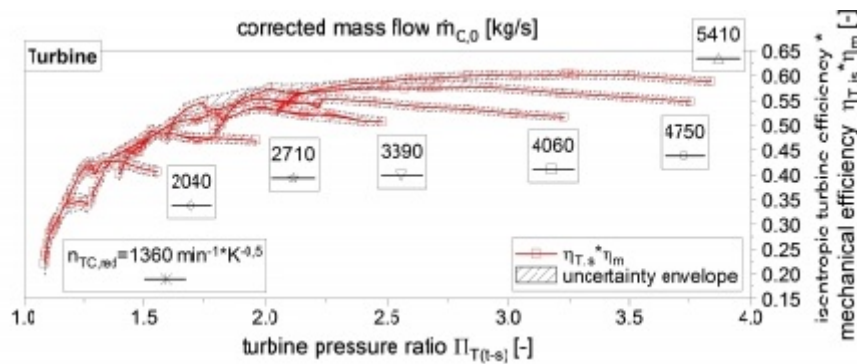


Figure 2.8: Typical turbine map.

equation

The last component is the Nozzle. In this phase the total enthalpy of the flux is considered constant since there is no work or heat added. The gas is therefore accelerated converting part of the enthalpy from pressure to velocity. This is simply expressed in terms of temperatures, and that is possible after converting the pressure in temperature through the isentropic equation ²:

$$T_{9'} = T_5 \left(\frac{p_9}{p_5} \right)^{\frac{\gamma-1}{\gamma}} \quad (2.21)$$

The real temperature considering the friction of the duct is:

$$T_9 = T_5 - \eta_n (T_5 - T_{9'}) \quad (2.22)$$

²This assumption is not truly valid since there is dissipation due to nozzle's wall friction. However, that can be bypassed introducing the efficiency of the nozzle η_n to pass from ideal $T_{9'}$ to the real one T_9 .

Now, since the thrust is generally expressed as :

$$F = \dot{m}_e u_e - \dot{m}_0 u_0 \quad (2.23)$$

is useful to obtain the expression for the exhaust velocity u_e . That proceeds from the conservation of energy between after turbine and exit (stage 5-9). The exhaust velocity is hence:

$$u_e = u_g = \sqrt{2c_{pg} (T_{t5} - T_9)} \quad (2.24)$$

Looking at the parameters that best describe the performance of a turbo jet, the main ones are :

- Specific Thrust (I_a):

$$I_a = \frac{T}{\dot{m}_a} \cong u_e \quad (2.25)$$

- Thrust-specific fuel consumption ($TSFC$):

$$TSFC = \frac{1}{\alpha I_a} \quad (2.26)$$

2.2.2 Gas Turbine Engines for UAVs Propulsion

Development of Micro Turbine Engines (MTEs) began from attempts of application of that propulsion source by group of enthusiasts of aviation model making. Nowadays, the domain of micro turbojet engines is treated on a par with “full size” aviation constructions. The dynamic development of these engines is caused not only by aviation modellers, but also by use of micro turbojet engines by army to propulsion of contemporary drones, i.e. Unmanned Aerial Vehicles (UAV) or Unmanned Aerial Systems (UAS) [17].

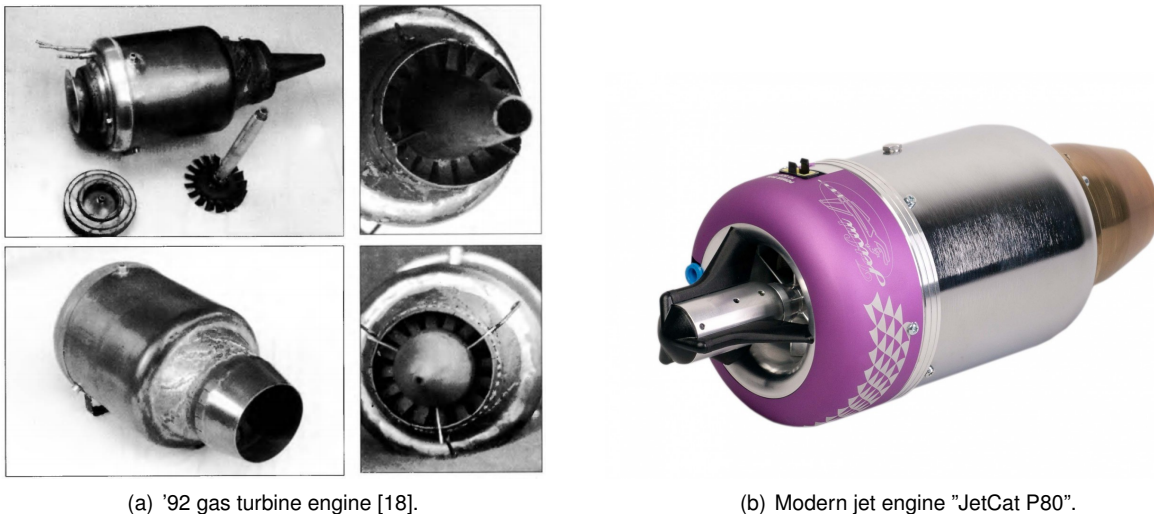


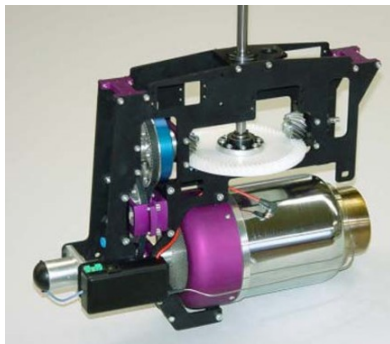
Figure 2.9: Old and modern micro turbine engines.

On the base of market demand, numerous companies specialized in the manufacturing of different kinds of micro turbine engines. There are several concepts of construction of these engines depending

on the custom demands and available technology.

It is possible to distinguish several types of MTEs taking into account their construction and destination:

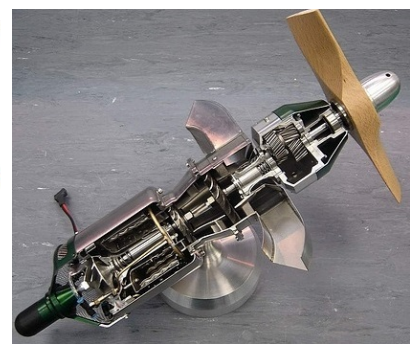
- turbojet MTE applied for propulsion by use of a thrust exclusively. There are two types of MTEs in this case:
 - with radial compressor and radial turbine;
 - with axial compressor and axial turbine (generally still experimental ones).
- turboshaft MTE applied for propulsion by use of the mechanical torque (power) delivered to the engine shaft (spool). In this case one can distinguish two kinds of construction:
 - single spool (single shaft) engines with gear box used for propulsion of helicopter drones;
 - two spool (dual shaft) engines for turboprop and helicopter aircraft drones.



(a) Single shaft MTE with gear box used for propulsion of helicopter.



(b) MTE with axial compressor.



(c) Single shaft MTE engine with gear box used to drive a propeller.

Figure 2.10: Some arrangements of MTEs.

Moving the attention toward the performances of these little engines, they present numerous advantages, but at the same time some deficiencies. The principal ones are listed below.

Advantages:

- high energy density potential of the fuel-based systems. Even with relatively low overall system efficiency the power per unit of weight of a gas turbine system will be much higher compared to existing or in the near future available batteries thus reducing the overall system weight significantly for missions requiring a high power output and a long duration.
- Increased Operational Flexibility with respect to battery based systems;
- Possibility to use composite fuel tanks that decrease the system weight;

Drawbacks:

- High overall temperature of the system, that is even further aggravated by the high temperature of the exhaust gasses;
- Contamination due to exhaust gases;
- Safety issues. A MTE based system has more hazards than and electric one [19].

2.2.3 Characterization of a Micro Turbine Engine

The market for the small-scale micro gas turbine is expected to grow rapidly in the coming years. Principally, employment of commercial off-the-shelf components is rapidly reducing the cost of ownership and maintenance, which is paving the way for vast use of such devices. However, to meet the high-reliability requirements of the similar big scale engines, there is an acute need of continue testing and data collection in order to have an accurate characterization of the unit. This because, although the rapid spreading, the statistic data of this tiny devices is still poor with respect to their ancestors.

The typology of required characteristic maps and output data, as it was mentioned above, differ from one type of engine to another. MTEs share some similarities with EDF motors, but at the same time there are dominant differences that affect testing approach. The common outcomes from a Jet engine characterization are disposed below with some examples in Figure 2.11 .

- "Performance curve", that shows the variation of the thrust through time;
- Thrust with respect to throttle curve and the inverse curve ;
- Thrust with respect to RPM curve and rhe inverse that are quite similar to the previous one, having as x-axes the revolutions per minute (RPM)instead of the command;
- Torque with respect to RPM (or to throttle);
- TSFC with respect to time (or to RPM);
- Specific thrust curves;
- Exhaust Gas Temperature (EGT) to RPM (or to throttle);
- Efficiency curves;
- Thermal analysis either through sensors or Thermal cameras;
- Vibration analysis;
- Wind tunnel analysis for further aerodynamic mapping.

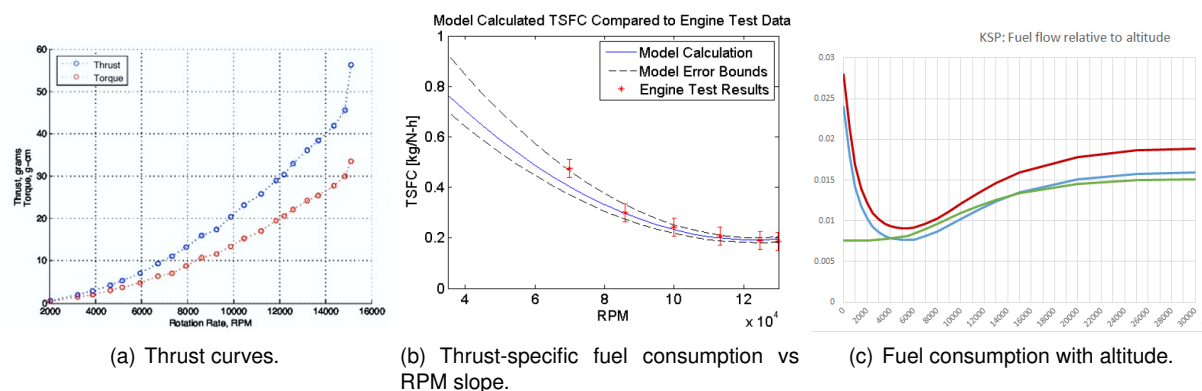
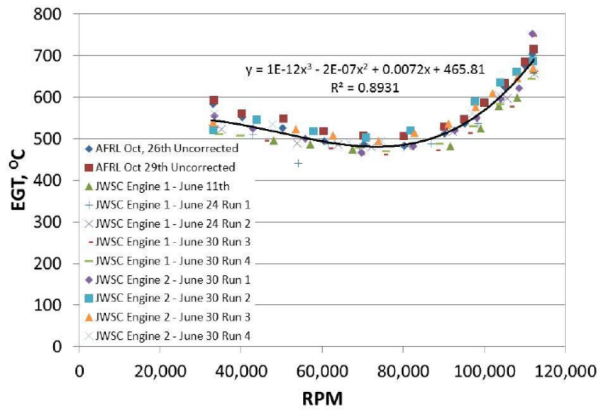
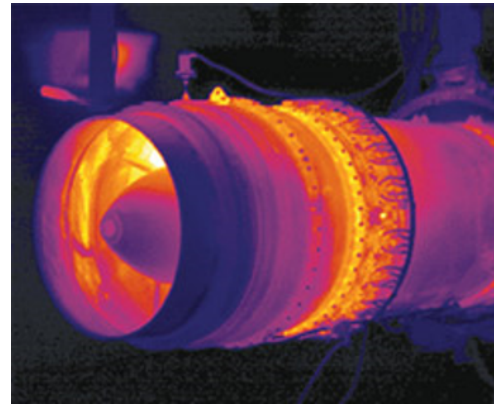


Figure 2.11: Gas turbine characterization outputs.



(a) Exhaust gas temperature to RPM curve.



(b) Thermal camera image during testing.

Figure 2.12: Gas turbine Thermal characterization.

The total or partial performing of the mentioned tests is always up to the enterprise disposable income and time. Once again, it must be underlined that all these tests and analysis intended to be done, regardless the grade of detail, must be performed with a high grade of attention and accuracy since the resulting model is often addressed to be applied on UAV's autopilot. Discrepancies in the model may cause catastrophic failures.

Chapter 3

EDF Testing

The aim of this work is to analyze the performance of the propulsion system of the FTV7%. The best way to achieve that is through test the main components of the system itself. As shown in Figure3.1, the 7% scale model mounts a pair of Electric Ducted Fans (EDFs) in the back of the aircraft . These have the objective of providing the required power during the flight, interfering the less possible with the other systems on board.



Figure 3.1: BWB EDF motors.

The selection of the propulsive system has been done during the design phase, and the chosen one was a pair of "Schubeler" EDF motors. These motors are known for their high performance and reliability, however, it's good practice to test them on ground before proceed with fly tests. Furthermore, tests are required also to obtain the accurate performance maps that return useful setting up the propulsion system model for the autopilot. Unfortunately, the latter phase has been omitted due to lack of time, and the flight tests have been made so far counting on a well done theoretical model. Luckily no catastrophic damage occurred so far, and the adopted model is showing high reliability. Nevertheless, in recent flights they have been noticed some abnormalities in the engines response, and these have been traced to the presence of inaccuracies in the model. All this lead to an necessity to accomplish finally a detailed

engine characterization in order to refine the present model.

The EDF's characterization is intended to be done in steps, since the test flights cannot be interrupted (due to tight deadlines), thus the model will be updated time after time. In this chapter will be shown a detailed experimental design and development of the tests on one of the EDF motors. An initial description of requirement list, useful to define the framework under which the tests will be executed, is followed by the analysis and explanation of all the fundamental achievements.

3.1 Schubeler DS-51-AXI

As previously mentioned, electric ducted fans (EDFs) have been chosen as mean to power the FTV7%, and this thanks to their blade design that is able to provide the propulsion necessary to give enterprise UAVs liftoff. The choice fell on Schübeler models, a well known company for the production of high-quality electric propulsion systems for aeromodelling. The house is leader in its sector, and can boast a solid track record in providing the highest quality systems available on the market [20].

The chosen model for the FTV7% is the "Schubeler DS-51-AXI" (Figure 3.2), and its main features are given in Table 3.1.



Figure 3.2: Schubeler DS-51-AXI.

Parameter	value	unit of measure
Max. RPM	45	1/min
Max. Power	4,27	W
Max. Thrust	55	N
Max. Exhaust Speed	95,6	m/s
Weight	114	g
Max. Motor Diameter	39	mm
Shaft Diameter	5	mm

Table 3.1: EDF parameters.

The performances of the motor itself are excellent, and the advantage of being an electric engine allows that casing could be made of composite material, and thus, to be light weight. So far it has been working properly, although a little drawback came out. Since the FTV7% is mounting a pair of engines, the best way to balance the torque produced by each engine would be that of having counter-rotating engines, that is not possible with this motors. Schubeler EDFs have the defect to rotate only one way, counterclockwise, and this creates an unsolicited unbalance, that need therefore, to be corrected continuously by the autopilot.

3.2 Objectives and Functional Requirements

The functional requirements were derived from the guidelines given by the engineer Stephen Warwick, Operations and Control/Instrumentation Lead at UVic Center for Aerospace Research (CfAR). The investigation focused on the listed tasks:

- Calibrate the ESCs ;
- Perform Thrust tests for engine mapping;
- Test the new LabVIEW GUI;
- Test the new cRIO data acquisition device;
- Investigate any anomaly encountered.

Unfortunately, the third and fourth tasks were not performed either due to lack of time, but mainly due to the detection of abnormal vibrations, which obviously took time to investigate. These have been carefully studied to discover the source, but also to check if the vibrations are somehow connected to others detected during flight tests.

3.3 Previous Work

This following analysis has the intention of continuing and help in upgrading what has already been done before. As mentioned above, there is already a current model that try to represent the behaviour of the propulsive system of the FTV7%. The latter have been developed in 2018 given the necessity to start flight tests at the end of the same year. The author of this model is Jenner Richards, former engineer at CfAR, and the subsequent description of the model is made adhering to the documentation he made [21].

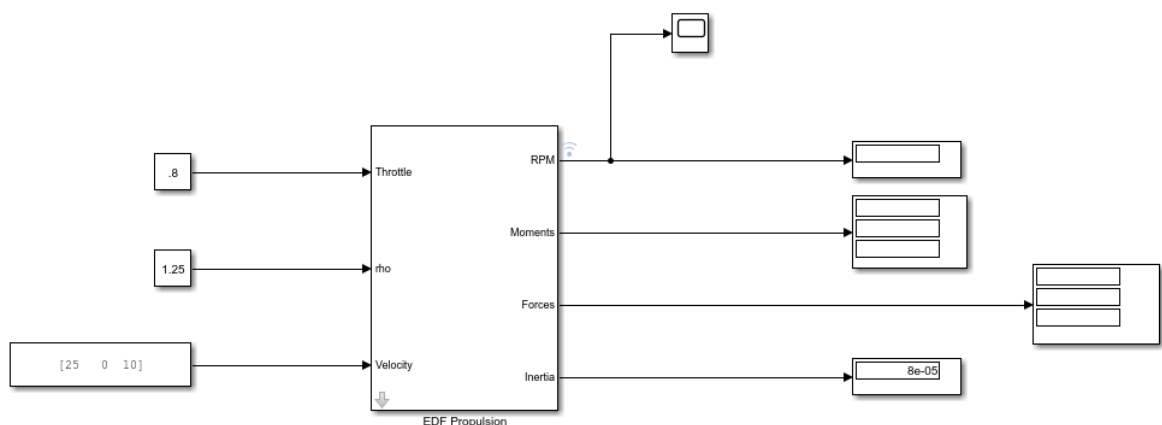


Figure 3.3: Example Implementation of Block Flying at 80% throttle, SL, 25m/s.

The EDF propulsion block (Figure 3.3) is used to model the forces on an aircraft due to an Electric Ducted Fan (EDF) and simplified battery model. The block represents a single EDF, so in the case of

the FTV7% model two would be required to simulate both engines. The diagram above represents the supplied model with some test inputs and outputs designed for trouble shooting where is possible to distinguish constants for inputs, scopes and displays on outputs.

The battery model is extremely simplified and uses a voltage based on a nominal cell voltage and the number of cells. The voltage drop under loading is caught using an internal battery resistance, but the battery discharge curve is not accounted. There is also no calculation of batteries mass or relative inertias, so the combined effects of the EDF/battery mass properties will need to be calculated and taken in consideration for elsewhere in the overall aircraft model.

Looking at the outputs, the block will be able to calculate the following:

- overall forces and moments in body axes based on the throttle setting;
- air density;
- aircraft velocity.

The moments only include those resulting from the blades rotational velocity, and don't account for gyroscopic effects. The EDF direction is taken in concern and can be changed in the parameters tab of the block mask. Forces are calculated from lookup tables for the EDF supplied by the furnisher (Schubeler), and 3 motor constants supplied by the manufacturer of the electric motors.

The main inputs and outputs of the block diagram are given in the tables below.

Table 3.2: Block Inputs.

Port Name	Units	Description
Throttle	n/a	Throttle fraction setting from 0-1
rho	kg/m ³	Air density
Velocity	m/s	3x1 vector of velocity components in body axis

Table 3.3: Block Outputs.

Port Name	Units	Description
RPM	Rev/sec	RPM of the EDF at curret time step
Moments	kg/m ³	Vectort of moments acting on the aircraft [3x1] in body axes.
Forces	m/s	Vector of forces acting on the aircraft [3x1] in body axes.
Inertias	Kgm ²	This is the sum of the EDF fan and motor inertias and does not account for the battery inertias. The overall mass and inertia effects are included in aircraft mass properties supplied from bifilar pendulum tests, thus this port will likely not be of any practical use in the overall simulation.

Furthermore, there are also block's mask parameters, which are indispensable to run the simulation. These will not be presented in this discussion, nevertheless the reader could find them easily in the *Appendix A* .

Another significant heritage from past years is represented by the LabVIEW GUI "THRUST-TORQUE TESTER.vi". This graphic interface is an important mean for testing, although it is not complete yet, and need further refinement. The cited GUI consists of a control panel that allows to send commands to the

test rig components, and at the same time to show and record data obtained from the Data Acquisition system. The main screen of this interface is shown in Figure 3.4.

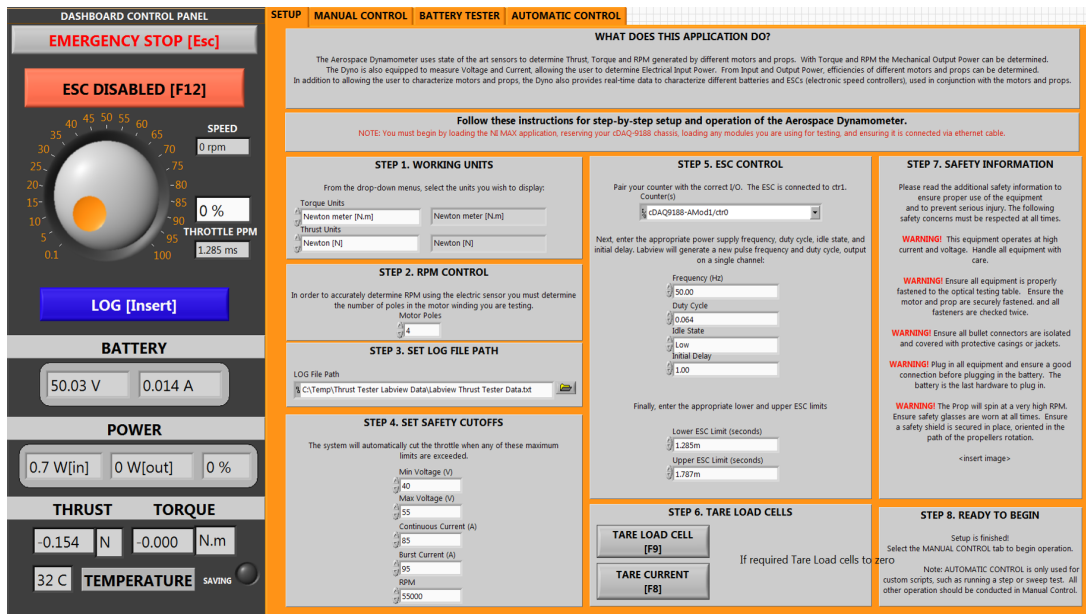


Figure 3.4: "THRUST-TORQUE TESTER.vi" interface.

3.4 Test Rig Design

The test bench must be designed so that it is possible to accurately characterise different types of UAV engines, and it is good practice if it could accommodate both electric motors and tiny internal combustion engines. However, here in CfAR it has been chosen to test the electric motors inside the shop, therefore no tests with internal combustion engines are allowed. Regardless the kind of engines in question, the test rig must be portable and simply installed to simplify assembling/disassembling, as well as storage of the components. At last, it must be said that output parameters of the test have always a direct dependency on the set installed in the test bench, and this reflects clearly on the design .

Since the requirements involve forces and momentum detection, the engine mount must be quite robust, even more so if tests are executed indoor. The Rotational Speed is another parameter to be detected. This depends only on the engine/motor involved in testing, however rotation devices induce always vibrations, reason why the test mount must be fixed and safety proof in case of any resonance phenomena. Temperature is not a big issue regarding the EDF motor, but the overheating of both ESC and batteries must be taken in consideration.

After discussing all these points with the rest of the team, it has been decided to use the same test stand used for a previous work. The stand was used to test a propeller driven by an electric motor with same power range of Schubeler EDF motor.

As first thing, it has been verified that the stand respects all the mentioned requirements, and it was found that the only modification that need to be done, was on the engine mount. To perform a more accurate testing it was found preferable to design and 3D print a mount that contains the shape of FTV7%

nacelles. The mount is shown in Figure 3.7 , while the remaining components and relative details will be introduced later in section 3.6.



Figure 3.5: EDF test rig.

3.4.1 Software Design

Recently, the software interface became a mandatory component of any engineering set up. The Graphic User Interface chosen was the same used in the previous, but with slight modifications. This LabVIEW interface inherited from previous engineers at CfAR had some little bugs and inaccuracies. During the readiness phase some of these failings have been fixed, but not all of them. One in particular is noteworthy because was considered a potential hazard. The program permits to control the throttle of the engine sending signal to the ESC, and the latter in turn to the EDF motor. The problem lies in the fact that it was possible to switch directly from 0% throttle to 100% using the knob shown in Figure 3.6. This capacity of passing instantly from engine off to engine at full power is very dangerous, and had to be fixed before start testing the motors. Luckily it was solved in few days, and no such problems occurred during the tests.

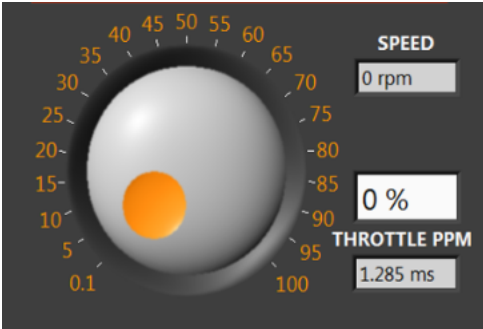


Figure 3.6: LabVIEW GUI knob.

During the tests though, some vibrations have been detected, and this lead to a need of studying the phenomena. The best way was that to use piezoelectric accelerometers, and customize both the data acquisition system, and the LabVIEW interface. Nevertheless, leak of time brought to carry the analysis

using the torque load cell data to analyze the vibrations. Before start working on the logged data, it was necessary a little modification to the program. The first version of the GUI contained a filter that records 1 sample each 1000 through using some filters. These have been removed in the last parts of the tests in order to perform at least four tests logging all the data that the load cell detected.

3.4.2 Test Planning

The objectives of the tests have been already shown in section 3.2. Is important to underline that before start programming all the tests, it has been done a review of the already made test card ², in fact safety procedures are part of test design, and it has been always a priority for CfAR .

The time has come to give a detailed outline of the tests that this investigation aims to accomplish. Here there is a list of how tests have been organized:

- Test the ESC device to find the higher and lower limits in milliseconds.

The tests consist of sending different signals to the motor from the GUI, and check for which value the device trills two times. This sound indicates that the ESC is ready to send the command to run the engine. The test are repeated two more times to be sure that is being registered the correct values.

- Test the EDF motor for Thrust mapping.

The tests consisted in a first one to check the integrity of the test stand, and the response of the other devices as well as to check if data is being recorded by through LabVIEW program. Subsequently the test have been split in four sets:

- 2 tests with 20% throttle steps with same set of battery³;
- 2 tests with 10% throttle steps in same conditions as the above one;
- 2 tests one with 10% and other with 20% using same battery;
- 2 test similar to previous but inverting the order.

The purpose from this partition is to avoid inaccuracies due to battery discharge, and limit the dependence of the testing from batteries behaviour.

Moving forward with testing, some abnormal and notable vibrations have been detected. This made be mandatory an analysis of the phenomena, but did not affected the planned tests, except for the modifications to LabVIEW program as mentioned in section 3.4.1.

²The test card is a checklist that must be compiled by at least two people before start running the tests.

³For each of the mentioned tests, the set of battery was checked to be sure that they are fully charged.

3.5 Experimental Set Up

After planning everything, and purchasing all the missing components, it was time to finally set up the test bench. The installation of all the components was done on one of the available optical tables at CfAR's shop. It was chosen to do that since the surfaces of these tables are designed to be very rigid with minimum deflection so that the alignment of the elements remains stable over time in addition to limiting vibrations.

The arrangement of the different components was easily accomplished thanks to the video guide made by CfAR in the previous year. Following step by step all the instructions, the test rig was ready in just a pair of days. Moreover, it is noteworthy that all the components have been tested one by one during the assembling, and no trouble occurred, except for a little wiring that have been fixed within few hours.

All the components of the test bench will be now presented.

Engine Mount

The engine mount consists of a vertical aluminium bar covered by plastic layer, that plays the role of keeping the EDF motor fix on its top. The mounts includes other two devices in addition to the engine., and these are: a Force load cell and a Torque load cell. The two load cells are connected to the other components through wires that pass inside the vertical beam, and exit from the bottom. EDF's wiring instead, are exposed. The scheme of the mount is given in Figure 3.7.



Figure 3.7: EDF mount.

Electric Speed Control (ESC)

An electronic speed control or ESC is an electronic circuit that controls and regulates the speed of an electric motor. It may also provide reversing of the motor and dynamic braking. Miniature electronic speed controls are used in electrically powered radio controlled models [22].

The model chosen by CfAR designers to be mounted on the FTV7% is the "Castle Phoenix Edge 120 HV" (Figure 3.8). Since the latter needs to be tested before go on board, it took part in all the performed tests. The device have been located between the EDF motor and the power box (will be introduced in the next part).

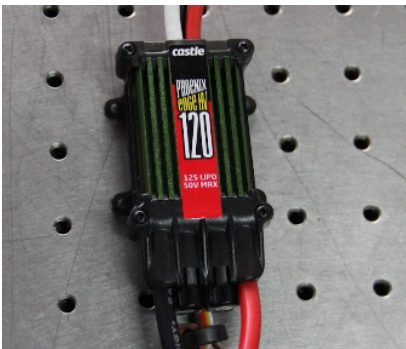


Figure 3.8: Castle Phoenix Edge 120 HV.

Specifications	
Input Voltage	3S-12S LiPo
Max Continuous Current at Full Throttle	120 A
Max Voltage	50.4 V
Dimensions	50.8 x 83.6 x 23.2 mm
Weight	148.8 g

Table 3.4: ESC parameters.

Power box

It was previously said that the EDF mount has two sets of cables in output: a set from the load cells, and the other from the EDF motor. Both wiring are then connected to the so called "power box" (Figure 3.9), although the EDF motor is connected first to the ESC device, as mentioned above, and then to the power box. This device is a pure production of CfAR engineers, and it has been modified several times based on the requirements. The apparatus is used mainly to supply and manage the electric signals going to the downstream devices (in this case towards EDF motor and load cells).

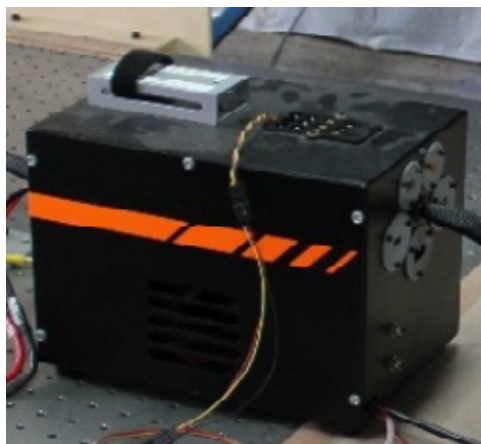


Figure 3.9: CfAR customized power box.

The CfAR power box is able to send different types of signals, with different frequencies, amplitude, analog or digital, periodic or aperiodic etc. After sending the desired command from the GUI, the power box processes it, and send it in turn to the wired devices. Furthermore, the device can take signals in input from the same downstream devices, and send them to the data acquisition system that in turn will communicate with the graphic interface.

Data acquisition system

Data acquisition is the process of sampling signals that measure physical parameters and converting the resulting samples into digital numeric values that can be manipulated by computer programs. The data acquisition system selected to detect the desired measurements is represented by National instrument devices (Figure 3.10). The choice was not that hard since the well known high-tec house has always demonstrated high reliability, and most of CfAR projects were performed counting on these devices.

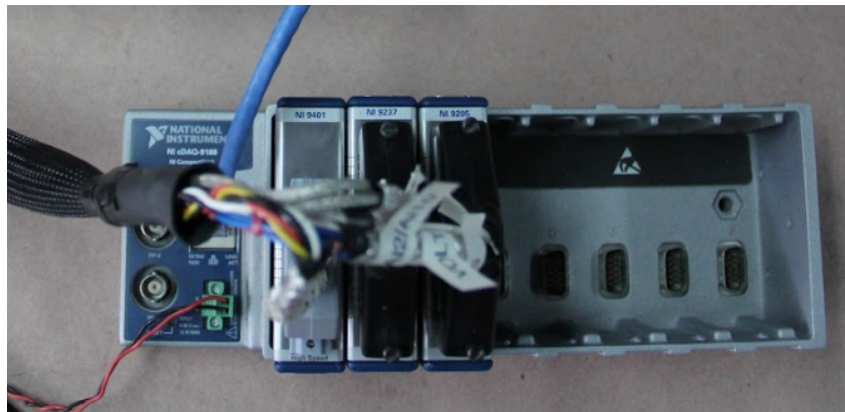


Figure 3.10: NI data acquisition devices.

Figure 3.10 shows the NI data acquisition system used for testing, while below are listed the elements that compose it:

- NI cDAQ¹ board. The compactDAQ is a portable, rugged data acquisition platform that integrates connectivity, data acquisition, and signal conditioning into modular I/O for directly interfacing to any sensor or signal [23];
- NI 9401 module. It is a configurable digital I/O interface for input or output in 4-bit increments. It is possible to use LabVIEW to program the NI-9401 for implementing custom, high-speed counter/timers; digital communication protocols; pulse generation; and more [24];
- NI 9237 module. It includes all the signal conditioning required to power and measure up to four bridge-based sensors simultaneously. The module provides strain or load measurements [25];
- NI 9205 module. It performs single-ended or differential analog inputs, with four programmable input ranges for each. The provides voltage and current evaluation [26].

⁴The cDAQ device is powered by the power box, while the output data are sent to the computer through a Lan cable.

EDF power source

The test bench components are fed through to power sources : LiPo batteries and the power box. The first fount is dedicated only to the EDF motor, since the latter will be powered by the same batteries on board of the FTV7%. The set of batteries consist of a pair of 8000mAh 6 cells batteries (Figure 3.11), and they are connected in parallel before be wired to the power box that in turn joint the EDF motor. The rest of the power is provided by the power box ⁵, which feed all the remaining instrumentation (i.e. load cells, ESC and cDAQ).



Figure 3.11: LiPo batteries.

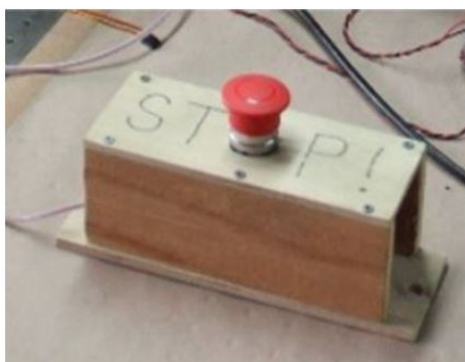
Specifications	
Capacity	8000 mAh
Voltage	22.2 V
Max Continuous Discharge	25 C
Weight	1174 g
Dimensions	165 x 65 x 53 mm
Discharge Plug Type	EC5

Table 3.5: battery parameters.

Safety equipment

Last but not least, there is the safety equipment. Regarding the test bench itself, since there electricity power in the game, it was made a simple but quite effective precaution to deal with inconveniences. This consists of a Safety Stop Button (Figure 3.12 a), that creates an open circuit when activated, thus interrupting the power feeding.

To conclude, is necessary that all the operators in the zone use the appropriate protective equipment, in particular safety glasses and safety caps (Figure 3.12 b).



(a) Safety stop button box.



(b) Safety protection.

Figure 3.12: Safety protection and Stop button.

Finally, the test rig is ready for EDF testing (Figure 3.13)

⁵The power box receives electricity from the socket.

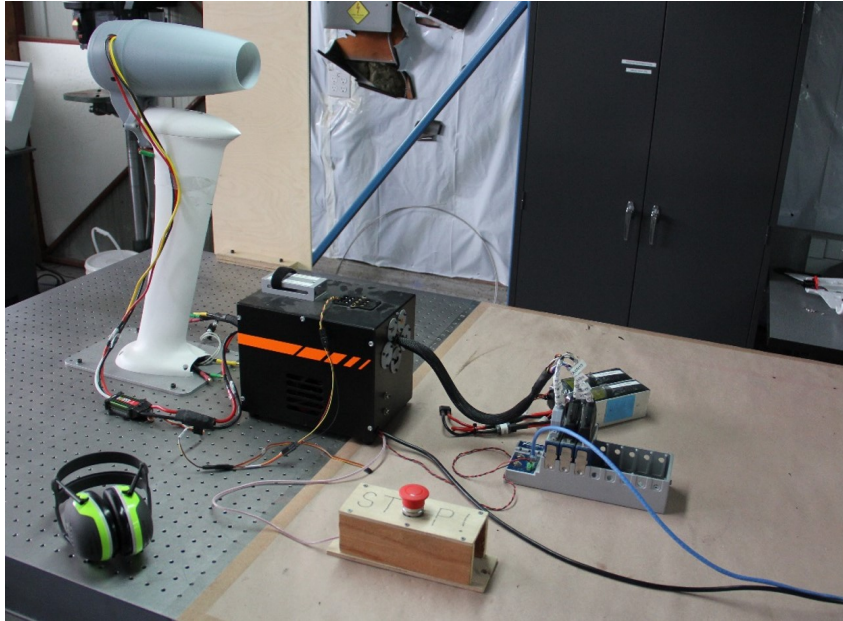


Figure 3.13: EDF test rig assembled.

3.6 Testing and Results

In this section will be presented the results obtained after having elaborated the data acquired from testing EDF motors. As said previously, the program used during the data acquisition was LabVIEW, but in addition it has been used Matlab ⁶ to obtain most of the graphs and tables that will be shown here. It would be useful to take a look to the scheme in Figure 3.14 to have an idea on how work has been organized. It must be said though, that the performed tests where more than those shown below, however the main analysis have been obtained working on these tests in particular.

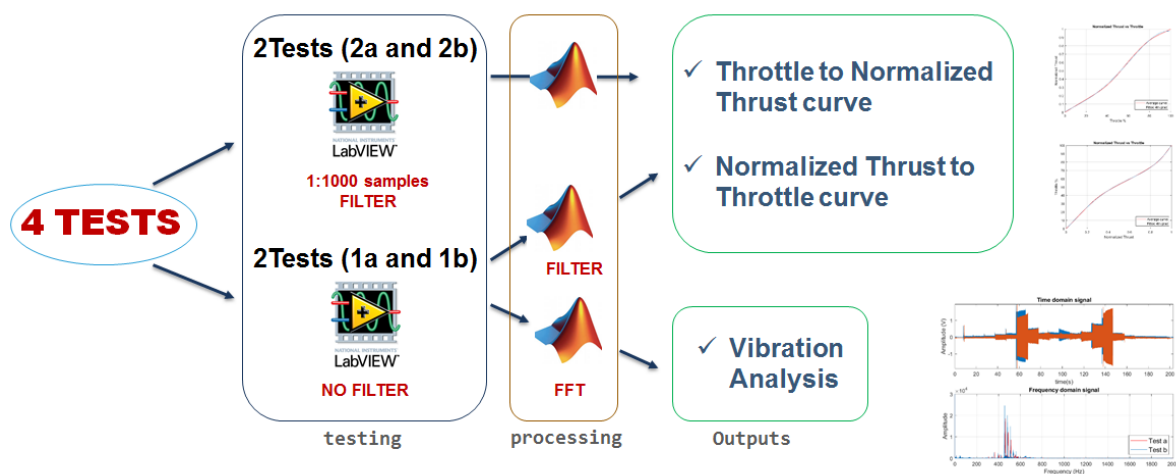


Figure 3.14: Scheme of the performed tests and analysis .

⁶The relevant Matlab scripts are given in *Appendix A*.

3.6.1 ESC Testing

Before start running the engine, it was mandatory to test the ESC first. Although most of CfAR prototypes uses the same device as speed controller, it was proved that not all of them have the same upper and lower limit for arming, and thus send the signal to run the engine.

Test the ESC was accomplished following the subsequent steps:

- Check all the wiring and devices;
- Plug the power box;
- Run the LabVIEW GUI;
- Check that ESC button is set on "disabled" otherwise the command will be sent to the motor, and the latter will start running;
- Type a "guess value" for the ESC limit, and follow the sequences shown in Figure 3.15;
- Deactivate the Stop Button;
- Wait 10 seconds to hear if the device beeps twice, that means that ESC is armed, and ready to send the signal to the motor.

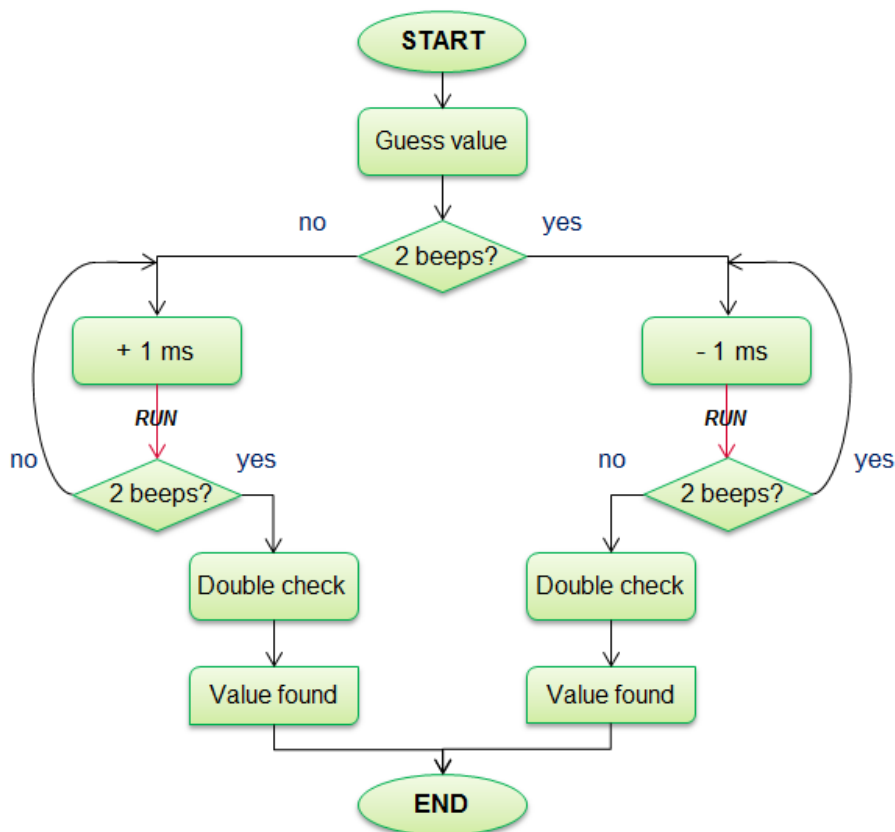


Figure 3.15: Iteration process to find ESC lower limit .

It is evident that the iteration shown is indicative, in fact it has been altered quite often during tests like for example making bigger steps instead of just adding/removing 1 ms per time. Regarding the upper limit, the iteration is pretty much the same, the only adjustment is that of inverting the signs).

3.6.2 Thrust Test Results

The main objective of the tests, as said in the beginning of this chapter, is that of obtaining experimental thrust maps. The data acquired from the numerous tests have been logged in the computer instant by instant, and then elaborated with Matlab software. The main outputs for the thrust mapping task are:

- Normalized thrust vs Throttle graph (and correspondent equation);
- Throttle vs Normalized thrust graph (and correspondent equation) ⁷.

It must be said that although all the planned tests, both 20% and 10% throttle steps, were executed, the thrust maps where made using only the 10% data. Nevertheless, the 20% ones have been used to compare and confirm the results obtained with the the others. The current discussion shows only the results performed with the 10% steps data. Both scripts are given in the *Appendix A*.

The results will be now shown commenting briefly each step executed.

First of all the data have been imported on Matlab, then the 4 tests mentioned have been filtered with Matlab, and each of the 11 throttle values (from 0 to 100) has been done the thrust average to obtain one value for each throttle signal sent. After that, using the spline command of Matlab, the thrust curves are obtained as displayed in Figure 3.16.

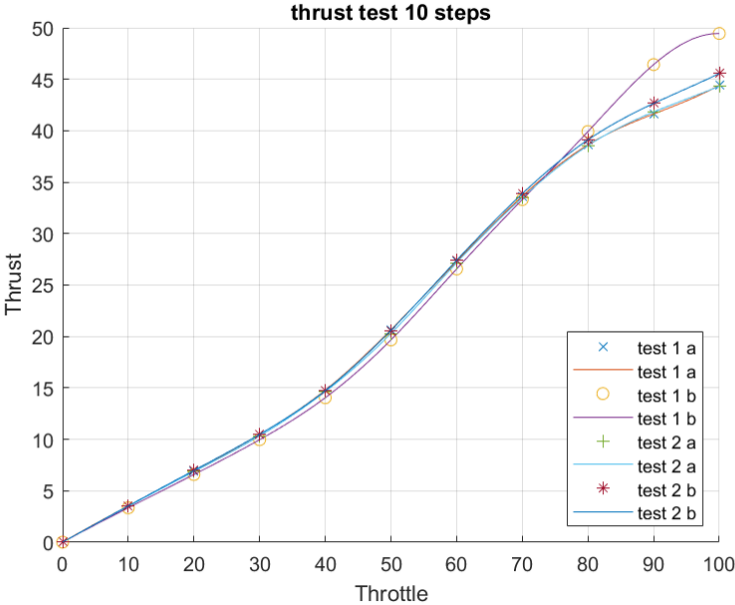


Figure 3.16: Experimental average values of thrust tests.

Looking at the previous graph, it appears immediately the presence of an abnormal behaviour from the test 1 b. From the other hand, it looks like all the other graphs follow the same trend. The anomaly

⁷Both graphs where required by the flight team, and they were processed separately in order to correct some discrepancies.

has been investigated, and further data has been processed to find the origin of this significant discrepancy. The study carried out led to a conclusion: The thrust behavior of Test 1 b differs from the others most likely because of the battery discharge. As evident in the graph 3.17, this was slower than in the other tests, that means that the battery succeeded in maintaining high voltage for high throttle better than the other cases. Since this behaviour was considered an isolated case⁸, it wasn't taken in consideration in the thrust study, but was used later in the vibration analysis (section 3.6.3).

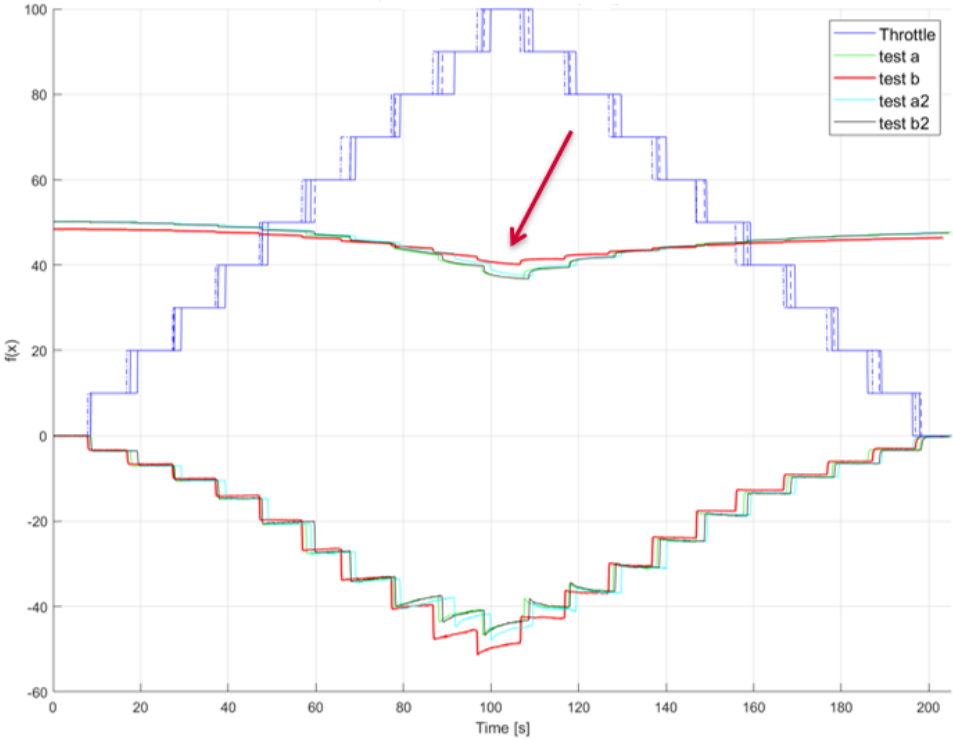


Figure 3.17: Throttle, Thrust (negative) and battery voltage for the four tests.

Moving forward, it was necessary then to make an average of the remaining tests, thus the mean curve has been made as in Figure 3.18 plot. Looking at this graph, is possible to note that for one half, the trend is pretty much the same, although the three tests have been done with different battery conditions, giving the analysis confidence in terms of accuracy, but also the success in reproducing exactly the same conditions for each test.

After obtaining the average thrust curve, it was appropriate to convert the absolute values of thrust in percentage ones expressed in the range between 0 and 1. Afterwards, the next step consisted of deriving the equation that best describes the trend of this experimental curve. The job was accomplished using Matlab tools, and the resulting curve with respective equation have been realized. It has been chosen a 4th degree polynomial equation since it tuned to be a good compromise between accuracy, and simplicity. Figure 3.19 shows both the fitting equation and the resulting graph, and also residuals are less than 5%.

The same procedure has been done to obtain the inverse curve, obtaining even better fitting as it seen in the graph below (Figure 3.20). It might be deceiving the fact that residuals seem high in

⁸that was demonstrated through other two quick tests, unfortunately not recorded here.

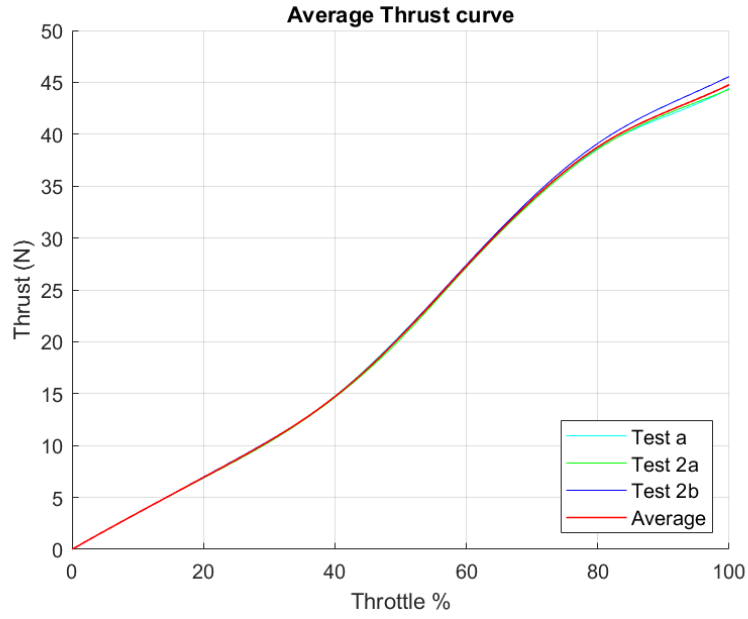


Figure 3.18: Average curve obtained from experimental thrust tests .

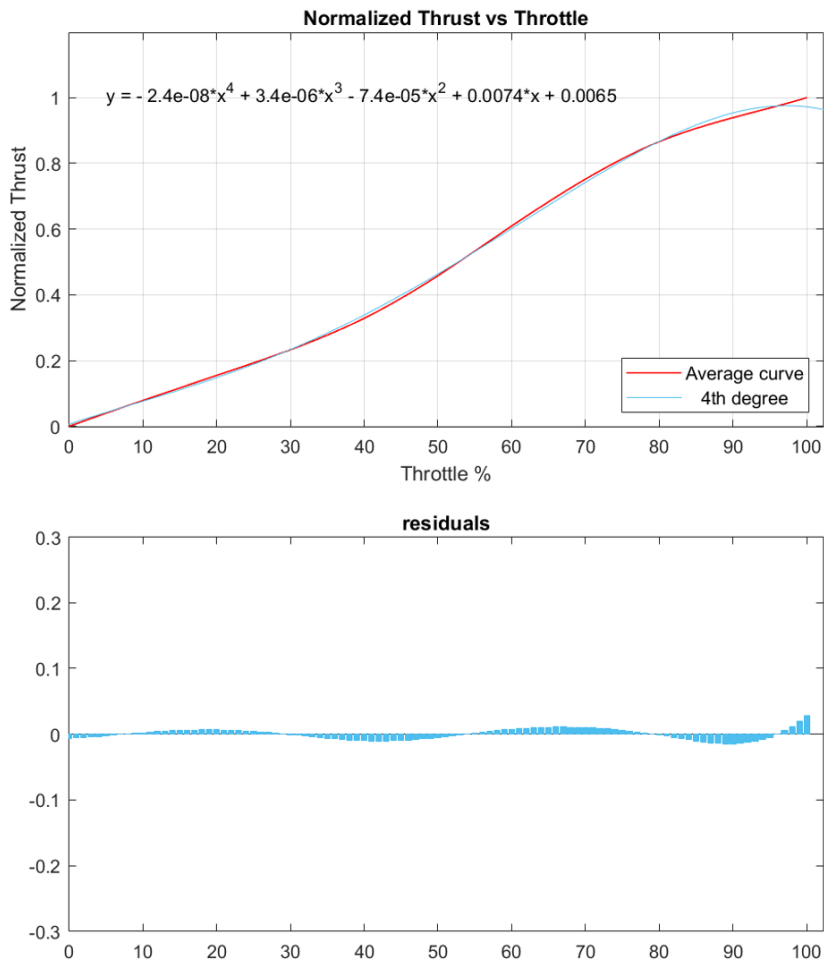


Figure 3.19: Fitting curve and related equation for N.thrust to throttle curve.

amplitude, but that is due only to the scale, in fact computing the relative error, it results to be even less than 1% .

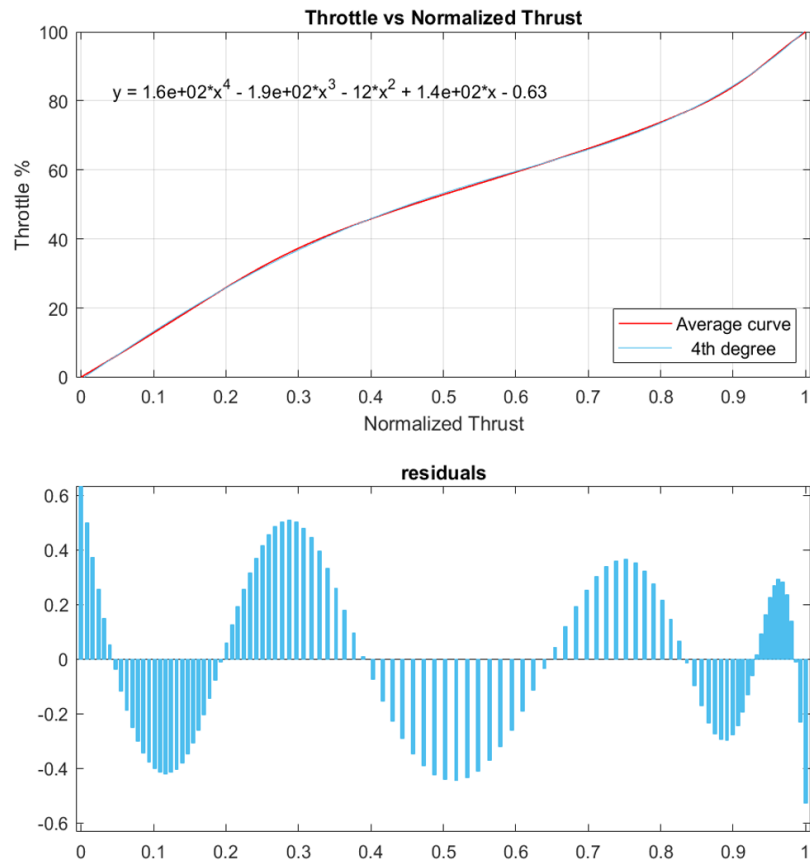


Figure 3.20: Fitting curve and related equation for throttle to N. thrust curve.

Looking at the results up to date, they can be presented in three different forms:

- average thrust curve with correspondent fitting one (Figure 3.21);

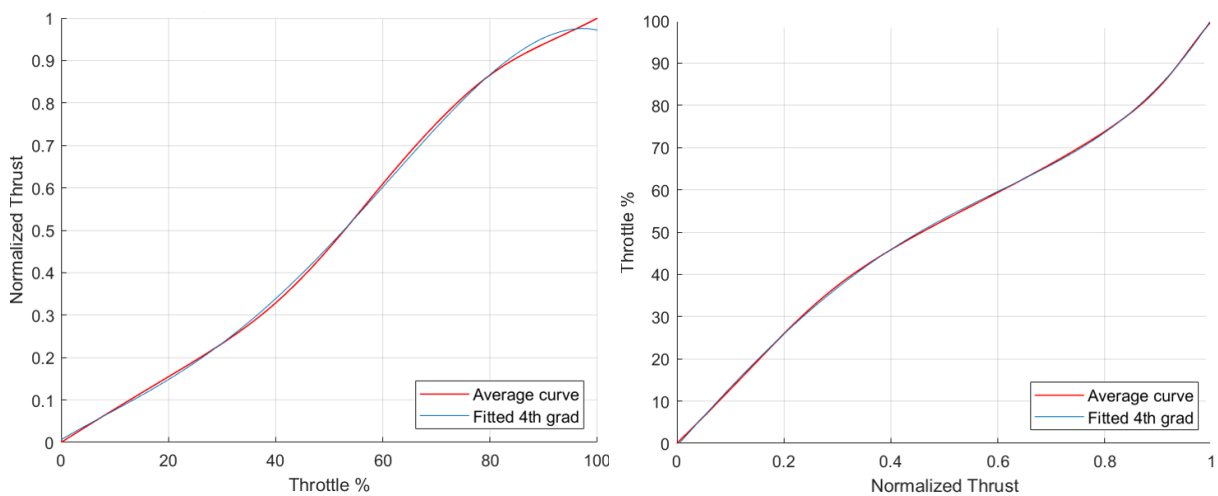


Figure 3.21: experimental thrust curves fitted by 4th degree equation.

- equations:

$$y = -2.4e^{-0.8} \times x^4 + 3.4e^{-6} \times x^3 - 7.4e^{-5} \times x^2 + 0.0074 \times x - 0.0065 \quad (3.1)$$

$$y = 16 \times x^4 - 19 \times x^3 + 12 \times x^2 + 14 \times x - 0.63 \quad (3.2)$$

- tables with relevant values.

Table 3.6: Thrust vs throttle relevant values.

Throttle%	Norm.Thrust	Thrust (N)
0	0,00	0,00
10	0,07	3,10
20	0,14	6,28
30	0,23	10,04
40	0,33	14,66
50	0,45	20,16
60	0,59	26,31
70	0,73	32,62
80	0,86	38,32
90	0,94	42,41
100	1,00	44,77

Table 3.7: Throttle vs thrust relevant values.

Norm. Thrust	Thrust (N)	Throttle %
0	0,00	0,00
0,1	4,48	13,20
0,2	8,95	25,87
0,3	13,43	36,81
0,4	17,91	45,87
0,5	22,39	53,27
0,6	26,86	59,61
0,7	31,34	65,92
0,8	35,82	73,58
0,9	40,30	84,39
1	44,77	100,00

All the values presented above have been given to the flight team, and they are ready to be implemented on Simulink.

3.6.3 Vibration Analysis

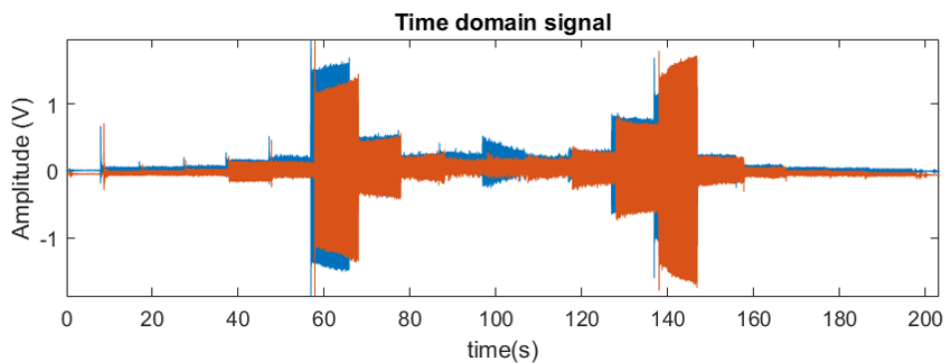


Figure 3.22: Torque load cell reading for test 1 and test 2 overlapped.

Conducting the tests it was remarkable the behavior of Torque load cell showing oscillation on L GUI graphs for certain Throttle commands. Inspecting directly on the test table and on the nacelle itself, outcomes of true vibrations, thus the possibility of calibration/malfunction of torque load cell was aborted. The analysis began modifying the LabVIEW GUI in order to recover all the data without any filter (discussed already in section 3.4.1). Furthermore it must be said that only 2 tests out of 4 were included in the analysis since the other 2 were done before removing LabVIEW filter.

In optimal conditions, a piezoelectric accelerometer would have been the best solution to study the phenomena, but since it was an unplanned test, the inquiry was carried out counting on the torque load cell sensor. The response of the torque load cell of the two tests, expressed in terms of voltage amplitude (proportional to the acceleration ⁹), is shown in the plot of Figure 3.22. The two graphs have been overlapped, and is quite evident the presence of consistency in the output.

FFT function of Matlab was used to study the presence of any dominant frequency for both tests, and the result is given in Figure 3.23. It is clear that there are 3 main peaks at high frequency in both plots, while the peak relative to the engine mount beam (low frequency), is irrelevant.

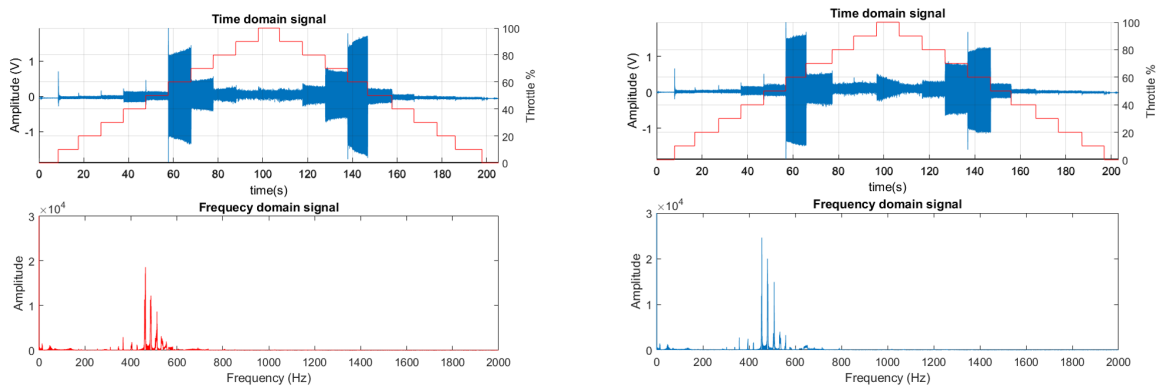


Figure 3.23: Time and frequency domain signal for test 1 and test 2

Singular throttle commands have been investigated as well to find out which value was more responsible for the oscillations and the respective frequency. In Figure 3.24 they have been highlighted in red the values of throttle responsible of the highest vibrations detected, in particular 60% and 70% values.

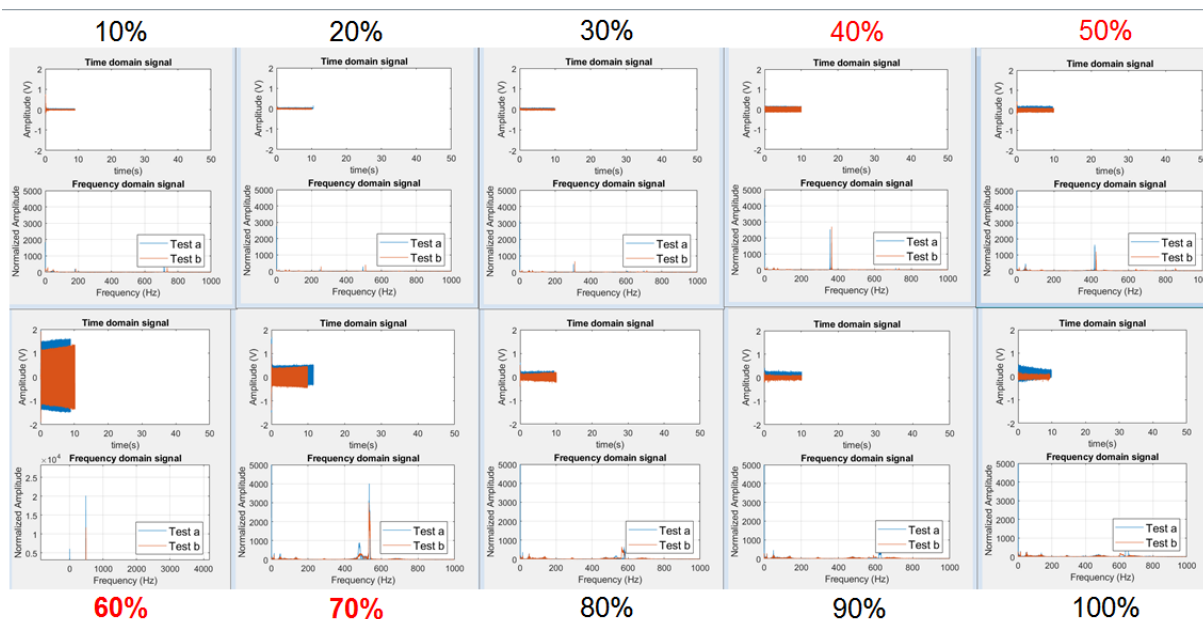


Figure 3.24: FFT results for each throttle command.

⁹That is valid since the load cell strain gauge is Wheatstone bridge based.

Since there is no direct connection between throttle and vibration frequencies, it was necessary to get the RPM values corresponding to the different throttle commands. Unfortunately, one of the bugs of the LabVIEW GUI was the wrong reading of RPM value, however, the problem was overcome using Castle Link usb programming kit, directly connected with the ESC. Using this device it was possible to extract the recorded data in the ESC, among which the RPM values.

Table 3.8: Throttle, RPM and frequency detected values.

Throttle	RPM	Frequency
40%	22000	360 Hz
50%	25700	420 Hz
60%	29300	480 Hz
70%	32300	530 Hz

After studying carefully the acquired data, it came to light that the vibrations were definitely caused by the rotation of the electric motor, in particular by the 6-poles rotor. It was possible to state that since the values derived from ESC and FFT analysis (shown in table 3.8), follow in good approximation the relation given below:

$$f = \frac{RPM}{2\pi \times 60 (s) \times 6 (poles)} \tag{3.3}$$

The examination carried so far had the only objective to find out the causes of the unexpected vibrations met during testing. Looking at the results, it was clear that for certain RPM values, the EDF motor start oscillating more than others, and this phenomena needs to be further investigated.

3.7 Concluding Remarks

The overall results of the accomplished tests were satisfactory, in fact most of the planned objectives were met. It is appreciable as well the study carried on the detected vibrations, since this was not included initially in the planned tests. The ESC limits were found quite easily, and it was found that they were pretty close to the usual ones found in similar devices, as well as they were between the range of values given by the supplier.

Furthermore, the EDF motor mapping in terms of Thrust to Throttle led to quite smooth results, although the results could be improved further acting on the environment of the tests to simulate even better the real conditions on the aircraft.

The vibration analysis described not to long ago, led to reliable outcomes, and dominants frequencies have been found, as well as the linkage between the RPM values and the latter.

In general, it must be recognized that although not all the functional requirements were met (due to lack of time), the few tests accomplished contributed to the achievement of satisfying outcomes. Moreover, the same results suggested to move forward with other tests to improve further (see Future Developments, section 5.1).

Chapter 4

Turbine Jet Testing



Figure 4.1: JetCat turbine jets.

In this chapter the attention will be focused on the propulsion system of the FTV16.5%. Unlike the previous prototype, this new 16.5% scale model is powered by two gas turbines instead of EDF motors. The reason lies on the fact that the full scale aircraft will be mounting gas turbines and not electric motors, thus the scale model is much close to the full scale one. Furthermore, as explained in chapter 2.1 (section 2.1.1), the weakness of the electric solution comes out when the dimensions of the system start increasing, and so the electric system as whole becomes too heavy to the point of being disadvantageous.

After selecting the propulsion system, the next step for the designers was that of selecting which one in particular will power the plane. The research ended with choosing two JetCat turbines, in detail the "P500/P550 PRO" model¹⁰. The company is well known for its reliability as well as for the reliability of its products. Nevertheless, it's good practice to test them on ground before proceed with fly tests both to check the integrity of the engines, and to get familiar with the device itself. Furthermore, tests are required also to obtain the accurate performance maps that return useful to implement the propulsion system model for the on board autopilot.

¹⁰In terms of hardware they are the same model, but the control unit of the engine can be configured in such a way to provide either 550 N or 500N maximum thrust. So on will be referred to only as P500.

The steps leading to the tests will be shown in the coming pages. They will be exposed the guidelines for the test bench design as well as all the necessary equipment, ending then with the set up and significant recommendations for the planned tests.

4.1 JetCat Engine



Parameter	Value	Unit of measure
Pressure ratio	3,6	/
Weight	4900	g
Max diameter	175	mm
Exhaust gas temp.	480–740	C
Idle speed	26000	1/min
Max rpm	80000	1/min
Thrust @ idle	28	N
Thrust @ maxRpm	492/544	N
Exhaust gas velocity	1986	km/h
SFC @ maxRpm	0,151	kg/Nh

Figure 4.2: JetCat P500 PRO.

Table 4.1: JetCat P500 PRO parameters.

The JetCat P500 PRO Engines (Figure 4.2) offer maximum integration and installation. All system equipment required for turbine operation is fully integrated under the turbine hood. This consist of the following components:

- ECU (electronic control unit);
- Integrated brush-less fuel pump;
- Fuel and kerosene start valves;
- fuel filter;
- kerosene starter;
- Barometric height / pressure sensor;
- 4-pole Molex extension plug (e.g. for smoke pumps / fuel pump);
- Vent opening with integrated one-way valve (e.g. for pressurizing the fuel system).

Apart from the supply battery, the fuel tank and the control signals, no further external subsystems are required. The control signals are output on a data cable terminated with a 15-pin SUB-D connector. Power is optionally supplied via the power cable with XT60 plug for direct battery connection [27]. The engine main details are given in Table 4.1.

Actually they exist two versions of the P500 PRO : GL and GH. The first one consist of a brush-less and non-contact starter/generator system. The generator is "soft coupled", i.e. it rotates at a lower speed

than the turbine shaft itself (patent pending). A built-in and integrated DC / DC converter with additional charge control enables buffering / recharging of the turbine battery. The charging system is able to supply charging energy to the Engine battery at idling speed. The electrical power of this charging system is approx. 85W. The "soft" coupling of the generator limits the power output.

The GH version instead, consists of a brush-less and non-contact starter/generator. The generator is "hard" coupled to the turbine shaft (but there is no mechanical contact), i.e. it rotates at the same speed as the turbine. This configuration allows a much higher power output of the generator, up to 900W [27]. The version that has been selected is the second, although it was much expensive. The reason lies on the fact that having a generator on board means saving weight in terms of batteries, something that all aerospace engineers "run after".

4.2 Objectives and Functional Requirements

The functional requirements for JetCat testing were given by Bombardier guidelines documents ¹¹, and quite often they change basing on unexpected events or necessities. Furthermore, it must be said that the initial objectives concerning JetCat testing have been reduced due to lack of time and delays by third parties. However, these tasks will be introduced in this dissertation, and the reader can find in the next chapter (Future Work, section 5.2).

After all, it was decided to focus all the efforts on the following tasks:

- Design a jet engine Test bench;
- Select and purchase the required sensors;
- Design and test the software graphic interface;
- Set up the test bench and test sensors;
- Check the engine response to the command sent (without firing the engine);
- Check the correct operation of the feed system;
- Run the engine to inspect if there is any anomaly.

Nevertheless, because of different delays in machining and shipping, but also the commitment of the team members in other priority work, the last three where postponed. Regardless all this, it must be said that the other tasks were accomplished with good results although the encountered difficulties.

Least but not last, it is right to say that the dissertation will not linger on the test rig CAD design simply because the author participated relatively to the performed work. From the other hand, all the remaining parts will be carefully treated.

¹¹The mentioned documents are not reported in the current thesis since because are considered confidential material.

4.3 Previous Work

It was mentioned above that the propulsion system was already selected during the design phase. Besides that, there is also a lot of work already done towards the preparation for testing, either with testing perspectives, or just because the design of the aircraft itself required certain steps. Anyhow, most of this goals turned useful during the tests rig design.

The relevant past achievements are summarized below:

- Fuel Tank. During the design of the 16.5% model it was unavoidable to deal with the fuel tank shape, reason why it has been already designed and sent to be manufactured by ATL company (Figure 4.3). However, since it turned to be pretty expensive, it was decided not to use it during the preliminary tests, thus is needed one for testing;
- Fuel Lines. JetCat provides already the latter, but the CfAR required also that the fuel lines are protected with jacketing ¹²;
- Engine mounting. This was designed during aircraft design as well, and is still being modified. The engine mounting given in Figure 4.3 is just one of the preliminary versions, and although is not the final one, it turns to be useful at least to have an idea before start designing the test bench;
- Engine nacelle. The design of the latter was considered completed until unexpected event came to light. After doing a detailed CFD analysis, Bombardier discovered that there is a little air stagnation on nacelle side walls just after the intake. The engineers stop the order of manufacturing, and start modifying the old design.

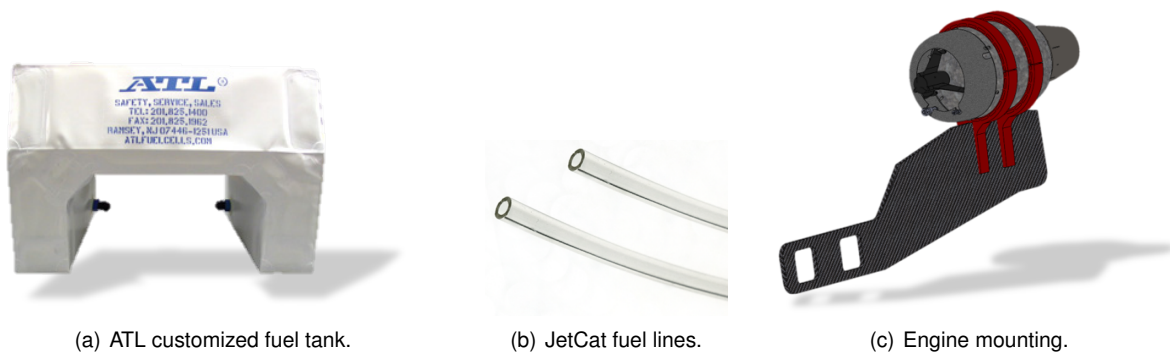


Figure 4.3: Propulsion system already chosen components.

Furthermore, it was contacted Bluewave Energy to see if it is possible to rent a portable Jet A1 tank and filter unit, and provide the Jet A1. The response of the company was positive, however, it has been decided to proceed, at least in the first tests, filling the fuel tank directly from airport supplier when needed.

¹²In the event of a burst in the injection pipe the leaking fuel will be collected by the jacket and piped away safely to an alarm device to notify operators of a potential problem.

Regarding the test rig itself instead, it was already done a preliminary design to have an idea about the dynamics of engine testing. Looking carefully at the left table in Figure 4.4, it is possible to recognize the presence of two fuel tanks. In fact, as said before, it is supposed to be used in a certain moment during ground testing before go inside the plane. These tests are mandatory since it is not a standard tank, but has a customized shape made to fit the aircraft design. Concerning the testing one (in blue), at the beginning it was thought that a marine fuel tank will be the solution, but during the research it came out that it was inappropriate (see section 4.4.3).

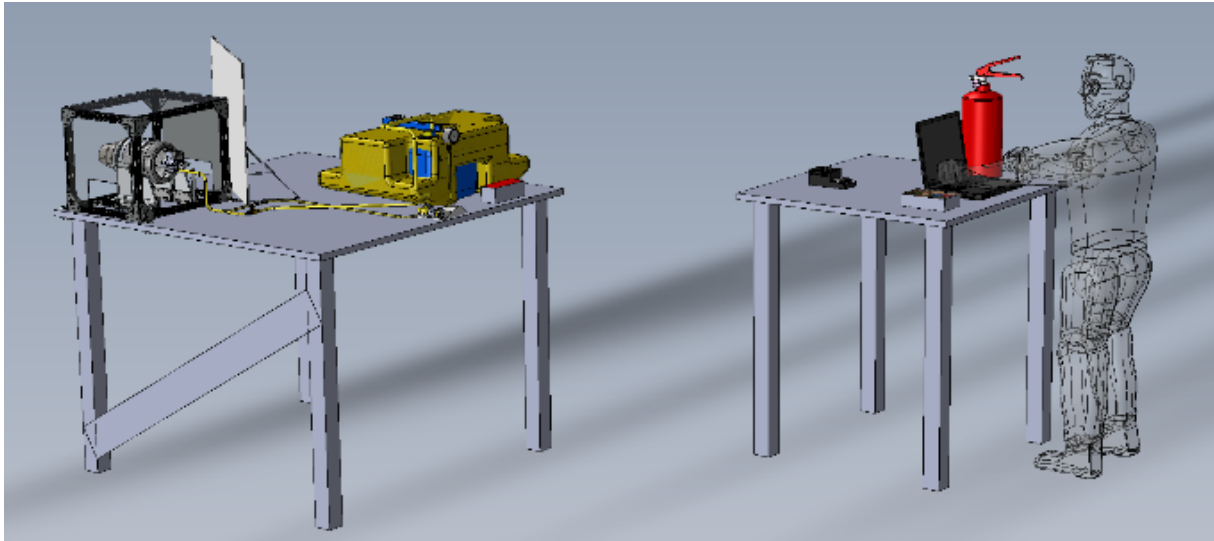


Figure 4.4: JetCat preliminary design.

Finally, with reference to software design for testing, unfortunately no particular program was inherited. That is quite understandable since the project itself just started this year, and at same time, there are many other projects running in parallel at CfAR, thus keeping designers busy.

4.4 Test Bench Design and Equipment Selection

4.4.1 Testing Location

An important task before proceed with test rig design is that of finding suitable location to execute the tests. This factor may seem irrelevant, but actually returns to be critical since it will affect most of the decisions that will be made for the test rig design. The procedure of choosing the post for testing must be chosen prudently paying attention to both safety and provider recommendations (see *Appendix B*). The JetCat P500 is capable of generating a thrust up to 540 N, and that leads to having an exhaust gas velocity close to 2000 km/h, and such velocity is around Mach number equal to 2. In this conditions shock waves become a relevant problem since they lead to noise hazard. Furthermore, in these conditions, the exhaust gas is pretty hot, and can reaches peaks of temperature up to 740 (Table 4.1). All these factors drove to abolish any opportunity to test the engine indoor, and at the same time, made the team be aware of the potential and delicacy of these "little" turbines.

Regarding the hazard awareness, JetCat provides their customers always an instruction manual including descriptions of possible risks and precautions. These recommendations were taken in consideration during the research, despite they were not respected to the letter. This occurred both because all that required space was not available nearby, but also because it supposed there is no need for all that since the final design includes a cage that must be able to contain any engine failure along the radial direction. After discussing all the available options, the final solution was that of running the tests in front of the hanger with the exhaust gas towards the empty field as shown in the map of Figure 4.5.



Figure 4.5: Test rig chosen location.

Although it has been considered the best solution found, the current location has its weaknesses. The principle drawbacks are the following:

- Testing outdoors means to have a constraint dictated by the weather. Tests will be executed only if the weather conditions allow that;
- The chosen zone is frequented quite often by pedestrians. This inconvenient may induce delays during testing because of quitting/pausing the tests when someone is passing nearby;
- Engine's noise may cause a form of disturb in the offing.

Probably only the second might be mitigated, in fact it was thought to surround the area with orange cones, and use an orange serene on top of the test cage in order to warn the passer-by.

4.4.2 Test Rig Design

The test bench must be designed in such a way that it is possible to accurately characterize different types of UAVs engines, preferably both electric motors and internal combustion engines. Since this

bench would cost pretty much respect to previous one present at CfAR, it was appropriate to consider the possibility of reuse it in future work as well, and do not limit its use to jetcat only.

Before proceed with the test rig design, it was considered the option of buying an on-the-shelf one. Thanks to the popularity of JetCat engines among both hobbies and centers of research, the was confident on the possibility of finding a ready tests bench to purchase. This choice would save a lot of time and effort giving the opportunity to accelerate engine testing. After some researches, it was finally found one by a French center of research. However, this option had a pair of defects: First of all, the engineers of that center stated that they did not have one ready at the moment, but they may build one. The second instead, it was the excessive cost demanding.

After brief discussions with the other engineers at CfAR, the option of buying the already made test rig was aborted, and the team start moving towards a homemade one.

The test rig CAD design was conducted in parallel with the equipment selection since one depends on the other. The main requests that bounded the CAD design are:

- The engine must have a shield cage to protect operators;
- The dimensions of the cage must be big enough to accommodate the FTV16.5 % nacelle too;
- The cage must be portable and easy installing on optical tables;
- The engine mounts must have the same bolt pattern and location as the FTV16.% 3D-printed mount;
- There must be the option of using thermal camera without being at risk ;
- Protected spots for sensors and wiring;
- Easy machinability of the components;
- Robustness of the structure. Over-sizing is not an issue;
- Failure proofed.

Applying all these instructions, the resulting test bench CAD is that shown in Figures 4.6 and 4.7.

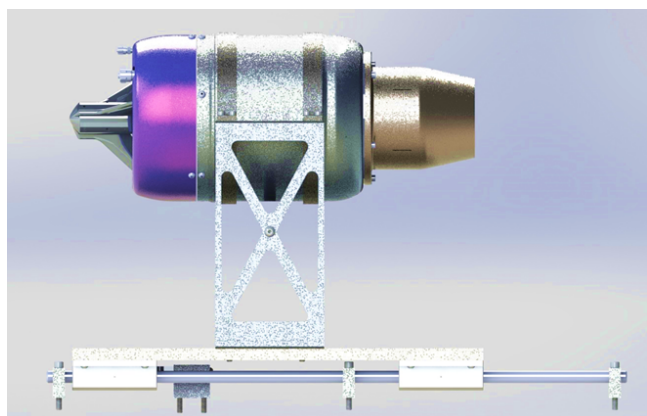
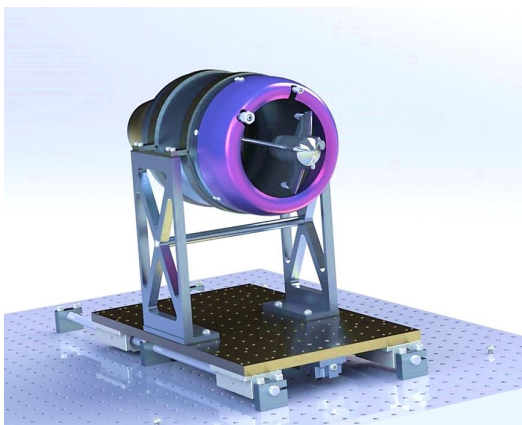


Figure 4.6: JetCat mounting.

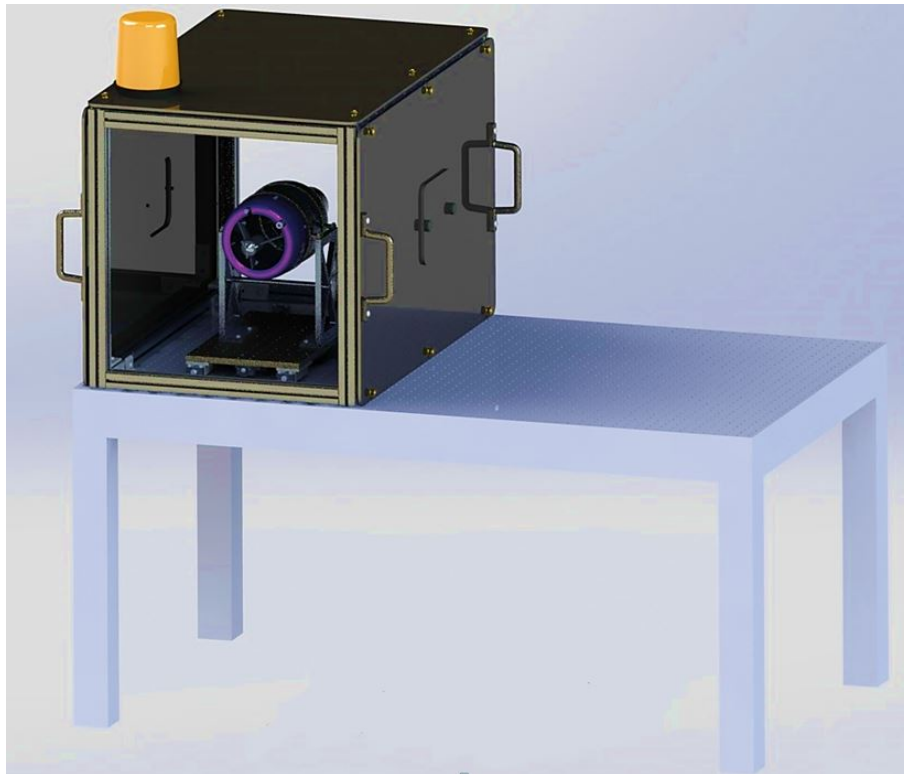


Figure 4.7: Test rig final design.

Analyzing the arrangement of the designed test rig, this can be considered composed by three main components : the engine mounts, the slider mechanism and the cage.

The main requirement for the slider is to provide a low friction rail so that the reading from the load cell is as accurate as possible. Therefore, many solutions were considered, and the final decision was to use a dual rod quad bearing system, this was the most cost effective solution to get low friction with minimal binding.

With the design of the test rig it was important that the JetCat engine can be mounted using the same bolt pattern and location as the aircraft mount that will have 3D printed out of titanium. This meant that a test mount needed to be designed so the testing could be run without the aircraft mount, granting the possibility of testing in parallel while the aircraft mount is being procured. The test mount consists of a simple plate and bracket solution, allowing to retain the same position as the aircraft mount while making it easy to install and machine.

The main purpose of the cage instead, is to protect the operators from engine failure, debris and heat. With this in mind, the simplest solution for this was to create an 8020 extrusion cage and close it with steel plating. The size of the cage is large enough to accommodate the engine and the respective nacelle. However, with these plates installed there is limited visibility of the engine, which makes taking FLIR images difficult, to remedy this it was designed an access port on either side of the engine, permitting to open and take images as needed through the test. To increase accessibility the steel plates are notched and located via bolts and thumb screws, making assembly and removal easy, as well as the possibility of having wiring pass through. With this cage testing can be executed safely and without big constraints.

4.4.3 Sensors and Equipment Selection

As already mentioned above, the test rig design included also the selection of sensors and other required equipment. The selection of the correct equipment is constrained by the presence of lots of variables making the "perfect sensor" almost utopia. In the foreground, the requirements of testing and subsequent outputs may cause a strict restriction. However, quite often the requirements are slightly modified in such a way to meet sensors features. Furthermore, most of sensors have certain standards, and cannot be customized to satisfy designers' objectives, and this leads to the necessity of taking critical decisions. All these aspects make sensor choice a challenging task.

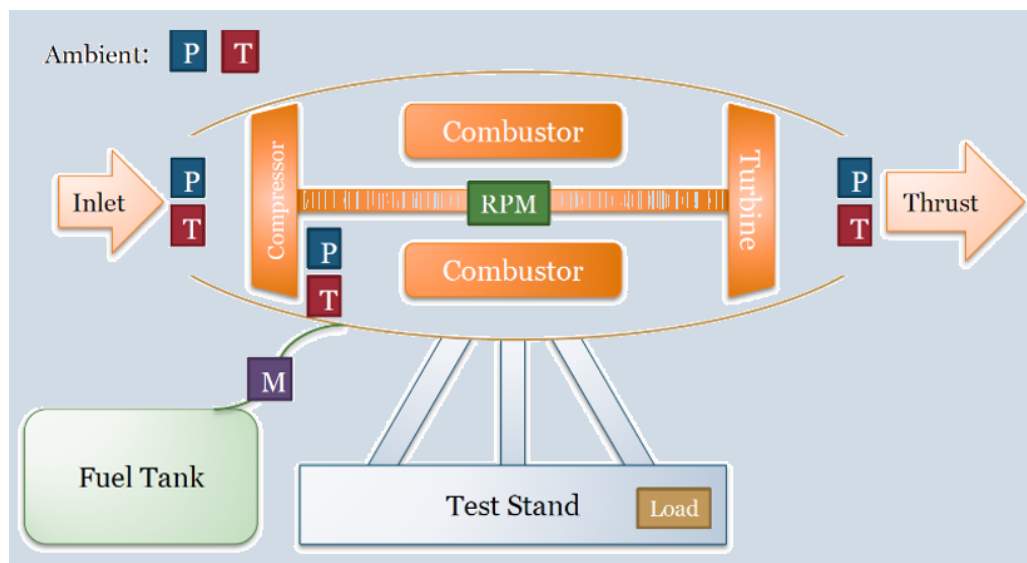


Figure 4.8: Sensors preliminary disposition.

The research carried out for test rig equipment was not easy, and has undergone several modifications. It must be said though, that the job was made a bit easier thanks to COMET team project documentation [28]. This aerospace team have been testing smaller JetCat models few years ago, and they performed engine characterization too. Although the level of detail of the latter was not that high, it was a good starting point. Figure 4.8 shows the arrangement of sensors for ideal testing, thus allowing the reading of all the required values for a theoretical approach. The knowledge of jet engines dynamics leads to recognize the difficulty of realizing similar disposition, in particular the after compressor and exhaust sensors. The first ones are known to be expensive, but at the same time they affect the engine integrity. The others instead, are critically expensive since they must be able to resist to high pressures and temperatures. All these constraints led to abandon the idea of using them, and start looking for considerable alternatives, like using Compressor and Turbine maps (*Appendix B*).

The coming paragraphs will be showing the main achievements of these research, as well as presenting the other instrumentation selected for JetCat testing.

Load cell

The first sensor to be processed is the load cell. This device is used to detect forces or momentum during testing. Since one of the main objectives is to obtain JetCat performance maps, the engine's thrust must be taken over. To take charge of this task is precisely the load cell. The sensor sends then data to the data acquisition system to send it in turn to the computer. The suitable model was an LCCD-1K S-shape load cell that measures up to 50 kgf, and this have been positioned below the engine mounts, parallel to engine's thrust direction (see Figure 4.9).

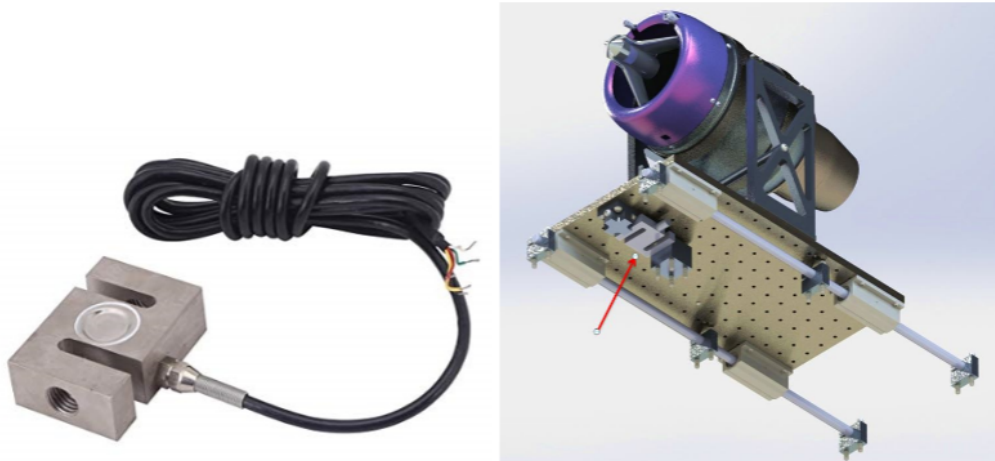


Figure 4.9: Load cell position.

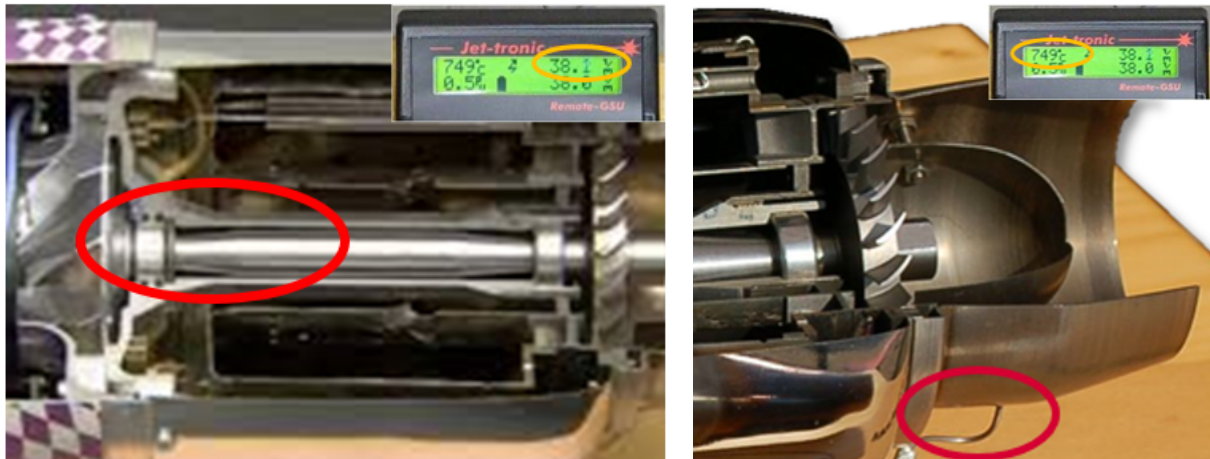
JetCat sensors

The objective of testing an engine is also that of checking the perfect functioning of all its components, therefore is appropriate to use sensors external to the engine. Nevertheless, either the complexity of some measurements, or the critical position (as said above) made the team move towards counting on some JetCat sensors. Figure 4.10 shows the main two sensors that have been decided to make participants at least in the first part of testing. The sensors are:

- RPM sensor;
- EGT thermocouple.

Moreover, the pictures show also the display of the JetCat GSU, a microcontroller of the latest generation, useful to monitor engine behaviour. In the first part of testing it is supposed to count on the GSU controller, and use LabView only as data acquisition program.

Another useful mean provided by JetCat is the ECU program interface. This software seems to be able to collect data relative to the engine performance, as well as furnish sensors' reading. Will be interesting then to find a way to make this program communicating with LabView GUI in order to pass the data to the latter, and end up with having only one and complete user interface.



(a) RPM sensor.

(b) EGT thermocouple.

Figure 4.10: JetCat sensors.

Accelerometer

The decision of whether to use piezoelectric force sensors or sensors based on strain gauges is a recurrent dilemma when dealing with vibrations measurements. Piezoelectric sensors are preferable, particularly when the application has one of the following requirements:

- Confined space for sensor installation;
- Measurement of small forces with a high initial load;
- Wide measuring range;
- Measurement at extraordinarily high temperatures (up to 300 ° C);
- Extreme overload stability;
- High dynamics.

Strain gauge-based sensors, too, offer advantages over piezoelectric force sensors; for instance, they enable tensile force to be measured and often are more economical. In addition, they provide better accuracy and static calibration. When it comes to reference measurements, there is no alternative to strain gauge measurement technology [29].

In any case, is recommended the transducer that meets most the requirements of the measuring task at hand in the best and most cost-effective way. When the decision to use a piezoelectric sensor has been made, there remains the question of which force transducer is the right one since they exist an infinity of them on the market.

The required sensor for JetCat testing consists of an accelerometer able to detect vibrations in all the 3 axis. After deep researches, the choice fell on two models of the PCB Piezotronics, a well known American company specialized in sensors. The selected models are shown in Figures 4.11 and 4.12 with relative specifications.



Figure 4.11: 3-axis PCB accelerometer

Specifications	
Sensitivity (10 %)	10 mV/g
Measurement Range	500 g pk
Frequency Range (10 %)	0.4 to 10000 Hz
Resonant Frequency	30 kHz
Price	700 \$

Table 4.2: PCB 356A43 specifications.



Figure 4.12: 1-Axis PCB accelerometer.

Specifications	
Sensitivity (10 %)	10 mV/g
Measurement Range	+/- 500 g pk
Frequency Range (10 %)	0.3 to 15000 Hz
Resonant Frequency	50 kHz
Price	700 \$

Table 4.3: PCB 352C04 specifications.

The choice between the two models was pretty hard. Looking at the specifications of both models it is obvious that second one enjoys better benefits, but from the other hand, three items of this device are needed to cover the three axis measurements, and that means three times the price of the 3-axis rival. At this point the decision to make was not easy, and numerous options came out. The first one was that to go for the cheap solution, and accept the lack of precision and shorter frequency range. Another suggestion made was that of choosing which axis are the most important for the vibration analysis, and therefore avoid to buy three sensors. Another choice finally, was that of making a deep theoretical analysis to find out if the resulting expected outputs will require that level precision or not. When it was being made an assessment of the decision to take, suddenly a new advantageous option came out. It was found that PCB offers the possibility of renting equipment for weeks or months, and all the components of the team agreed on this solution. The plan was to proceed with JetCat testing, and when time for vibrations analysis is getting close, three 1-axis sensors can be rent.

Data acquisition system

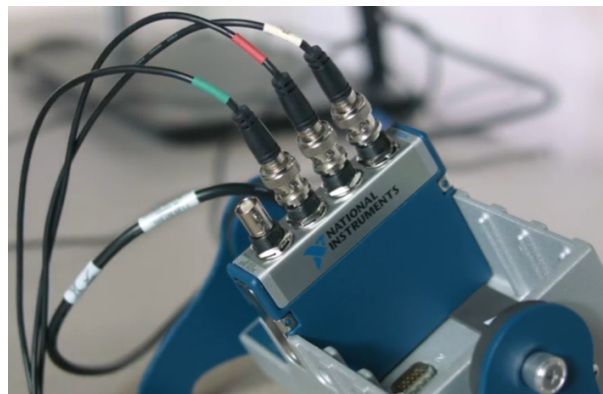
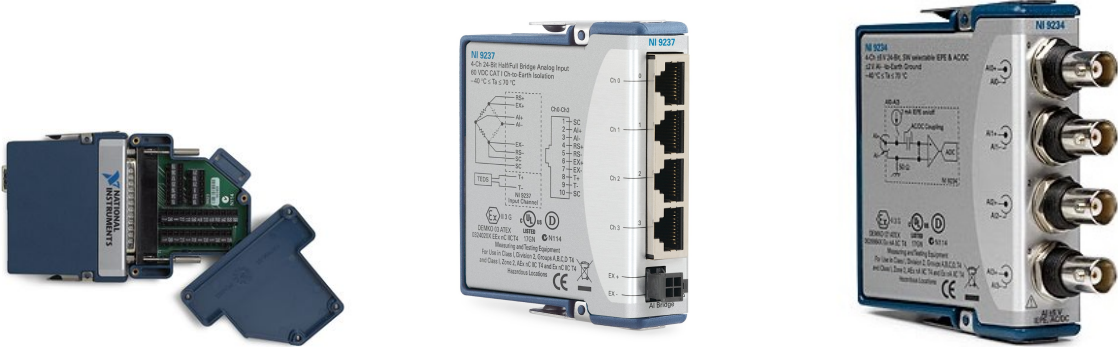


Figure 4.13: National Instruments cDAQ board.

Once again, as for the EDF testing (see section 3.6), the data acquisition system selected is represented by National instrument devices (Figure 4.13). The choice was confirmed after the high performance of the latter during the previous tests. The NI modules instead, are not all the same, in fact it will be used NI 9234 (Figure 4.14 c)to detect vibrations instead of the NI 9401 used for digital communication protocols.



(a) Internal combustion engine. (b) Electric Ducted Fan. (c) Gas Turbine for UAVs.

Figure 4.14: National Instruments modules.

Fuel tank and feed system

JetCat products are all provided with a fuel pump, and concerning the P500, this has it even integrated in the casing. The fuel lines are supplied buy the house as well, and the only missing component from the feed system before start running the engine results to be the fuel tank. As said previously, the first option proposed was to use a marine tank, but searching deeply, it came out that these type of tanks are made only for gasoline purposes, and in case of kerosene storage, the latter will be contaminated. This discovery brought the team to start seeking another alternative. The research concluded selecting an alluminium fuel tank from BoydWelding company (Figure 4.15).



Figure 4.15: Test rig Fuel tank.

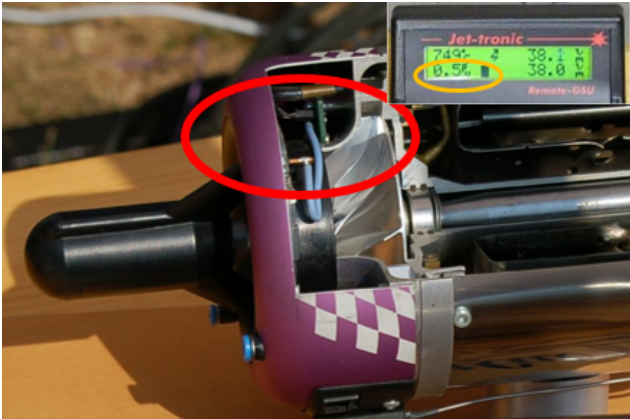
The chosen tank satisfies the minimum features required, in fact it had the required rectangular shape, 15 gallon volume and capable of storing kerosene for long term. Furthermore, it was chosen to buy a high quality one also to guarantee the longevity of the device in order to make use of it in future projects too.

Another additional device introduced in the line was the Air Trap. This accessory avoids the presence of air bubbles in the fuel line, and in addition works also as filter (Figure 4.16).

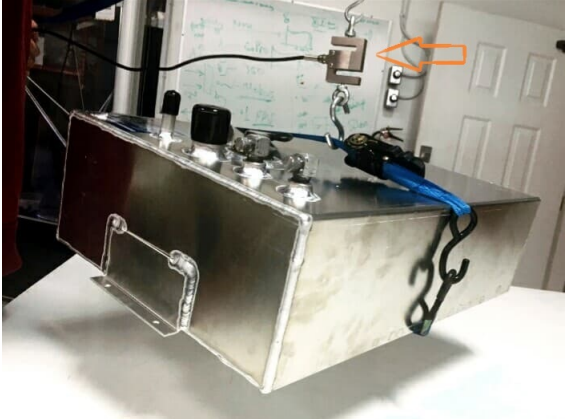


Figure 4.16: Fuel line air trap.

One more component was required, the flow-meter. This device is not necessary for the correct functioning of the apparatus, but was needed for fuel consumption measurements. After few researches it has been decided to avoid buying one, and use simple alternatives. First of all, the ECU of the JetCat is supposed to give in output an estimation of the fuel consumption. However, since there is no flow-meter either inside the engine or in the fuel line, it was obvious that the only way to give that information was through the measurement of fuel pump voltage (see Figure 4.17 a). This kind of calculation is not that accurate, and this led to seek a better alternative, at least to compare with ECU evaluation. After a several proposals from the team components, it was decided to go for the simplest idea, use a load cell to weigh the fuel tank while testing. This concept shown in Figure 4.17 b is as simple as effective, and the presence of numerous load cell at CfAR shop made the solution inexpensive.



(a) Fuel pump voltage measurement.



(b) Load cell mechanism for fuel consumption.

Figure 4.17: Alternatives to flow-meter sensor.

Safety stop button system

The last system to be described, but probably the most important, is the safety measures. To deal with such powerful engines is highly risky, and requires absolutely different levels of prevention. First of all, it is already confirmed the presence of two fire extinguishers (CO2 type as specified by JetCat manual present in *Appendix B*), one close to the engine and the other on the computer station.

Once again, as for the EDF testing, the presence of a manual stop button was retained mandatory. This time though, it was decided to make it in metal instead of wood to prevent it from catching fire since it will be mounted on the engine table. The stop button itself was easy to make, but the main issue has been where to install it exactly. At the beginning, they were suggested to options:

- Option A. This choice consisted of allowing the stop button to cut the connection between the Pro interface and the engines. This interruption of the signal may stop the engine;
- Option B. This preference instead, acts on the power line of the Pro interface, therefore, interrupting the power interface (thus the engine also) will stop running.

The two options were considered both applicable. Nevertheless, reading delicately the manual, it was found that JetCat strongly recommend not to interrupt either signal or feeding from and to interface (in particular from the pro interface to the engines). Luckily, it was found also that the Pro interface is provided with a little shut off pin, reason why the stop button will be positioned there without fear of running into malfunctions. The scheme given in Figure 4.18 explains what have been said so far.

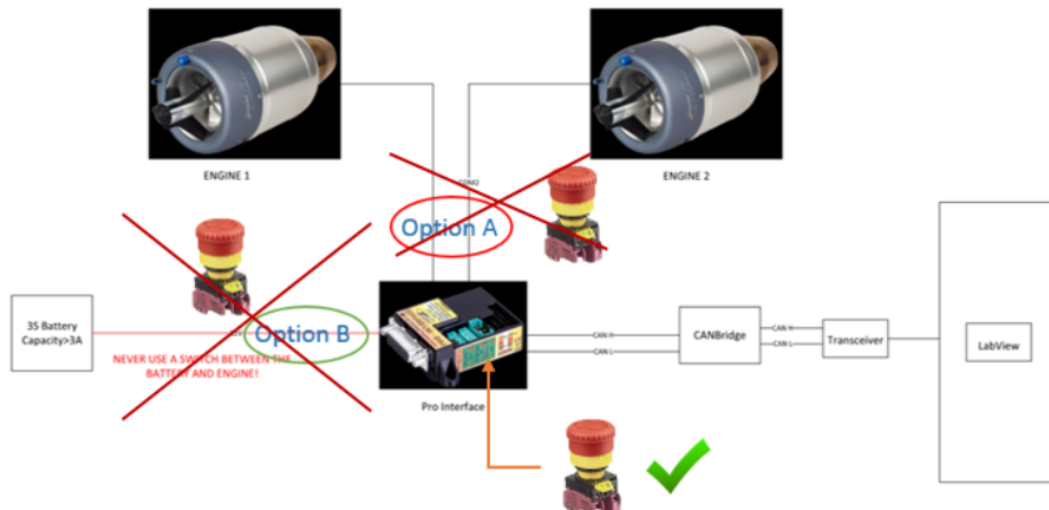


Figure 4.18: Stop button location.

Finally, before start any of the planned tests, there is a checklist to be filled out. This important document is not ready yet since it must be carefully reviewed when all the wiring and devices are set up. A first version is given in the *Appendix B*.

4.5 Software Development

In this part it will be shown which software will be used during and after tests, and will be also given a first version of what the graphic interface will look like. To conclude, they will be delineated the further developments that the interface will have. Before start describing the software, it is appropriate to take a look to the diagram present in Figure 4.19.

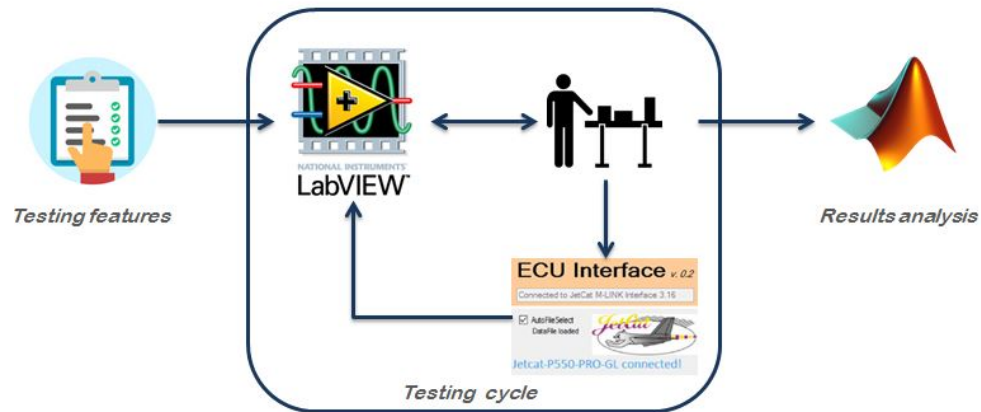


Figure 4.19: Multidisciplinary proces for JetCat tests.

Moving from left to right, the starting point is represented by testing features. The requirements and desired outputs mark the characteristics of testing, and therefore also those of the graphic user interface. The latter is made by LabView program, and as the diagram shows, this interact with other two components : test bench and JetCat ECU interface. The first one has a bipolar interaction, in fact Labview gives commands in output towards test bench devices, but ad the same time receives in input acquired measurements. The communication with the ECU interface program is different, in fact the latter is working as an interface between the JetCat engine and Labview.

Regardless the data is coming from the test rig apparatus, or pass through the ECU program, all the received information is saved on the computer to be processed at a later time. The program involved in the analysis of this logged data will be in the foreground Matlab (last step of the diagram to the right). So far only the LabView GUI has been designed, and still in need of further tests and upgrades. Concerning Matlab program, it was considered time taking the design of data processor before obtaining the data their selves. This makes sense since most of times process of testing is altered by unexpected factors, and the acquired data may shift from what have been planned.

4.5.1 LabView GUI Design

The graphic user interface is an important tool to send commands and signals to the test bench equipment as well as record collected data. In this project, there was the necessity of creating a new GUI since it was not made one for this typology of tests. The process of software design had also the purpose of provide CfAR a useful tool to be used whenever similar tests are made, reason way is it must be as accurate as general to fit any future application.

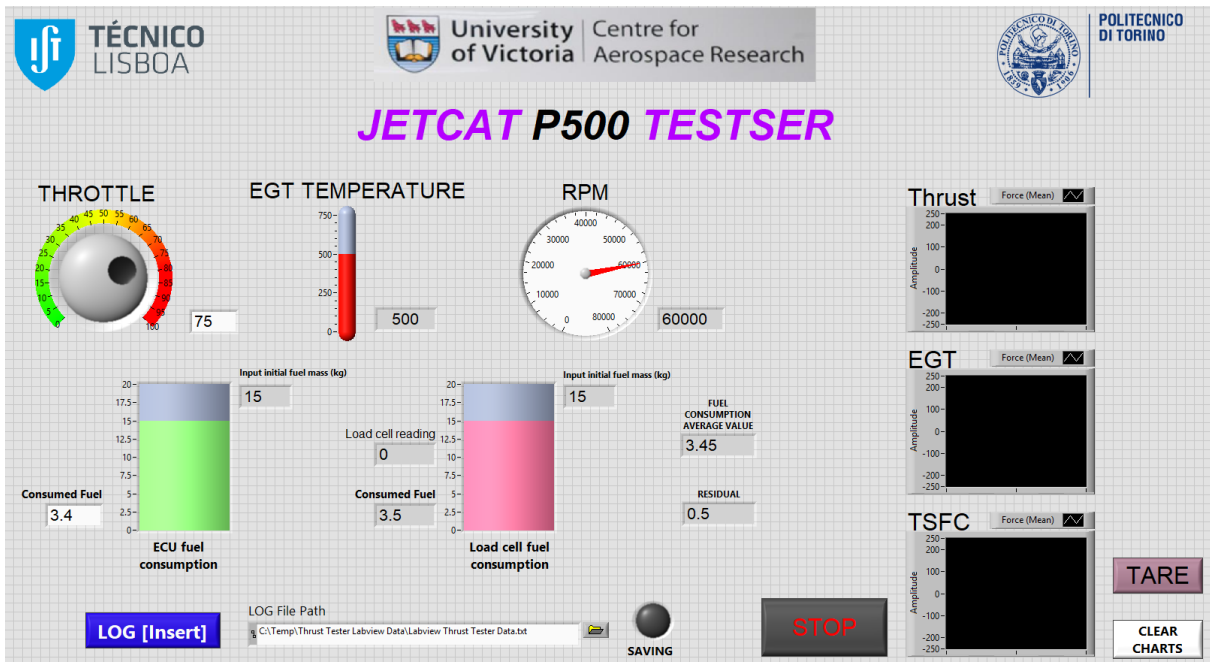


Figure 4.20: LabVIEW GUI for JetCat testing.

After taking care of all the requirements given, the resulting GUI is the one shown above (Figure 4.20). The principal components of this GUI are:

- Throttle knob. Using this gadget it will be possible to send signal to the Pro interface that in turn will send to the engine. All the values used during the tests are recorded if button "LOG" is pressed;
- EGT Temperature thermometer. This element will be showing the temperature relieved by the JetCat sensor which will be given by ECU interface program to LabView;
- RPM indicator. As per the previous one, this data from the ECU interface program, but this time the measurement is the RPM of the engine shaft.
- Fuel tank indicators. Is possible to notice in Figure 4.20 that there are two fuel tanks indicators. This is because, at least in the beginning, they will be used two methods to obtain fuel consumption parameter. For now it will used an average value, and after few more tests, if the two values match, it will be removed the one relative to load cell mechanism (see section4.4.3);
- LOG button. This button, with the log file path, allows to record the acquired data. When this is pressed, a green led present to the right of the path become green, indicating that data is getting recorded;
- Charts. The three charts have the purpose to show in real time the respective readings. The TSFC one in particular, is showing the average values of fuel consumption after being computed to obtain the Thrust Specific Fuel Consumption;
- STOP, TARE and CLEAR CHART buttons. The job of these switches is predictable from their names.

The program just explained was tested only in part, and that because the tests have not been done yet. Actually what have been explained above is not the definitive version, and the GUI is still under upgrades.

To conclude, it must be said that tests will not start directly with this version, but will be used other variants simpler in order to test first all the apparatus, and then proceed with the upgrades (see the next chapter, section 5.2.1).

4.6 Experimental Set Up

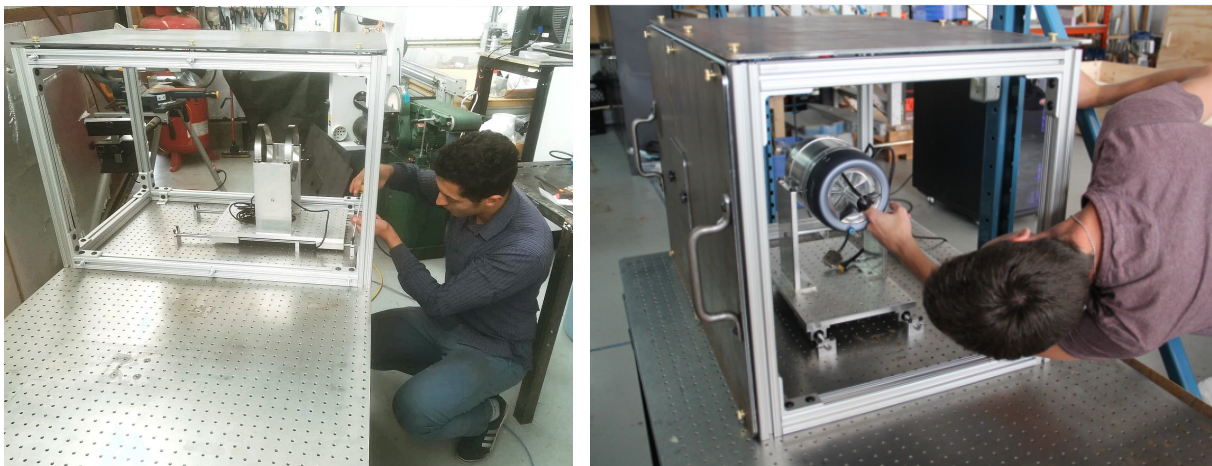


Figure 4.21: Test bench set up.

After planning everything, and purchasing all the designed components, it was time to finally set up the test bench. The installation of all the components was done on one of CfAR's optical table. Once again, it was chosen one of these tables because of the features of the rigid surface with minimum deflection so that the alignment of the elements remains stable over time. The arrangement of the different components was easily accomplished thanks to the video guide made by CfAR in the previous year. Following step by step all the documentation made during the CAD design stage, the test rig was ready in few days. The cage has been first mounted on another table to test fit it, and later on, was moved to the dedicated one. Moreover, it is noteworthy that the collocation on the table has been modified from the designed one in order to satisfy other instrumentation location as well as wiring. Finally, it must be said that all the components have been tested one by one during the assembling, and no trouble occurred.

A new issue occurred during the set up was the fuel tank location. At the end, it was chosen to put it below the test table for the following reasons:

- to protect it from any unexpected events;
- to reduce fuel lines length;
- to fit the load cell mechanism for fuel consumption measurement.

Finally, after arranging each component at its place, the resulting test rig is given in Figure 4.22.

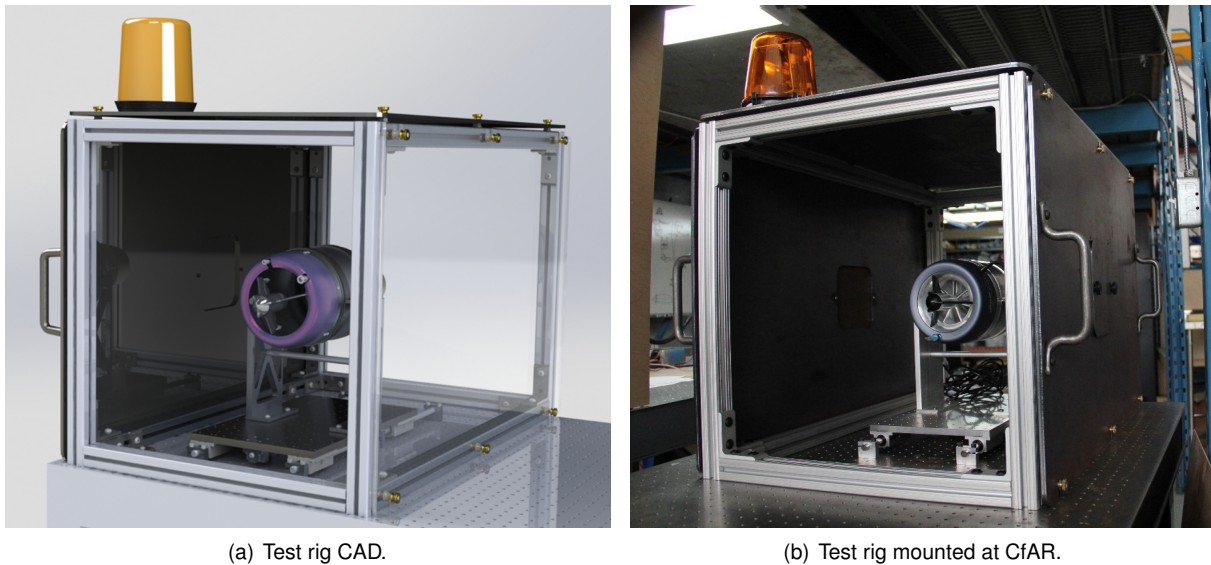


Figure 4.22: Test rig realization.

4.7 Concluding Remarks

The overall design of JetCat test rig was more than satisfactory, and the resulting test rig was matching most of the requirements made during preliminary design phase. In the set up stage, all the components were fitting perfectly, meaning that tolerances were made with a high level of accuracy, as well as the machining made by third parties.

Regarding the equipment and sensors, most of them are now available at CfAR, and ready to be used on the test rig once the tests will be ready to run. Regrettably, the tests were not performed in the arch of time reserved for this thesis work. This was principally due to delays either from third parties machining or shipping times. Is right though, to assume a bit of own responsibility, as some delays were caused by design mistakes or delays in the equipment selection.

However, it must be said as well that design in general "enjoys" the feature of being unpredictable and challenging. These characteristics are those which make engineers' work and effort worthy.

In the overall, it is appropriate to appreciate the satisfactory results obtained, and keep working on the remaining parts of the requirements, and move forward with testing. Some of the planned test are proposed in the next chapter, section 5.2.

Chapter 5

Future Work and Reccomandations

Is always a good practice to give an idea about the future advancements, both to use it as a starting point for the upcoming project tasks, but also to complete the picture of argument treated.

This chapter will be presenting possible improvements and continuation regarding what have been already done for both propulsion systems. Each section will give an overview of both testing and software expected developments.

5.1 EDF motor

5.1.1 Software Updates

In regard to the EDF motors, the main expected developments are concerning the satisfaction of the partial completed requirements. The main tasks remained incomplete are the testing of the EDF motors using the new cRIO data acquisition board (Figure 5.1). The benefit from using this new device of the National Instrument is the possibility of working with real time signals both in Input and output, without the constraint of dealing with computer processor lags. In detail, this new data acquisition apparatus allows the user to send signals that are not affected by delays or lags thanks to the presence of a little processor inside the board itself, enabling the device to make its own time sampling.



Figure 5.1: cRIO data acquisition system.

The direct consequence from using this type of communication is the possibility of start studying the time response of the engine, and therefore, transaction phase after receiving the command signal. If has been noticed, the chapter 3 treated only average values for all the examination performed, thus being a static analysis.

The presence of this new device required certain updates on the software side. However, instead of modifying the existing LabVIEW GUI, it has been decided to design a new one. The reason behind that was to avoid dealing with the previous program bugs, and make a new one capable of satisfying only the required duty. The materialization of this software was by another team member, and the resulting interface is given in Figure 5.2.

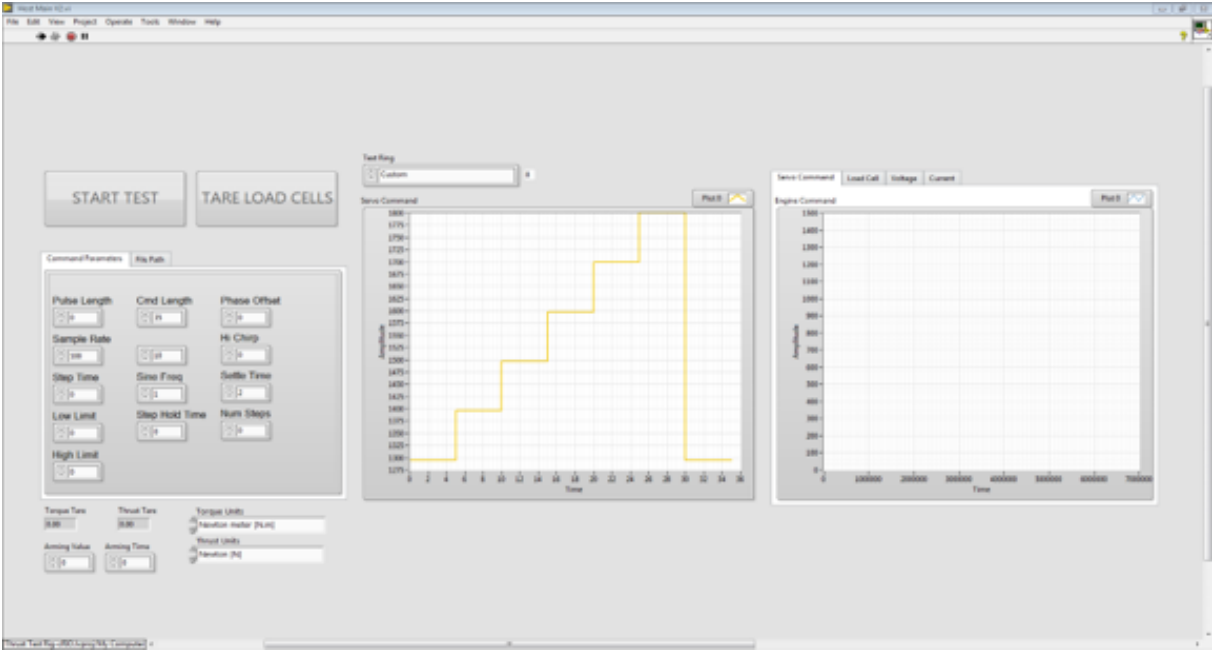


Figure 5.2: New LabVIEW GUI for EDF testing.

5.1.2 Testing

In connection with the software development, for sure it will be a continuation of testing. After checking both the correct functioning of the new cRIO device, and the corresponding graphic user interface, further tests will be performed. The foremost experiments are itemized below:

- Check the transient response of the EDF motor;
- Test the vibration behaviour when the EDF motor is mounted on the FTV7%. This means also to provide suitable accelerometers to stick on the motor instead of counting only on load cell measurement as done previously;
- Make thrust tests with the engine integrated on the plane for better mapping.

If all these tests are performed properly, a significant improvement of Simulink model is expected.

5.2 Turbine Jet Engine

A few ideas for JetCat testing are given since no test occurred so far. The choice of which test to perform has been made in order to satisfy BA requirements. Concerning the software updates, this is suggested by the author in order to improve the GUI before and during testing.

5.2.1 Software Updates

The main updates suggested here are still regarding the LabVIEW interface program. In the previous chapter (section 4.5.1), a first version has been already presented. Nevertheless, as for all programs, it needs to be always updated before reaching completeness. Furthermore, it must be said that it has been considered a bit risky to start working directly with the GUI, and it was preferred instead to go through stages as shown in the list below:

1. phase: The first tests will be executed using LabVIEW only for Load cell reading, while other variables like temperature, RPM and Voltage (for fuel consumption measurement) must be inserted manually. The commands to control the engine are sent from through the JrtCat GSU.
2. phase: Connect the JetCat interface to LabVIEW and upgrade the interface to interact with JetCat sensors in real time thanks to ECU program interface. Furthermore, will be tried to communicate straight way with the engine without resorting to the GSU;
3. phase: Introduce the piezoelectric sensors to the testing for vibrations detection. This may require a further update of the program introducing also vibrations reading and recording the correspondent data;
4. phase: Introduce the can bus in the wiring harness since they will be used on board the aircraft. Check that the GUI is working properly, and is not affected by the presence of this new system.

All these updates will be later followed by the implementation of a Matlab code to process the logged data. As explained in advance, there is no need to propose a preliminary version of the Matlab program before acquiring the test results.

5.2.2 Testing

At the end of chapter 4 it was stated that the test rig is almost ready to start the tests. This is true, in fact the only things missing are the wiring, the review of the checklist (given in *Appendix B*) and fuel. Once all these three tasks are completed, the engine can start running. However, it has been chosen to start with checking the engine response to the command sent without firing the engine. After that, the fuel system must be tested as well, and when all this is achieved, the JetCat testing can take place at CfAR. Here are briefly the main tests that hopefully will be running in the upcoming months.

Single Engine Thrust Test

This is the main test, and it is needed to map the engine as done previously with the EDF motor. The aim from this tests is to map the engine, and understand its behaviour to familiarize with it before mount it on board of the plane. Furthermore, is always a good practice to check the accuracy of the data sheet specifications.

Feeding System Tests

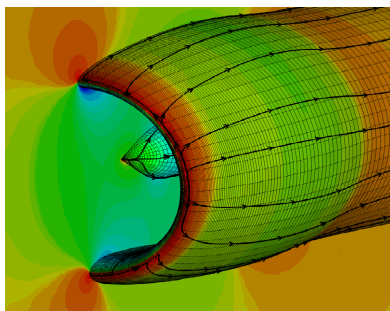
The following test is a continuation of the preliminary one mentioned above. The main objectives this time is to demonstrate that the feeding system can is working properly also in presence of bubbles in the fuel line as well as check the Jetcat response to such phenomena. Moreover, it is intended to try also different positions and inclination of the fuel tank to simulate typical flight situations.

Nacelle Tests

The Nacelle is the housing of the engine, and must be certainly tested. The planned test for regarding this components are two:

- Intake test. This is needed to check the influence of the presence of the nacelle on the normal performance of the isolated engine. A wrong position of the nacelle with respect to the coming air floe may reduce drastically the operation of the engine. In the same way though, a bad design of the internal walls may cause phenomena of circulation or even stagnation. All these aspects require deep investigation;
- Thermal testing. Since the engine in question is an internal combustion turbine, is opportune to test the resistance of the nacelle to the high temperatures that the engine may achieve when running at maximum power.

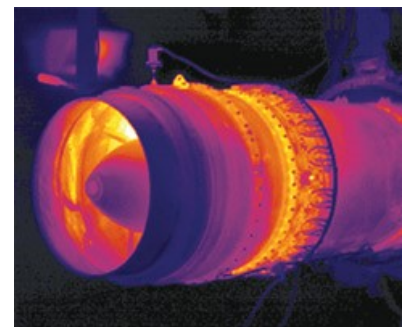
An idea of the tests outputs is given by Figure 5.3



(a) Intake testing output.



(b) Jetcat nacelle.



(c) Thermal testing.

Figure 5.3: Nacelle tests.

Dual Engine Control

Another important test, that has been omitted for the FTV7%, is that of testing two engines at the same time (Figure 5.4). The importance of this tests lies on the fact that although the two engines will be synchronized by the autopilot, problems may occur if there is something wrong with the feeding system. This problem did not appear for EDFs since the electric power is pretty reliable in these circumstances, while the pipes a bit less. Once these tests will be all done, and the results will be satisfying, it could be given the allowance to be mounted on board the FTV16.5%.

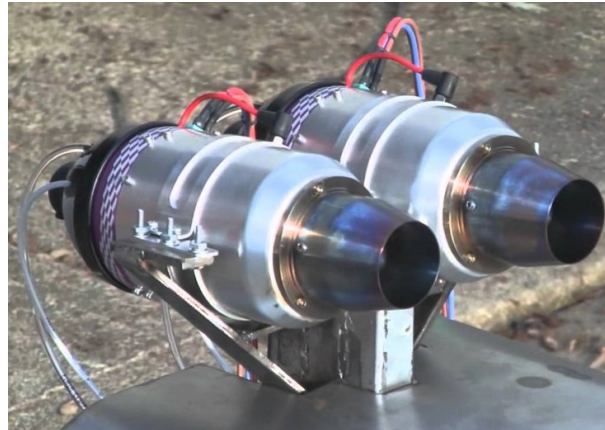


Figure 5.4: Dual Engine Control.

Integrated Engines Thrust Test

The final test before flight tests will be probably the integrated engines thrust tests. These are a good mean to check if the propulsion system is working properly on the aircraft, and above all, that there is no interference between this and the other systems on board. The execution of this kind of test will be pretty hard given the size of the aircraft, therefore it probable that third parties will take care of that, letting the CfAR team take care of the analysis of the results.

5.3 Recommendations

Being working on parallel with two different propulsion systems was a good opportunity to understand the diversity and similarities between MTEs and EDF motors. Furthermore, is noteworthy how different is the procedure to equip the test rig for the two systems, although they are expecting more or less the same outcomes.

There are several lessons learnt from both experiences, but the main one has to deal with the JetCat test rig design. As said in the design section of chapter 4, during the design phase, it must be always choices to make, and one of them was that of building a customized test bench instead of buying one. The success of the resulting test rig is indisputable, but what about the time it took to achieve the readiness? This aspect is still questionable as it was when the decision has been made.

Chapter 6

Conclusions

The thesis work started with the objective of testing and characterize the two propulsion systems of both FTV7% and FTV16.5%. To achieve that, it was required to start a test bench design and development for both systems. In the case of EDF motors, luckily the test was almost ready, and few adaptations have been made before proceed with testing. From the other hand, the JetCat test rig did not exist yet, and was made from the bottom brick. However, at the end of the work, both test rigs were ready and have met all the pre-established requirements.

Unfortunately, although all the efforts on the readiness of the JetCat rig, it was not possible to start testing within the available time for the present dissertation. Nevertheless, a little chapter has been dedicated to describe the upcoming tests.

Returning to the EDF part, here the test have been performed with success, and lots of fascinating results have been achieved. Despite this good results, it was appropriate to suggest further developments in order to improve even more the model already made.

In conclusion it must be admitted the difficulty of designing respect to testing, at least in this experience after the enormous effort and time dedicated to JetCat project. All this may not stop CfAR engineers from moving forward on their design tasks, making every challenge encountered, just a step before triumph.

Bibliography

- [1] ICAO. Unmanned Aircraft Systems. *ICAO's circular 328 AN/190*, 2016.
- [2] Y. Gibbs. Past projects: X-48b blended wing body. <https://www.nasa.gov/centers/dryden/research/X-48B/index.html>, 2017. [Online; accessed on March 2019].
- [3] Bombardier and Q. Aerospace. Horizon - flying demo specs for the new generation ftv. 2018.
- [4] CfAR and Q. Aerospace. Bba 7pcnt (operational documentation and scaling process). 2018.
- [5] K. S. Shrikrishna Sane. Experimental characterization of propulsion system for mini aerial vehicle. 2004.
- [6] A. Tiwari. Slideshare - testbench development. https://www.slideshare.net/Abhishekt11/test-bench-development?qid=b4b3d26c-3add-4afd-b236-583e4e26960d&v=&b=&from_search=7, March 2011. [Online; accessed on October 2019].
- [7] M. Adamski. Analysis of propulsion systems of unmanned aerial vehicles. <https://doi.org/10.1080/20464177.2017.1383337>, 2017. [Online; accessed on October 2019].
- [8] A. Akturk and C. Camci. Experimental and Computational Assessment of a Ducted-Fan Rotor Flow Model. <https://arc.aiaa.org/doi/10.2514/1.C031562>. JOURNAL OF AIRCRAFT, Vol. 49, No. 3, Pennsylvania State University, May–June, 2012, [Online; accessed on October 2019].
- [9] P. C. R.A. Sharman, B.Sc. Electric ducted fan – theory and practice. <https://www.rcgroups.com/forums/attachment.php?attachmentid=6384145>, 2006. UNIVERSITY COLLEGE UNIVERSITY OF NEW SOUTH WALES, 7 October, 2006, [Online; accessed on October 2019].
- [10] V. Prisacariu. Flying wing with electric ducted fan (edf) propulsion. https://www.researchgate.net/publication/308607927_Flying_wing_with_Electric_Ducted_Fan_EDF_propulsion, 2013. [Online; accessed on October 2019].
- [11] J. Longbottom. Investigation into the reduction of the drag area of a paramotor. <https://www.rcgroups.com/forums/attachment.php?attachmentid=6384145>. chapter 4 UNIVERSITY COLLEGE UNIVERSITY OF NEW SOUTH WALES, 7 October, 2006, [Online; accessed on October 2019].

- [12] P. Bjarnholt. Electric propulsion in passenger jet airplanes. <https://www.diva-portal.org/smash/get/diva2:1115014/FULLTEXT01.pdf>. chapter 2, paragraph 4, KTH School of Industrial Engineering and Management, 5 October 2014, [Online; accessed on October 2019].
- [13] M. Boyce. *Gas Turbine Engineering Hand Book, Second edition*, volume pp. 55–56. Butterworth-Heinemann, 2002.
- [14] T. Nada. Performance characterization of different configurations of gas turbine engines. <https://www.sciencedirect.com/science/article/pii/S2212540X14000571>. chapter 2, National Authority of Remote Sensing and Space Sciences, Cairo, PO box 1564 Alf-Maskan, Egypt, 2016, [Online; accessed on October 2019].
- [15] J. F. W. Naveed Ur Rahman. A numerical investigation into the effect of engine bleed on performance of a single-spool turbojet engine. <https://www.semanticscholar.org/paper/A-numerical-investigation-into-the-effect-of-engine-Rahman-Whidborne/e1fd3152edfea272fb26c6b1fab2d9bfd36b0532>. chapter 2, Dynamics Simulations and Controls Group, Cranfield University, Bedfordshire, UK, 2008, [Online; accessed on October 2019].
- [16] R. L. Daugherty. *Fluid mechanics with engineering applications*. McGraw Hill, New York, 1997.
- [17] J. Dutczak. Micro turbine engines for drones propulsion. <https://iopscience.iop.org/article/10.1088/1757-899X/148/1/012063/pdf>. IOP Conf. Ser.: Mater. Sci. Eng. 148 012063, 2016, [Online; accessed on October 2019].
- [18] K. Schreckling. *Gas Turbines for Model Aircraft*. Taplet publication limited, 1994.
- [19] P. D. I. R. Decuyper and I. D. Verstraete. Micro turbines from the standpoint of potential users. <https://pdfs.semanticscholar.org/1c80/8e3c8d6db53de9632630be5abfa101bb41ea.pdf>. Royal Military Academy of Belgium Applied Fluid Mechanics Department (MFTA) , 2005, [Online; accessed on October 2019].
- [20] S. T. GmbH. <http://schuebeler-technologies.de/en/>. [Online; accessed on October 2019].
- [21] J. Richards. Edf simulink block used for 7% simulation. 2018.
- [22] S. Vorkoetter. An electronic speed control primer. <http://www.stefanv.com/electronics/escprimer.html>. Sailplane Electric Modeler Magazine , 1997, [Online; accessed on October 2019].
- [23] N. Instruments. http://www.ni.com/pdf/manuals/378020a_02.pdf, . [Online; accessed on October 2019].
- [24] N. Instruments. <https://www.ni.com/en-ca/support/model.ni-9401.html>, . [Online; accessed on October 2019].
- [25] N. Instruments. <http://www.ni.com/en-ca/support/model.ni-9237.html>, . [Online; accessed on October 2019].

- [26] N. Instruments. <https://www.ni.com/en-ca/support/model.ni-9205.html>, . [Online; accessed on October 2019].
- [27] Jetcat. <https://www.jetcat.de/en/productdetails/produkte/jetcat/produkte/Professionell/P550%20PRO%20-%20GH>. [Online; accessed on October 2019].
- [28] C. Team. https://www.colorado.edu/aerospace/sites/default/files/attached-files/COMET_PDR.pdf. Colorado University, 2013, [Online; accessed on October 2019].
- [29] P. M. f. f. s. a. H. Thomas Kleckers. <https://www.hbm.com/en/6810/selection-guide-for-piezo-sensors/>. [Online; accessed on October 2019].

Appendix A

EDF Documentation & Software

A.1 Coupled Electric Motor and EDF Aerodynamics Model

Port Name	Units	Description
Motor Params		
Kv Rating	RPM/V	Motor characteristic, will be supplied by CfAR
No Load Current	A	Motor characteristic, will be supplied by CfAR
Armature Resistance	Ohm	Motor characteristic, will be supplied by CfAR
Motor Vis Drag	Nms	Motor characteristic, typically not used
Motor Inertia	Kgm2	Motor characteristic, will be supplied by CfAR
EDF Parameters		
EDF Structure	n/a	This should not be changed here. It is referencing a workspace variable (a matlab structure) that represents the EDF. This will be supplied with the block but will need to be opened in the workspace when the block or aircraft model is opened. For example, if a starting script is run on launching of simulator then the command <code>'load('HSD51_EDF_params_for_Simulink.mat')</code> could be added to load the "EDF_Params" variable corresponding the the HSD51 EDF to the workspace
Motor Direction	n/a	This value should only be set to 0 or 1. If set to 0 then it is assumed that the EDF will spin clockwise when viewed from behind the aircraft and if set to 1 then the EDF is spinning counterclockwise when viewed from behind
Fan Inertia	Kgm2	EDF characteristic, will be supplied by CfAR
EDF Thrust Line	degrees	[2x1] vector where the first entry corresponds to the down thrust of the motor axis and the second entry corresponds to the pan of the motor (+ve would point the engine left)
Battery Parameters		
Number of Cells	n/a	Motor characteristic, will be supplied by CfAR (typically 12 for 7%)
Nominal Voltage per Cell	V	When the battery is fully charged it is typically ~4V (ie right at launch). During most of the flight it will be around its nominal value of 3.7V until it starts to run out at which point it could drop down to 3.2-3.5V
Cell Resistance	Ohm	Battery characteristic, will be supplied by CfAR

Figure A.1: Block's mask parameters [21].

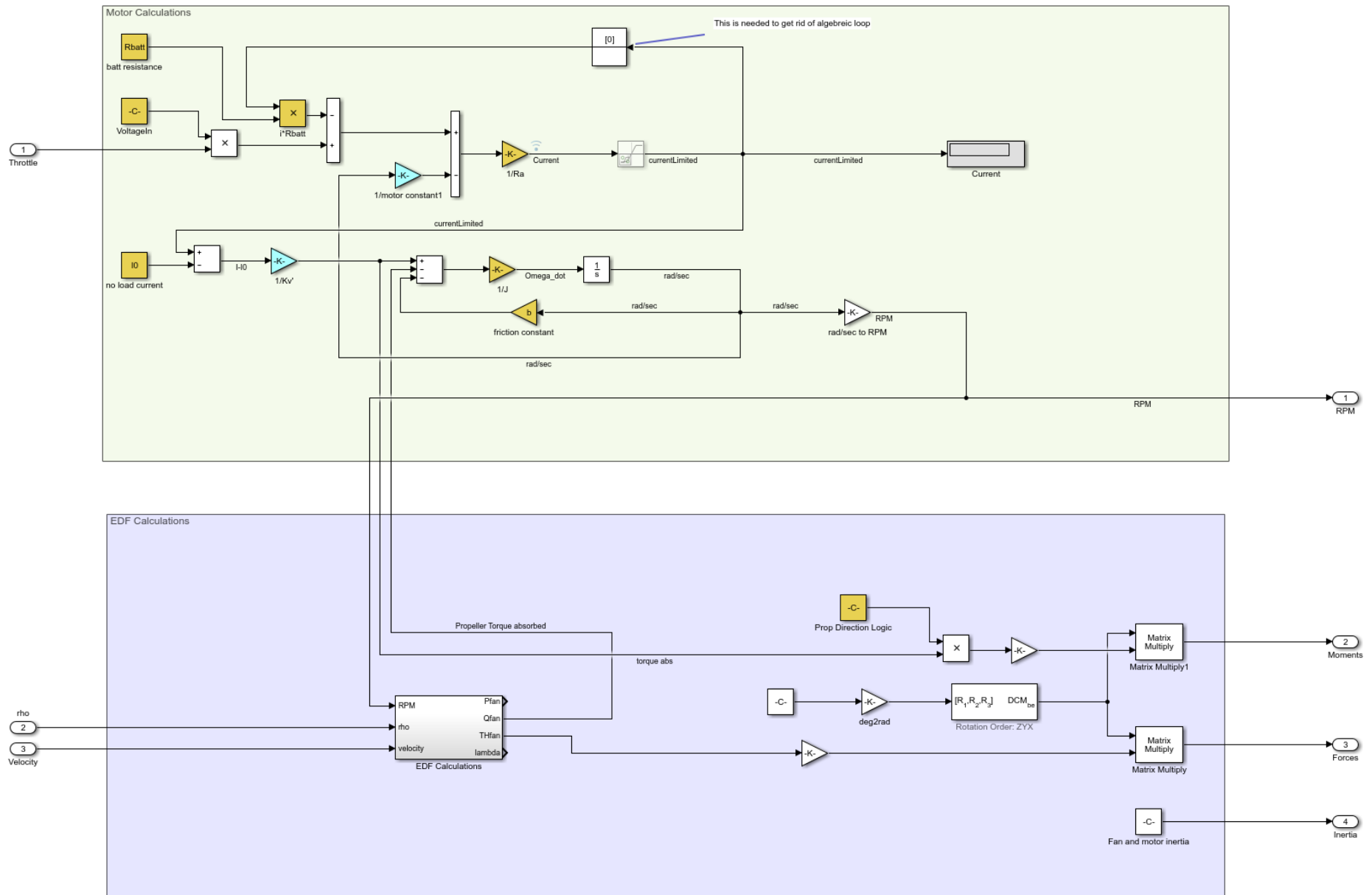


Figure A.2: Simulink diagram [21].

A.2 Matlab script

```
1 %% EDF Schubeler ds-51-axi Matlab tool %%
2
3 % The program consists of 4 parts
4
5 % – Normalized Thrust vs Throttle ;
6 % – Throttle vs Normalized Thrust;
7 % – RPM calculation from Castlelink logged data for the Test 1a;
8 % – Vibration analysis.
9
10 %% Normalized Thrust vs Throttle
11
12 % the following code creates a table with 3 columns and n rows containing
13 % throttle , normalized thrust and Real thrust;
14
15 clc
16 clear all
17
18 n= 100; % Select the number of steps between initial
19 Throttle_vector=linspace(0,100,n); % and final value of throttle
20
21 max_thrust= 44.77;
22 p1 = -2.4207e-08; % Coefficients obtained from fitting the
23 p2 = 3.3848e-06; % experimental curve;
24 p3 = -7.3797e-05;
25 p4 = 0.0073929;
26 p5 = 0.0064605;
27 fitted_y = @(x) p1*x.^4 + p2*x.^3 + p3*x.^2 + p4*x + p5;
28
29 ThrustF_vector = fitted_y(Throttle_vector);
30 Table_Throttle_vs_Thrust = [Throttle_vector; ThrustF_vector ;
31 ThrustF_vector*max_thrust ]';
32
33 Table_Throttle_vs_Thrust(1,2:3)= 0;
34
35 figure
36 hold on
37 plot(Table_Throttle_vs_Thrust(:,1), Table_Throttle_vs_Thrust(:,2) , 'r', '
38 LineWidth',1, 'DisplayName', 'Fitted 4th grad');
```

```

36 grid on;
37 legend ( 'Location', 'southeast', 'FontSize',10);
38 title ( 'Normalized Thrust vs Throttle' );
39 xlabel( 'Throttle %' );
40 ylabel( 'Normalized Thrust' );
41
42 %% Throttle vs Normalized Thrust
43
44 % the following code creates a table with 3 columns and n rows containing
45 % normalized thrust, Real thrust and throttle;
46
47 clc
48 clear all
49
50 n= 100; % Select the number of steps between initial and
51 Thrust_vector = linspace(0,1,n); % final value of Norm thrust
52
53 max_thrust= 44.77;
54 p1 = 163.09; %Coefficients obtained by fitting the experimental curve;
55 p2 = -190.92;
56 p3 = -12.301;
57 p4 = 141.29;
58 p5 = -0.63167;
59
60 fitted_y_inv = @(x_inv) p1*x_inv.^4 + p2*x_inv.^3 + p3*x_inv.^2 + p4*x_inv
+ p5;
61
62 ThrottleF_vector = fitted_y_inv(Thrust_vector);
63 Table_Thrust_vs_Throttle = [Thrust_vector; Thrust_vector*max_thrust ;
ThrottleF_vector ]';
64 Table_Thrust_vs_Throttle(1,3)= 0;
65
66 figure
67 hold on
68 plot(Thrust_vector , ThrottleF_vector , 'r', 'LineWidth',1, 'DisplayName', '
Fitted 4th grad');
69 grid on;
70 legend ( 'Location', 'southeast', 'FontSize',10);
71 title ( 'Normalized Thrust vs Throttle' );

```

```

72 xlabel('Throttle %');
73 ylabel('Normalized Thrust');
74
75 %% RPM from Castle Link
76
77 % This part of code I sent you is to let you check if I have done any error
78 % in calculating RPMs from CastLink logged data for test 1a
79
80 clc
81 clear all
82
83 RPM = 7;
84 throttle = 2;
85 s= 10;
86
87 load('matlabCastleLink1a.mat');
88 Throt= 10:10:100;
89 Castle_throttle = [9.804 19.608 29.804 40 49.804 60 70.196 80 90.196 100];
90 average_rpm= zeros(1,s);
91
92 for i = 1:10
93 p= find(Castlelink_data(:,throttle)== Castle_throttle(i));
94 rpm_vect = Castlelink_data(p(1):p(end),RPM);
95 average_rpm(i)= round(mean(rpm_vect),-2)/2;
96 end
97
98 Tabele_RPM = [Throt; average_rpm ]'
99
100 %% Vibration analysis
101
102 % the following program get data acquired from labVIEW in input, and plots
103 % vibration graphs in both time and frequency domain
104
105 clc
106 clear all
107
108 THRO = 2;
109 t = 5;
110 A = 6;

```

```

111 V = 8;
112 TOR = 10;
113 THRU = 12;
114 PWM = 4;
115 RPM = 18;
116
117 cut0= find(LabviewThrustTesterData10a(:,THRO)== 100);
118 cut1= find(LabviewThrustTesterData10b(:,THRO)== 100);
119
120 dataSelect_a = LabviewThrustTesterData10a(1:cut0(end),:);
121 dataSelect_b = LabviewThrustTesterData10b(1:cut1(end),:);
122
123 throt= 100 ; % insert the desired throttle
124 Ts= 0.0001; % Data acquisition sampling
125 Fs= 1/Ts;
126
127 %10a
128
129 m=find(dataSelect_a(:,THRO)== throt);
130 lung_a = length(m);
131 time_a = dataSelect_a(m(1):m(end),t);
132 Tf= round((time_a(end) - time_a(1)),7);
133 dt_a = 0:Ts:Tf;
134 y_fft_a = dataSelect_a(m(1):m(end),TOR);
135 y_fft_a= detrend(y_fft_a, 'constant');
136 nfft_a = length(y_fft_a);
137 nfft2_a = 2^nextpow2(nfft_a);
138 ff_a = fft(y_fft_a, nfft2_a);
139 fff_a = ff_a(1:nfft2_a/2);
140 xfft_a= Fs*(0:nfft2_a/2-1)/nfft2_a;
141
142 %10b
143
144 m=find(dataSelect_b(:,THRO)== throt);
145 lung_b = length(m);
146 time_b = dataSelect_b(m(1):m(end),t);
147 Tf_b= round((time_b(end) - time_b(1)),7);
148 dt_b = 0:Ts:Tf_b;
149 y_fft_b = dataSelect_b(m(1):m(end),TOR);

```

```








150 nfft_b = length(y_fft_b);
151 nfft2_b = 2^nextpow2(nfft_b);
152 ff_b = fft(y_fft_b, nfft2_b);
153 fff_b = ff_b(1:nfft2_b/2);
154 xfft_b = Fs*(0:nfft2_b/2-1)/nfft2_b;
155
156 % Comparison
157
158 figure
159 subplot(2,1,1);
160 plot(dt_b, y_fft_b);
161 title('Time domain signal');
162 xlabel('time(s)');
163 ylabel('Amplitude (V)');
164 axis([0 50 -2 2]);
165
166 hold on
167 plot(dt_a, y_fft_a);
168
169 subplot(2,1,2);
170 plot(xfft_a, abs(fff_a), 'r', 'DisplayName', 'Test a');
171 grid on;
172 title('Frequency domain signal');
173 xlabel('Frequency (Hz)');
174 ylabel('Normalized Amplitude');
175 axis([0 1000 0 5000]);
176
177 hold on
178 plot(xfft_b, abs(fff_b), 'DisplayName', 'Test b');
179 legend('Location', 'southeast', 'FontSize', 12);
180 hold off

```


Appendix B

Jet Turbine Documentation & Software

B.1 JetCat Instruction Manual & Test Checklist

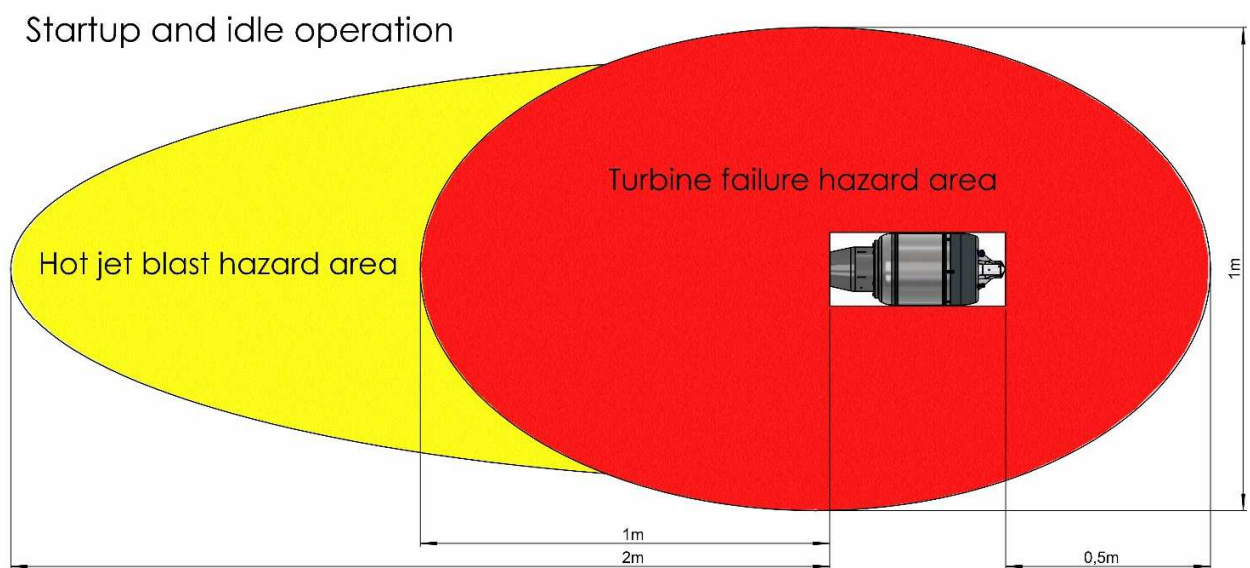
	<p>WARNING! In case of a mishap, fire extinguishers should be on hand at all times. JetCat recommends the CO/2 variety. Powdered extinguishers will corrode the precision components inside the engine and void your warranty.</p>
	<p>WARNING! When the engine is running, never place your hands closer than six inches into the area of the intake. An extreme suction which can grasp a hand, fingers or other objects in an instant exists in this area. Always be aware of this source of danger! Prevent foreign materials from entering the intake or exhaust when working with the engine. Before operation, make sure there are no loose parts or debris near the engine. Objects being sucked in can cause severe damage. If your installation allows, we highly recommend using a “Jet Net” to protect the intake.</p>
	<p>WARNING! Never run the engine in a closed room, or an area near any kind of flammable matter. Do not fly engine-powered aircraft near flammable materials, nor in forested tracts or areas experiencing drought or dryness. Obey all forest fire regulations and warnings by refraining from operating the JetCat engine in restricted fire zones.</p>
	<p>WARNING! The overflight of people, especially at low altitude, is strictly prohibited</p>
	<p>Attention! Always exercise caution around the hot parts of the engine, to avoid burns. The outer case at the engine stage and nozzle reaches 450-600 (Celsius), while the exhaust gas may exceed 800 C.</p>
	<p>WARNING! Assure that the fuel is mixed with approximately 5% synthetic oil. Use only synthetic engine oils available at local airport fuel suppliers. Synthetic engine oils are dangerous and should only be handled as per the manufacturer's MDS sheets. JetCat has available a compatible oil that is less harmful that also contains an antistatic ingredient. Contact JetCat for more information.</p>
	<p>WARNING! To avoid hearing damage, always use hearing protection when you are near a running engine!</p>

Hazard Areas

The following diagrams show the hazard areas during engine operation.

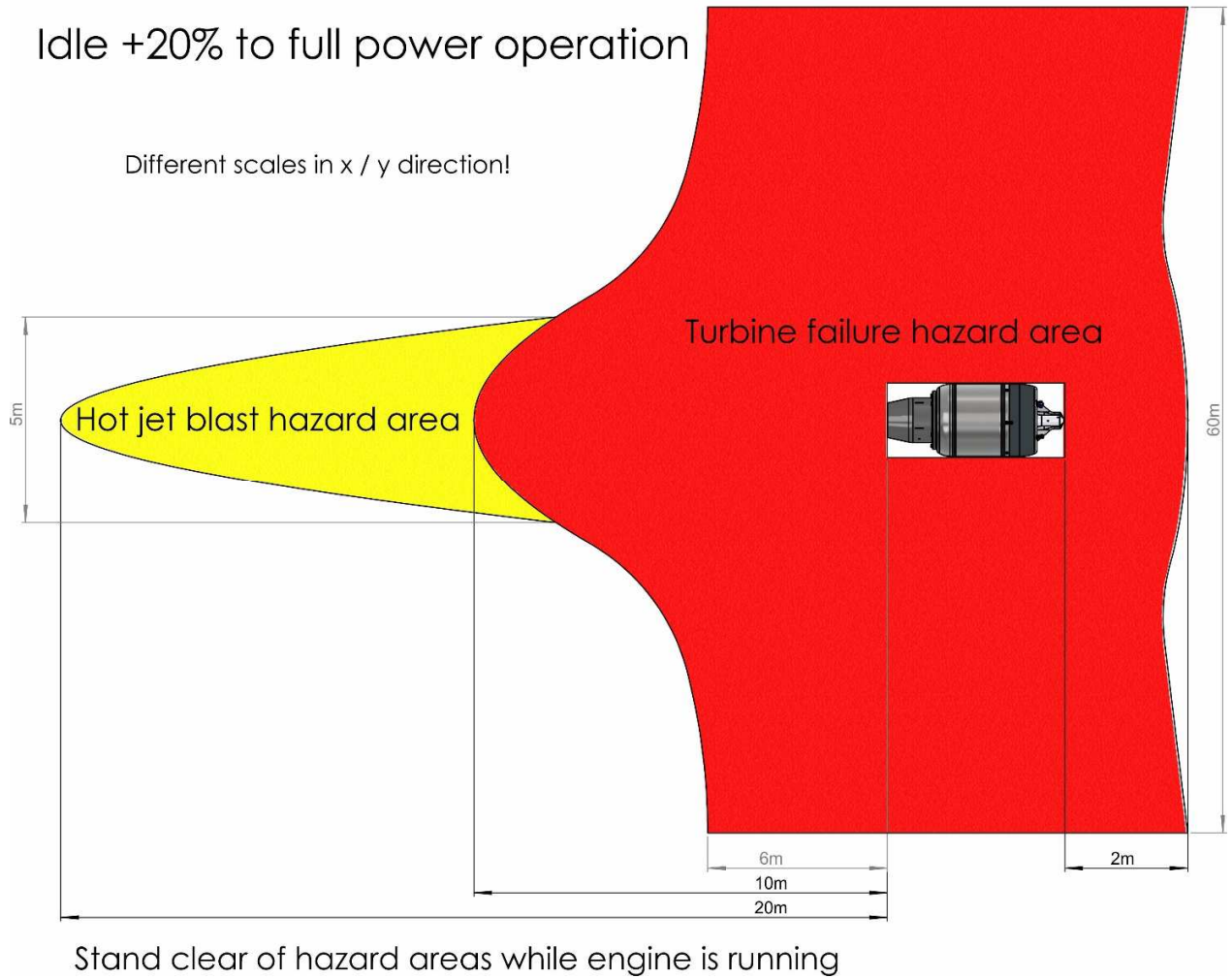
- Please make sure that these safety areas are kept free of persons during operation.
- Always wear safety glasses when operating a jet engine.
- Make sure intake area is free of any parts/obstacles possibly being sucked in by the compressor (FOD)!
The engine will produce an immense suction able to aspirate unsecured parts in quite a large radius!
Keep fingers away from intake area!
- Make sure that fire extinguishing equipment is present (CO2 fire extinguisher with at least 5kg content)

Hazard areas on engine startup and idle operation



Stand clear of hazard areas while engine is running

Hazard areas on engine idle +20% to full power operation



Testing Safety

In order to ensure the safety of all persons present at the test site, the safety checklist, Table 3, must be completed prior to every engine run.

Table XII.3: Safety Checklist

Test:	Date:	
Personal Protection/Test Site Rules	Yes	No
Are ear muffs and plugs being worn by everyone present?		
Are safety glasses being worn by everyone present?		
Was the engine manual used to make all the connections for running the engine?		
Is the jetengine cage locked properly?		
Are the blast shields set up 3m away from the engine?		
Are the wheels locked on the test stand?		
Are there heavy boxes in place on and around test stand?		
Is the testing area clear of all debris and extra objects?		
All extra personal 25 m away?		
Fire Preparedness		
Are fire extinguisher available and their uses known?		
Are fire extinguishers easy to see and reach?		
Does everyone know the 'stop, drop and roll' rule if clothing is on fire?		
Does everyone know to get immediate medical attention for smoke inhalation or any burn, even if minor?		
Visual Inspections:		
Has the engine been inspected for signs of damage?		
Mounting hardware check for flaws?		
All high-pressure connections inspected for signs of damage/ fatigue?		
Fuel lines secure and without leaks?		
Fuel gaskets in good condition?		
Connection/Equipment		
Is wiring permanent, not temporary?		
Are extension cords in good condition and adequate for the job?		
Are there any extension cords or power strips connected in series?		
Are electrical outlets kept from being overloaded with devices?		
Are motors and machine tools kept clean and lubricated?		
Is overloading of motors, circuits, and outlets avoided?		
Is overheating of engine and bearings avoided?		
Are the connections kept from touching the engine?		
Flammable Liquids		

Are flammable liquids stored in approved, airtight metal containers?		
Are they used only in areas with adequate ventilation?		
Are they used only in needed quantities?		
Are spills cleaned up promptly and leaks repaired?		
Is clothing that has absorbed flammable liquids have been removed immediately?		
Components		
Are all the components in the correct place?		
Are the temper sensors being monitored to ensure safe operation limits?		
Is the load cell in place?		
Are the pressure and temperature sensors in their position?		
Is the rear of the engine clear of obstruction?		
Is the fuel on the opposite side of the test stands as the personnel?		
Weather/Field Conditions		
Is there sunlight?		
Is the wind mild? If so, is the wind in line with the engine?		
Do all other flyers/team mates know about the test?		

Completed By: _____

Check List Complete: _____

Emergency Procedures

In the event of an emergency while the engine is running, including (but not limited to) fire, electrical failure, loss of engine control, mechanical failure, the following emergency procedures must be followed:

1. All persons must remain behind blast shields until the engine has stopped moving with PPDs on at all times.
2. Hit the 'EMERGENCY STOP' button
3. Place throttle to "Stop" position (all the way down)
4. Unplug extension cord from the generator
5. Wait for engine to completely stop before approaching- DO NOT TOUCH the engine or test cart until at least 15 minutes after shutdown, since it may be very hot.
6. Call 911 (as necessary)

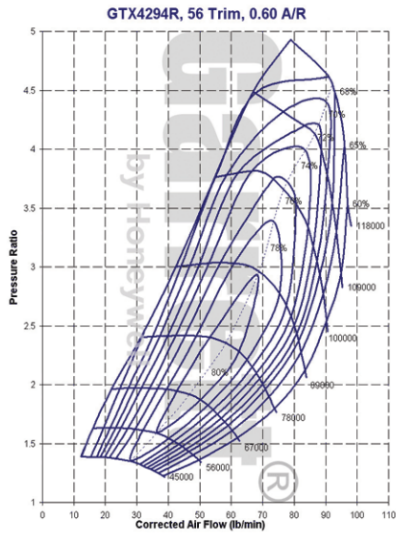
In case of fire:

7. If it is safe to do so, use the CO2 Type fire extinguisher to extinguish the fire by spraying the chemical retardant at the base of the fire.
8. If the fire is uncontrollable, evacuate the area and call 24 hour airport operations at

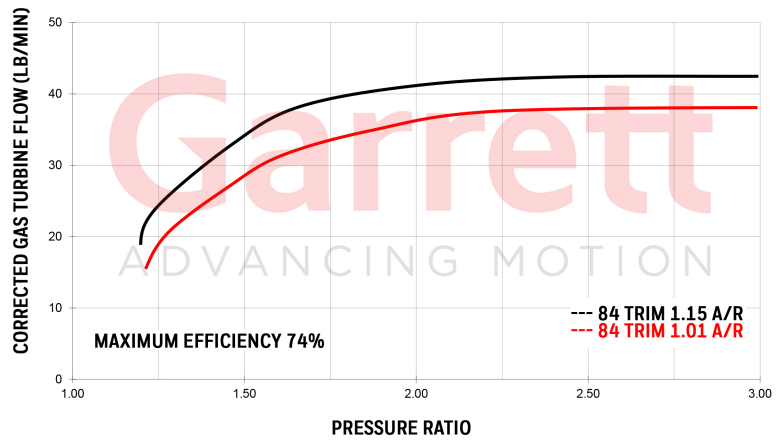
+1 250-953-7500

B.2 Compressor and Turbine maps

Since Jetcat was not able to provide CfAR with the Compressor and Turbine map, the alternative was that of seeking similar documentation on the net. Luckily it was found that the GT42 turbocharger shares almost the same features (in terms of dimension, pressure ratio etc.) with the JetCat P500, and the relative maps are available on the house website. The maps are shown below in Figure B.1.



(a) Airbus A320



(b) Bombardier CRJ200

Figure B.1: compressor and turbine maps.